THE ISOLATION AND CHARACTERISATION OF PROTEASES FROM *EUPHORBIA TIRUCALLI, E. TRIANGULARIS* AND *CARICA PAPAYA* LATEX

by

AKIRA BOODHOO

BSc (Hons) Biochemistry

Submitted in fulfilment of the academic requirements of

Master of Science

in Biochemistry

School of Life Sciences

University of KwaZulu-Natal

Pietermaritzburg

South Africa

2023

PREFACE

The experimental work described in this dissertation was carried out in the School of Life Sciences, University of KwaZulu-Natal, Pietermaritzburg, under the supervision of Professor T.H.T Coetzer. The studies represent original work by the author and have not otherwise been submitted in any other form to another University. Where use has been made of the work of others, it has been duly acknowledged in the text.

09/02/2023 

Akira Boodhoo

As the candidate's supervisor, I agree to the submission of this dissertation.

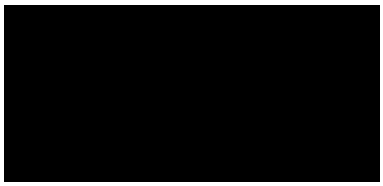

09/02/2023 _____

Prof T.H.T Coetzer

DECLARATION – PLAGIARISM

I, Akira Boodhoo, declare that:

1. The research reported in this dissertation, except where otherwise indicated, is my original research.
2. This dissertation has not been submitted for any degree or examination at any other university.
3. This dissertation does not contain other persons' data, pictures, graphs, or other information, unless specifically acknowledged as being sourced from other persons.
4. This dissertation does not contain other persons' writing unless specifically acknowledged as being sourced from other researchers. Where other written sources have been quoted, then:
   a) Their words have been re-written but the general information attributed to them has been referenced
   b) Where their exact words have been used, then their writing has been placed in italics and inside quotation marks and referenced.
5. This dissertation does not contain text, graphics or tables copied and pasted from the Internet, unless specifically acknowledged, and the source being detailed in the dissertation and in the reference sections.

09/02/2023 

Akira Boodhoo

ACKNOWLEDGEMENTS

I would like to thank my supervisor Prof T.H.T Coetzer for all her support and guidance throughout my postgraduate studies. I am very grateful to have worked under your guidance and learned so much from you during my studies.

Thank you to Dr. Faiaz Shaik and the late Dr. Lucky Marufu for their help, guidance, mentorship and friendship, you all have really helped me throughout my studies whenever I needed help. Thank you to all my lab colleagues Arishka, Ryan and Bhavana.

Thank you to my fellow post-graduate friends: Suhavna, Dhamini, Tehrim and Tim for all the good times and days filled with laughter and for all the encouragement and support.

Thank you to the National Research Foundation and Prof T.H.T Coetzer for financial assistance.

Thank you to Mrs. Alison Young for all the help in collecting my samples for my research project.

Lastly, thank you to my parents, Naveen and Seema Boodhoo for their support and patience throughout my studies. My aunt Natasha Maharaj, for the immense support, thank you for always being there on the good and bad days. Thank you for being my pillar of strength. A thank you to my partner Shane Govender for the continuous encouragement and for never letting me give up.

I dedicate this thesis to my parents for showing me to never give up.

ABSTRACT

Plant proteases play an important role in the food and industrial sectors from meat tenderisers to milk clotting agents and even anti-parasitic agents. Proteases have been identified in plant latex, but many proteases have not been isolated and characterised. This research aimed to isolate and characterise proteases from the latex of *Euphorbia tirucalli*, *E. triangularis,* and *Carica papaya*. Three-phase partitioning (TPP) of *E. tirucalli* plant latex revealed the presence of two active proteases on gelatin-containing zymograms, that were subsequently separated by size exclusion chromatography. These proteases were classified as a 75 kDa serine protease (*E. tiru* SP), inhibited by PSMF, and SBTI and a 37 kDa cysteine protease (*E. tiru* CP), inhibited by E-64. Analysis of *E. triangularis* latex by TPP and *p*-aminobenzamidine affinity chromatography showed the presence of three serine proteases inhibited by PMSF and SBTI, *E. laris* SP1 (>97.4 kDa), *E. laris* SP2 (68 kDa) and *E. laris* SP3 (38 kDa). These proteases showed stability in constant ionic strength buffers from pH 4 to 9, both with and without the presence of the reducing agent cysteine. Papain was isolated from the latex of *Carica papaya* for use as a control protease in zymograms on account of the anomalous behaviour of commercial papain preparations on these gels. Papain was isolated by two methods: ammonium sulfate precipitation followed by TPP and CM-cellulose cation exchange chromatography. The isolated papain was detected by rabbit anti-papain antibodies in a dot blot and western blot and showed inhibition by E-64. The latex from all three plant species showed milk clotting activity with higher activity in the presence of calcium chloride. These findings suggest that isolated plant latex proteases from the *Euphorbia* species can be used in the food industry as milk clotting agents. Further characterisation of these isolated proteases should identify further uses in biotechnology.

TABLE OF CONTENTS

List of Figures

List of Tables

List of abbreviations

5-CQA	5-caffeoyl quinic acid
ALE1	abnormal leaf shape 1
AMC	7-amino-4-methylcoumarin
AMT	acetate-MES-Tris
APA1	*Arabidopsis* aspartic protease
BCA	bicinchoninic acid
BSA	bovine serum albumin
C35	cyanidin 3-sambubioside
CBD	chitin-binding domain
CDR 1	constitutive disease resistance 1
CM	Carboxymethylated
CMTI-I	*Cucurbita maxima* trypsin inhibitor-I
CN	catalogue number
CP	cysteine protease
C-terminus	carboxyl terminus
DEAE-C	diethylaminoethyl cellulose
DEK 1	phytocalpain defective kernel 1
dH_2O	distilled water
DTT	Dithiothreitol
E-64	(1*S*,2*S*)-2-(((*S*)-1-((4-Guanidinobutyl)amino)-4-methyl-1-oxopentan-2-yl)carbamoyl)cyclopropanecarboxylic acid
EDTA	ethylenediaminetetra-acetic acid
FACs	fatty acid-amino conjugates
g	relative centrifugal force
h	hour(s)
HRP	horse radish peroxidase
IgG	immunoglobulin G

IgY	immunoglobulin Y
kDa	kilo-Dalton
MCA	milk clotting ability
MEC	molecular exclusion chromatography
MES	2-(N-morpholino)ethanesulfonic acid
min	minute(s)
MPA1	meiotic prophase aminopeptidase 1
M_r	relative molecular mass
N-terminus	amino terminus
P69	subtilisin-like serine protease
PAGE	polyacrylamide gel electrophoresis
PBS	phosphate buffered saline, pH 7.2
PCS 1	Promotion of cell survival 1
PEG	polyethylene glycol
pI	Isoelectric point
PMSF	phenylmethylsulfonyl fluoride
PR-P69	pathogen related 69 kilo-Dalton proteinase
PSI	Plant specific insert
PVDF	polyvinylidene fluoride
RT	room temperature
SBTI	soybean trypsin inhibitor
SCPL	serine carboxypeptidase-like acyltranferase
SDS	sodium dodecyl sulfate
SFTI-I	sunflower trypsin inhibitor-I
SMEP 1	soybean metalloendoproteinase 1
SP	serine protease
SSD1	stomatal density and distribution 1

t	time
TBS	Tris-buffered saline
TCA	trichloroacetic acid
TLCK	tosyl-L-lysyl-chloromethane hydrochloride
TPCK	tosyl phenylalanyl chloromethyl ketone
TPP	three phase partitioning
Tris	2-amino-2-(hydroxymethyl)-1,3-propandiol
UCH1/2	ubiquitic C-terminal hydrolase 1 and 2
v	volume
VAR2	yellow variegated 2
VEPs	vacuolar processing enzymes
WAMPs	Hevein-like antimicrobial peptides found in wheat
Z	benzyloxycarbonyl

Chapter one
Literature review

1.1 Applications for plant-derived compounds

Plant proteases are used in various industries, such as a milk clotting agent and meat tenderising agent in the food industry and in industrial applications such as beer production (Balls and Hoover, 1937, Tomar et al., 2008, Shouket et al., 2020). Plant proteases have been used in the baking industry to hydrolyse gluten, in the detergent, leather and cosmetic industries, as therapeutic agents in the treatment of different diseases and in biotechnological applications for waste management (Feijoo-Siota and Villa, 2010, Silva-López and Gonçalves, 2019, Troncoso et al., 2022).

Medicinal plants and plant-based medicines have been used in many traditional cultures world-wide as a natural alternative to synthetic chemicals (Wyk and Wink, 2017). Knowledge of the use of medicinal plants has been passed on from generation to generation and is currently still being used independently or with manufactured drugs. Although a few countries have adopted medicinal plants for drug manufacturing, many medicinal-based drugs are used for self-medication (Petrovska, 2012). The increase in the use of herbal medicine may be ascribed to a belief that medicinal plants are more effective than chemically manufactured drugs, adverse side effects and high cost of current medicines and resorting to herbal medicines where modern medicine proved to be ineffective (Bandaranayake, 2006, Ekor, 2014).

The first natural (plant) product used in therapeutics was morphine (Veeresham, 2012), an active compound isolated from opium resin of the dried latex from the opium poppy (*Papaver somniferum* L.) (Brook et al., 2017). One of the most commonly used drugs is aspirin, isolated from the bark of the willow tree, which is used as a pain reliever and anti-inflammatory agent (Desborough and Keeling, 2017, Miner and Hoffhines, 2007). Artemisinin from the bark and leaves of *Artemisia annua* L. (sweet wormwood) is used for the treatment of malaria due to its fast-acting properties against *Plasmodium* spp. and its low toxicity (White et al., 2015, Faurant, 2011). Capsaicin, isolated from the placental tissue surrounding the seeds of *Capsicum annuum* L., known as sweet and chili pepper (Basith et al., 2016), is used in pain relievers (Veeresham, 2012). Various plant-derived components are used for the treatment of inflammatory pain, such as curcumin from *Curcuma longa* L., an important component in turmeric spice (Khumalo et al., 2022). Although the treatment of certain diseases using medicinal plants has not been scientifically proven, some have been effective such as the

treatment of dermatologic diseases in small ruminants. In Argentina, the Wichí people use the latex of *Euphorbia serpens* Kunth (matted sandmat) for the treatment of rashes, conjunctivitis and pimples by direct application (Suárez, 2019).

Proteolytic enzymes (proteases) from plants have other biotechnological applications such as a teeth whitening agent in toothpaste (Chakravarthy and Acharya, 2012, Kalyana et al., 2011), oral diseases such as dental caries, gastrointestinal disorders, antifungal and antimicrobial agents (Balakireva et al., 2019). These proteases also have pharmacological applications such as a hydrophilic extract from *Fucus vesiculosus* L. (bladder wrack), for the treatment of pancreatic cancer (Balakireva et al., 2019, Geisen et al., 2015). Proteases found in plant extracts have been used fopr wound healing and blood clotting; hence an interest in the procoagulant and anticoagulant properties of plant proteases (Balakireva et al., 2019).

1.1.1 Plant proteases

The focus of this study is plant proteases, enzymes responsible for the hydrolysis of proteins into smaller peptides and single amino acids. Plant proteases aid in regulating biological processes such as meiosis and seed coat development by degrading non-functional proteins such as misfolded and abnormal proteins into amino acids (van der Hoorn, 2008, Sharma and Gayen, 2021). Plants are able to adapt to changing environmental conditions due to stress responses such as light exposure, temperature, water and nutrition; or the plant can become susceptible to diseases or attacks by insects and herbivores. In response to drought, an example is, serine protease subtilase SBT3.8 that processes the precursor of phytosulfokine, a peptide hormone that plays a role in drought resistance in *Arabidopsis*. The precursor is cleaved by SBT3.8 at the C-terminus of the phytosulfokine pentapeptide before an aspartic residue (Stührwohldt et al., 2021). Developmental factors involve internal processes such as cell differentiation in which cells are developed for specific functions (David, 2017) such as cell wall development or for plant defence against predators. An example of a cell wall protease is papain-like cysteine protease CEP_1 that is located in the cell wall of xylem cells of *Arabidopsis*, and is responsible for secondary wall thickening during xylem development (Han et al., 2018). This protease removes cellular contents during programmed cell death (PCD) in xylem development, a mutation on CEP_1 results in delayed PCD that causes thicker secondary walls. In PCD, the secondary walls contain lignin, an organic polymer found in cell walls which provides mechanical strength thus increasing its defence against predators (Huang et al., 2018, Liu et al., 2018).

Plant proteases are used in the food, medical and biotechnological industries due to their activity over a wide pH and temperature range, high stability and broad substrate specificity (Tomar et al., 2008). The cysteine protease ficin from the latex of *Ficus carica* L. (common

fig), is used for milk clotting, meat tenderisation (Ilany and Netzer, 1969, Bekhit et al., 2014, Baeyens-Volant et al., 2015) and as a hemostatic and an anti-parasitic agent Morellon-Sterling et al. (2020). Actinidin isolated from kiwi fruit [*Actinida* spp: *Actinidia macrosperma* C.F. Liang, *Actinidia arguta* (Siebold & Zucc.) Planch. ex Miq. and *Actinidia deliciosa* cv. Abbot] hydrolyses α-amylase (Martin et al., 2017, Dhiman et al., 2021). Kiwi fruit actinidin inactivates α-amylase thus reducing the glycaemic index of foods rich in starch, thus eating starchy foods with kiwi fruit slows down starch digestion resulting in low blood sugar production therefore assisting diabetic patients to maintain the low blood sugar levels. The serine protease cucumisin from melon fruits (*Cucumis melo L*.) (Yamagata et al., 1994) showed milk clotting ability (Uchikoba and Kaneda, 1996). Papain from the latex of papaya fruits (*Carica papaya*) (Istrati, 2008) can be utilised for the treatment of diarrhoea or the prevention of chest pains (Pavan et al., 2012). Bromelain from the stems and peels of pineapples (*Ananas comosus* (L.) Merr.) (Campos et al., 2019) and papain are used for meat tenderisation; papain and zingibain from ginger rhizomes (Gagaoua et al., 2015) showed milk clotting ability. Milk clotting is a process used in the food industry for the production of cheese. According to Balakireva et al. (2019) plant proteases have collagenolytic activity that can be used to treat wounds and removing damaged tissue caused by burns.

Plant latex provides a good source of proteases, by simple purification methods and removal of interfering compounds such as rubber, secondary metabolites, terpenes, alkaloids and phenolics during purification (Tomar et al., 2008, Gracz-Bernaciak et al., 2021). For example, wrightin, a serine protease isolated from the latex of *Wrightia tinctoria* R. Br. (pala indigo plant) can be used in food and industrial applications such as baking, cheese production and protein hydrolysis to improve food quality such as digestibility due to its high temperature stability (Tomar et al., 2008, Tavano, 2013). A glycosylated cysteine protease, isolated from the latex of *Euphorbia nivulia* Buch.-Ham. (leafy milk hedge), showed potential use in the leather processing and detergent industries (Badgujar and Mahajan, 2013a).

1.1.2 Classes of proteases

There are seven different protease classes: serine, cysteine, metallo-, aspartic, glutamic and threonine proteases (Lopez-Otin and Bond, 2008) as well as asparagine peptide lyases (Rawlings et al., 2011). The four main classes are serine, cysteine, aspartic and metallo-proteases. The catalytic mechanisms of these protease classes are different as aspartic, metallo- and glutamic proteases use water as a nucleophile, while asparagine peptide lyases and cysteine, serine and threonine proteases use a specific active site amino acid residue as the nucleophile (Lopez-Otin and Bond, 2008). Nucleophiles are electron donors that donate a pair of electrons in order to form a covalent bond. Glutamic proteases and asparagine peptide

lyases have not yet been found in plants but threonine proteases have been detected in some plant species such as *Populus* and *Arabidopsis* (García-Lorenzo et al., 2006) but not in Euphorbia spp. The proteases in each of the different catalytic classes are grouped into different families based on the analysis of their amino acid sequences and are further grouped into clans which represent distantly related families (Barrett and Rawlings, 1996).

Proteases play an important role in proteolysis by regulating the fate and activity of proteins, producing new bioactive modules, protein-protein interactions and aids in the processing of cellular information (Lopez-Otin and Bond, 2008). The ability to detect target protein substrates is based on the substrate specificity. Protein substrates are cleaved by proteases either near the N- or C- terminus (exopeptidases) or internally (endopeptidases) following binding of the protease active site to the substrate residues, thus flanking the cleavage site as shown in Figure 1.1 (Song et al., 2011). The protease active site residues comprise contiguous pockets called subsites and each subsite pocket will bind to a corresponding residue in the substrate sequence. The nomenclature for the description of protease subsites is according to Schechter and Berger (1967). The amino acid residues of the substrate sequence are numbered outwards from the cleavage site towards the N-terminus of the substrate as P_1, P_2, P_3, etc. and towards the C-terminus as -P_1', P_2', P_3', etc. and the corresponding subsites in the active site are numbered from the scissile bond to the N-terminus as S_1, S_2, S_3, etc. and towards the C-terminus as -S_1', S_2', S_3', etc. The scissile bond is located between the P_1 and P_1' amino acid residues. (Song et al., 2011).

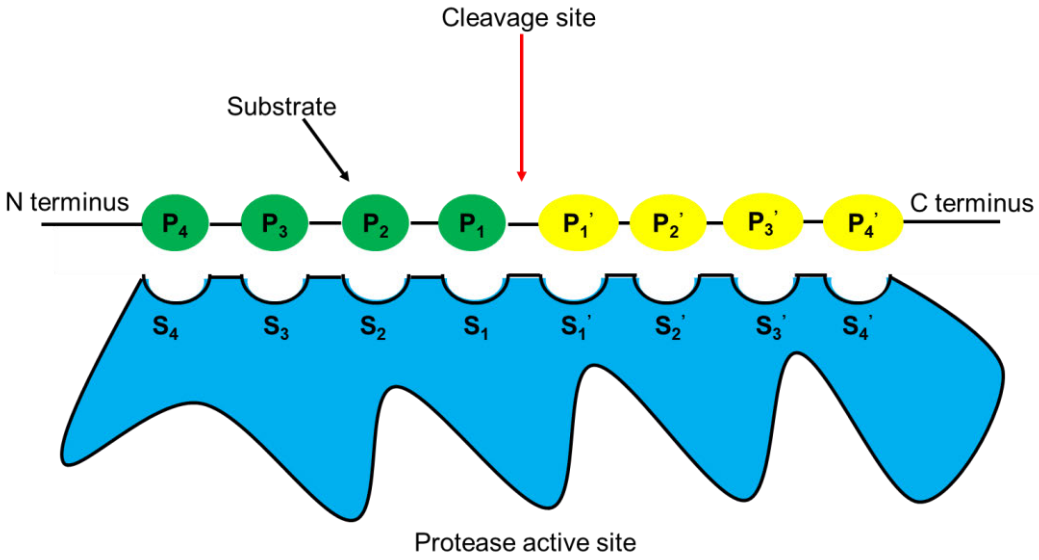

Figure 1.1: Protease substrate specificity nomenclature. The amino acid residues are numbered from the cleavage site towards the N-terminus of the substrate as -P_1, P_2, P_3 etc. and towards the C-terminus as P_1', P_2', P_3', etc. The corresponding subsite pockets in the active site are numbered from the scissile bond to the N-terminus as S_1, S_2, S_3, etc. and towards the C-terminus as -S_1', S_2', S_3', etc. The cleavage site (scissile bond) is highlighted by the red arrow between P_1 and P_1'. The non-prime

side residues (P_1-P_4) are coloured green and the prime side residue (P_1'-P_4') are coloured yellow. The Figure was adapted from Song et al. (2011).

1.1.1.1 Serine proteases

One third of all known proteases are serine proteases being found in many kingdoms of life (Di Cera, 2009), including plants where they form the largest class of proteases (Sebastián et al., 2018). A serine protease classification system based on their catalytic activity and on the similarity between ancestral proteases was developed by placing them into 40 families and 13 clans (Di Cera, 2009); of which plant proteases belong to 14 families and 9 clans (van der Hoorn, 2008). The largest family of serine proteases belong to clan PA, have a trypsin fold and include digestive enzymes such as trypsin and chymotrypsin (Di Cera, 2009). Clan PA proteases are responsible for important biological processes such as complement activation in which the proenzyme of serine proteases are activated in a signaling pathway to produce effector molecules by limited proteolysis (Sebastián et al., 2018) and blood coagulation (Di Cera, 2009). Serine proteases hydrolyse peptide bonds in a two-step mechanism as illustrated in Figure 1.2. In the first part of the reaction the carbonyl carbon atom of P1 undergoes nucleophilic attack by the catalytic serine residue. This creates both a covalent acyl-enzyme intermediate and a new peptide amino terminus on P1. In the second part of the reaction the acyl-enzyme is hydrolysed by a water molecule, which releases a carbonyl group and the serine residue is restored to its original state (Zakharova et al., 2009). An oxyanion hole is formed by the backbone nitrogen atoms of Ser-195 and Gly-193 and is responsible for stabilising the high-energy acyl intermediates (Zhang et al., 2002, Bobofchak et al., 2005).

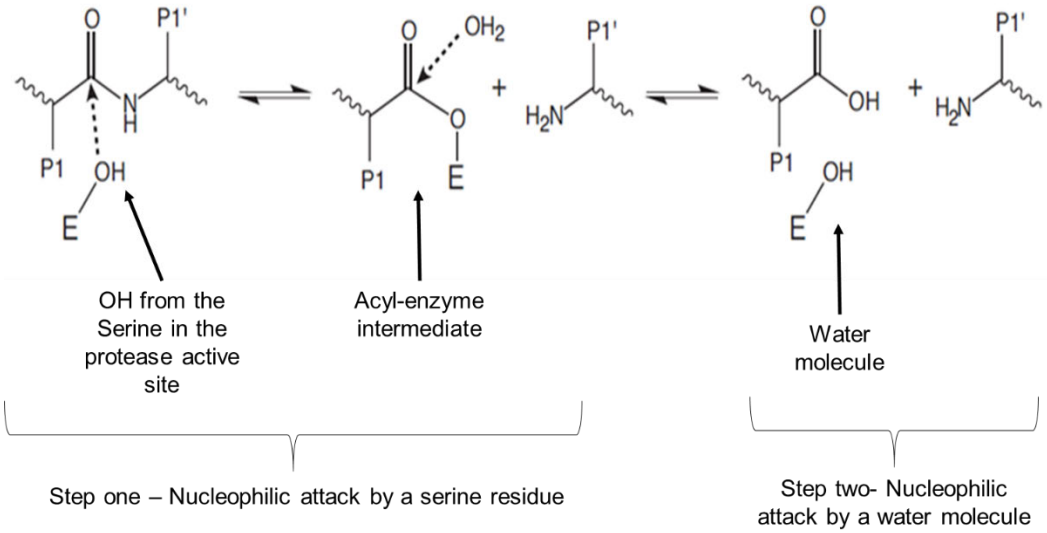

Figure 1.2: Catalytic mechanism of serine proteases. In step one, the serine residue undergoes nucleophilic attack, creating a covalent acyl-enzyme intermediate and a new peptide amino terminus on P1. In step two of the reaction, a nucleophilic attack by a water molecule releases a carbonyl group resulting in regenerating the serine hydroxyl. Figure adapted from Zakharova et al. (2009).

Plant proteases that belong to the S8, S9, S10 and S33 families are considered to be the largest families, with S8 being the largest amongst them. Plant subtilisin-like proteases belong to family S8, clan SB and contain a catalytic triad consisting of Asp, His and Ser residues (Dodson and Wlodawer, 1998). Substilisin-like proteases, stomatal density and distribution 1 (SSD1) and abnormal leaf shape 1 (ALE1) were found in the *Arabidopsis* genome and are responsible for regulation of stomatal development within the epidermis and cuticle development during embryogenesis respectively (van der Hoorn, 2008). Substilisin-likeproteases can play a role in plant pathogen defence, such as the 69 kDa protease PR-P69, a pathogen related protein produced in tomato plants (*Lycopersicon esculentum*) that has a functional similarity to substilisin-like proteases (Tornero et al., 1996). Carboxypeptidase-like proteases belong to family S10, clan SC and contain a catalytic triad of Ser, Asp and His residues and these proteases differ to other serine proteases as they are only active at acidic pH levels (van der Hoorn, 2008). Serine carboxypeptidase-like (SCPL) acyltransferase are classified as plant natural biosynthetic enzymes and facilitates transacylation reactions by using energy-rich 1-O-β-glucose esters to produce bioactive compounds (Mugford and Milkowski, 2012) and plays an important role in a plant growth and development (Wang et al., 2022).

1.1.1.2 Cysteine proteases

There are 140 cysteine proteases that are derived from plant genomes which belong to five clans and 15 families (van der Hoorn, 2008). The most studied proteases are the papain-like proteases (Grudkowska and Zagdańska, 2004). In plants, these proteases play a role in programmed cell death by responding to pathogens and developmental cues while other cysteine proteases play a role in regulating flowering time, pollen and embryo development (van der Hoorn, 2008). Cysteine proteases contain a catalytic triad of Cys–His–Asn residues within the active site. Papain-like cysteine proteases consist of two domains, a N-terminal helical domain and a C-terminal β-sheet domain (Verma et al., 2016). Figure 1.3 represents the domain structure of cysteine proteases showing the catalytic triad where the cysteine residue's nucleophilicity is enhanced by the histidine residue. The catalytic mechanism of cysteine proteases is shown in Figure 1.4. A histidine and a cysteine residue in the active site form a stable thiolate-imidazolium ion pair. Following a nucleophilic attack by the cysteine on the carbonyl carbon of the peptide substrate, a tetrahedral intermediate formed. When the peptide bond is cleaved, an acyl enzyme intermediate is formed. The acyl enzyme undergoes hydrolysis which releases the cleaved peptide and regenerates the active site residues (Fricker, 2010).

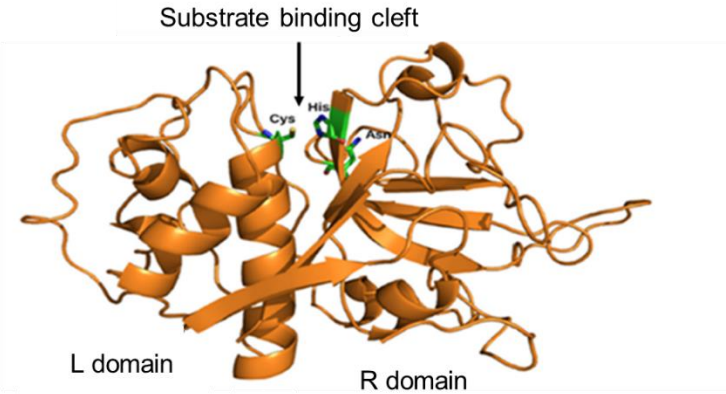

Figure 1.3: Mature domain structure of a cysteine protease. The active site contains a Cys-His-Asn triad (stick figures) within the substrate binding cleft and the alpha helix and beta sheets are indicated by arrows. Cysteine is the nucleophile for proteolysis. Figure adapted from Verma et al. (2016).

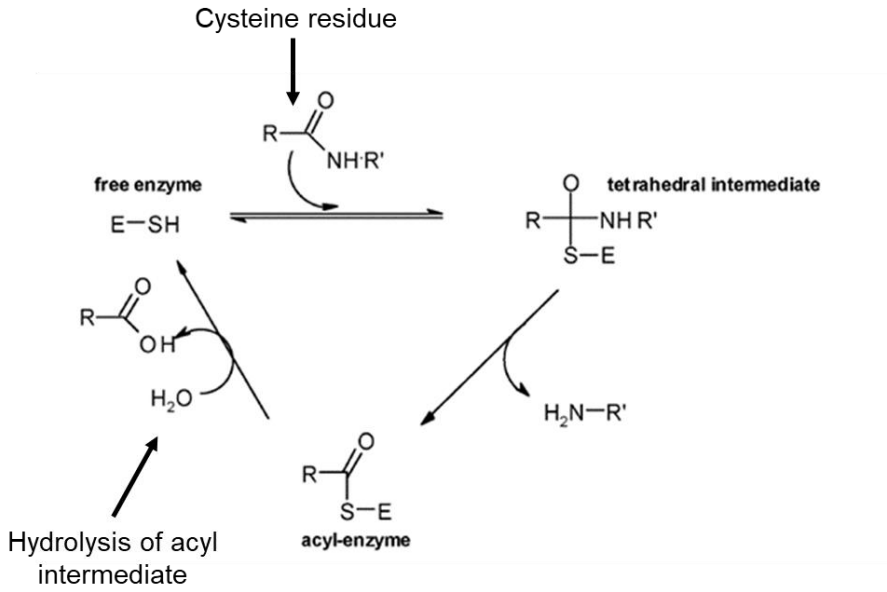

Figure 1.4: Catalytic mechanism of cysteine proteases. The carbonyl carbon of the peptide substrate undergoes nucleophilic attack, forming a tetrahedral intermediate. An acyl enzyme intermediate is formed when the peptide bond is cleaved and undergoes hydrolysis, which releases the cleaved peptide and regenerates the active site residues. Figure adapted from Fricker (2010).

Papain, isolated from the latex of *Carica papaya*, is the archetypal subfamily C1A cysteine protease. It is a single chain protein of molecular weight 23.4 kDa and contains four disulfide bridges that stabilise the tertiary structure. Papain is folded into two domains, that each have their own hydrophobic core with the L-domain comprising mostly α-helices and the R-domain β-sheets (Figure 1.3). The substrate binding pocket is located in the cleft between these two domains (Kamphuis et al., 1984). The active site of papain consists of three residues Cys25,

His159, and Asn175, in which the sulfhydryl group on Cys25 acts as the nucleophile during catalysis. The precursor of papain is a 39 kDa pro-papain zymogen molecule that is glycosylated and can be auto-catalytically processed to the active form by removal of the pro-peptide (Vernet et al., 1991). The optimal conditions for precursor activation is between pH 3.7 and 4.2 and at a temperature range of 30°C to 65°C in the presence of cysteine (Vernet et al., 1991). Industrial applications of papain include being used as a meat tenderiser, milk clotting agent and in beer production by digesting dissolved proteins, increasing the clarity of beer (Balls and Hoover, 1937, Shouket et al., 2020).

Bromelain is another C1A subfamily cysteine protease , isolated from either the stems (stem bromelain) or fruit (fruit bromelain) of a pineapple (*Ananas comosus*) (Verma et al., 2022). Bromelain is isolated as a glycosylated (on the Asn117 residue), monomeric protein with a pI of 9.55 and optimal pH range of 6-7, containing seven cysteine residues forming three disulfide bonds, with the seventh Cys- residue in the active site (Harrach et al., 1995, Novaes et al., 2014, Azarkan et al., 2020). The structure of bromelain also consists of two domains (L and R domain) with the active site cleft located between the domains (Azarkan et al., 2020). The residues GIn20 and Asn179 of the oxyanion hole forms a hydrogen bond on the protonated side of His158, resulting in the formation of the imidazolium ring (Menard et al., 1991, Vernet et al., 1995). Fruit bromelain showed optimal activity at 55°C when incubated with substrates azoalbumin at pH 7.5 and azocasein at pH 6.5 (Corzo et al., 2012). Bromelain is activated in the presence of cysteine, calcium chloride and benzoate (Dubey et al., 2012). Bromelain is used in the food industry as a meat tenderising agent and is an active ingredient in tooth whitening (Arshad et al., 2014).

Ficin is a 23.1 kDa cysteine protease isolated from the latex of the fig tree, *Ficus carica* (Englund et al., 1968, Haesaerts et al., 2015). Ficin has peak activity at pH 7 and is completely inactive below pH 3 (Milošević et al., 2019) and can be used as a milk clotting agent and the production of milk protein hydrolysates (Siar et al., 2020, Aider, 2021).

Other plant cysteine proteases include phytocalpain defective kernel 1 (DEK1) which is responsible for the development of the embryonic epidermal layer and the outer layer of the endosperm (aleurone) in the seed development of *Zea mays* L. (maize) and *Arabidopsis thaliana* (L.) Heynh. (thale cress) (Ahn et al., 2004, Lid et al., 2002). Calpains (family C2, clan CA) are related to papain in having the same order of catalytic residues (Cys, His, Asn), but require calcium for catalytic activity (Hosfield et al., 1999). Since plant genomes only contain one calpain, it is known as phytocalpain (van der Hoorn, 2008). Papain-like protease Rcr3 from tomato (*S. lycopersicum*) plays a role in the defence against fungal pathogens such as *Cladosporium fulvum* Cooke (Paulus et al., 2020). The immune response of Rcr3 is signaled

by P69B (substilisin) and other subtilases (Paulus et al., 2020). Another papain-like protein is *Nicotiana benthamiana* Cathepsin B (*Nb*CthB) that partakes in host and non-host plant disease resistance (Gilroy et al., 2007) and is responsible for the transduction of signals in recognition of some avirulent pathogens (van der Hoorn, 2008). Deconjugating enzymes ubiquitin C-terminal hydrolase 1 and 2 (UCH1/2) functions in protein deubiquitination and are found in the genome of *Arabidopsis* (van der Hoorn, 2008, Wang et al., 2018). Caspase-like proteases belong to family C14, clan CD and are noted for PCD (van der Hoorn, 2008). An example of a caspase-like protease are vacuolar processing enzymes (VPEs) found in plant seeds and vegetative organs (Hara-Nishimura et al., 1998). This protease activates proprotein precursors and mediates PCD by rupturing the vacuole initiating the PCD signal response (Yamada et al., 2020). Programmed cell death is the process of cell suicide in response to developmental changes such as removal of unwanted tissues and to stress responses such as change in temperatures, nutrient deficiencies and drought (Raju et al., 2021, Mareri et al., 2022). Vacuolar processing enzymes are expressed in the inner cell layers of developing seeds and trigger PCD to reduce the thickness of the seed layers to form the seed coat (Hatsugai et al., 2015). When aphids feed on plant leaves, VPEs are triggered as a response to biotic stress, causing the leaves to curl up and become deformed (Ramasamy and Ravishankar, 2018, Vorster et al., 2019).

1.1.1.3 Metalloproteases

Plant genomes contain approximately 100 types of metalloproteases, which belong to 11 clans and 19 families. Metalloproteases use zinc in the active site to activate a water molecule that causes a nucleophilic attack on the carbonyl carbon of the substrate (Figure 1.5). A proton transfer to the amine nitrogen is facilitated through the glutamic acid residue resulting in the formation of a tetrahedral gem-diol intermediate. The substrate is then broken down and the water molecule is released (Cui et al., 2017). Stabilisation of the peptide occurs at the active site by the interaction between the N-terminal substrate residue and S_1' binding pocket as well as the new hydrogen bonds formed between the water molecule, glutamate and N-terminal residues (Laronha and Caldeira, 2020).

Plant metalloproteases include clan MA metalloprotease meiotic prophase aminopeptidase 1 (MPA1) which aids in chromosome pairing and is important in the first steps of both male (stamen) and female (pistil) meiosis in plants (Peer, 2011). A metalloprotease of the M1 subfamily is encoded by *MPA1* and is sensitive to puromycin and is essential in meiosis of *Arabidopsis thaliana* (Sánchez-Morán et al., 2004). This protease regulates progression of the cell cycle during prophase I in meiosis for both male and female gametophytes (Wattarantenne, 2017). The metalloprotease, yellow variegated 2 (VAR2) encodes a FtsH5

protease, responsible for chloroplast differentiation in *Arabidopsis thaliana* in which parts of green tissues appear yellow or white (Takechi et al., 2000, Miura et al., 2008).

Matrix metalloproteases, also known as MMPs or matrixins are a subfamily of metalloproteases (Pelmenschikov and Siegbahn, 2002) that belong to the family of metzincins (Stöcker and Bode, 1995), which are zinc dependent proteases (Pelmenschikov and Siegbahn, 2002). The first MMP from higher plants, ethylenediaminetetraacetic acid (EDTA)-sensitive azocoll-degrading enzyme was isolated from the leaves of soybean (*Glycine max*) (Ragster and Chrispeels, 1979). This 15 kDa protein was purified by DEAE-cellulose chromatography and later renamed as soybean metalloendoproteinase-1 (SMEP-1) (Graham et al., 1991). A study by Zimmermann et al. (2016) showed that MMPs, Sl_2-MMP and Sl_3-MMP from tomato (*Solanum lycopersicum*) regulate cell death starting in tomato seeds by inactivating P69B (subtilisin-like protease) that acts as a substrate for Sl_2-MMP and Sl_3-MMP.

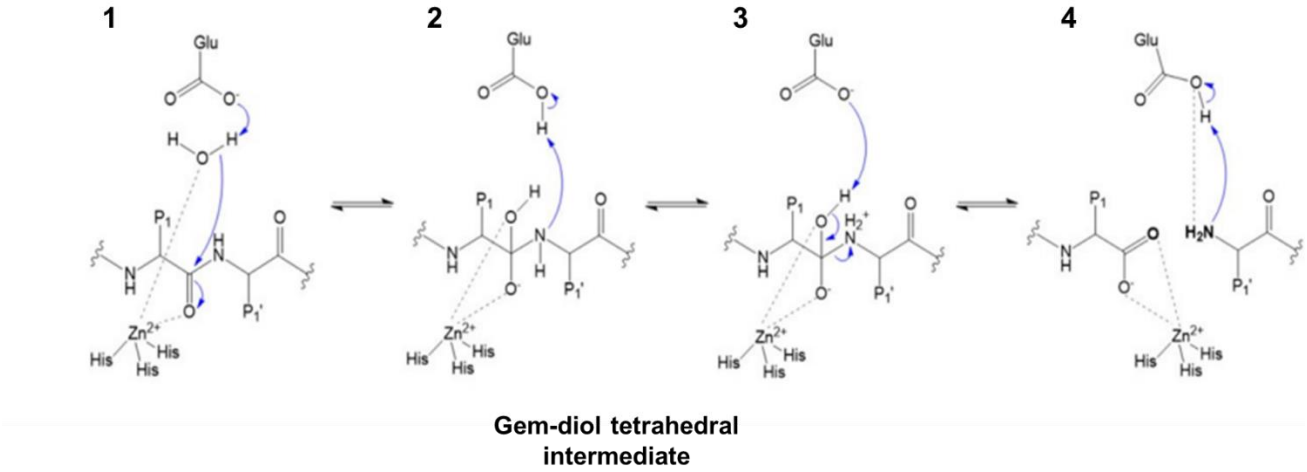

Figure 1.5: Catalytic mechanism of metalloproteases. Activation of water molecule by zinc and nucleophilic attack on carbonyl carbon of substrate **(1)**. Transfer of a proton to the amine nitrogen **(2)** and the formation of the gem-diol tetrahedral intermediate (**3)**. Breakdown of substrate and release of water molecule **(4)**. Figure adapted from Laronha and Caldeira (2020).

1.1.1.4 Aspartic proteases

Aspartic proteases are the second largest class of proteases, with serine proteases being the largest class overall. There are 14 families, further classified into six clans, with plant aspartic proteases belonging to families A1, A3, A11 and A12 (clan AA) and family A22 (clan AD) with most plant proteases belonging to the A1 family (Simões and Faro, 2004). The archetypal aspartic protease is mammalian pancreatic pepsin. The catalytic mechanism of aspartic proteases involves two highly conserved aspartic residues present in the active site for catalytic peptide cleavage (Figure 1.6). The aspartic residue activates water by removing a proton which allows the water molecule to attack the carbonyl carbon of the scissile bond of

the substrate which then creates a tetrahedral oxyanion intermediate. The nitrogen on the tetrahedral intermediate becomes protonated by internal proton transfer via the Asp residue from a hydroxyl of the carbon of the tetrahedral intermediate and finally the tetrahedral intermediate breaks down (Polgár, 1987, Trezza et al., 2020).

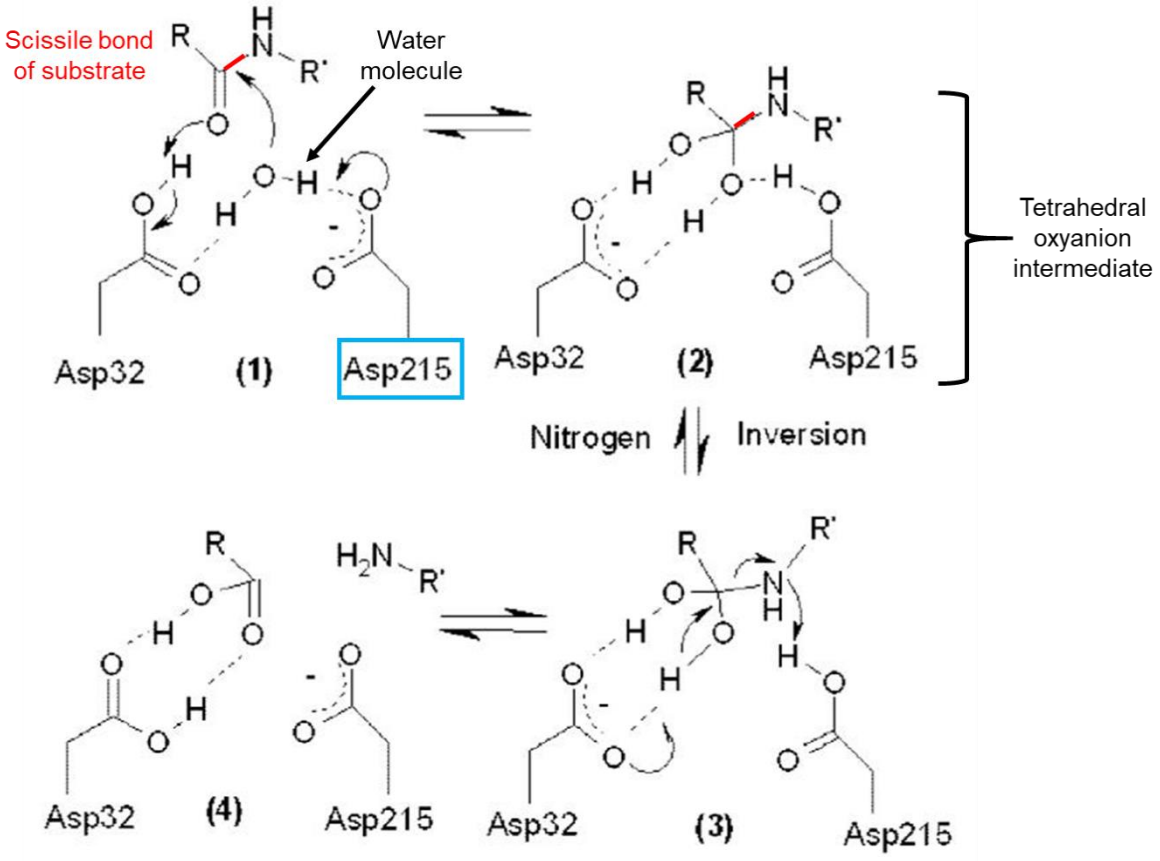

Figure 1.6: Catalytic mechanism for aspartic proteases. (1) The Asp 215 residue activates water by proton removal allowing the water molecule to attack the carbonyl carbon of the scissile bond of the substrate. **(2)** A tetrahedral oxyanion intermediate is formed. **(3)** The nitrogen on the tetrahedral intermediate is protonated by internal proton transfer through the Asp residue from a hydroxyl of the carbon of the tetrahedral intermediate. **(4)** The tetrahedral intermediate breaks down. The arrows represent proton transfers. Figure adapted from Coates et al. (2008).

The A1 family of plant aspartic proteases are divided into typical, nucellin-like and atypical aspartic proteases (Soares et al., 2019). Typical plant aspartic proteases contain a plant-specific insert (PSI) in the C-terminal region. This PSI and the pro-segment are not found in nucellin-like aspartic proteases, while atypical aspartic proteases contain intermediate features from both typical and nucellin-like aspartic proteases (Mutlu and Gal, 1999, Simoes and Faro, 2004). Plant aspartic proteases play a role in a plant's defence response to abiotic stresses such as heat, cold and drought and plant-pathogen interactions (Figueiredo et al., 2021). The overexpression of *Arabidopsis* aspartic protease (APA1) in the epidermal and

stomata cells of the leaves, is important in drought tolerance as it reduces the stomatal index, thus reducing water loss (Sebastián et al., 2020). A 37 kDa aspartyl endoprotease isolated from the leaves of the wild tomato, *Lycopersicon esculentum* Mill., showed the degradation of P69 and PI (pathogen-related proteins) when infected with citrus exocortis viroid thus reducing its overaccumulation (Rodrigo et al., 1989). Plant thistle aspartic proteases are also utilised in a semi-industrial sector for cheese making due to their high proteolytic activity in comparison to enzymes from animals (Folgado and Abranches, 2020). An example is the aspartic protease from *Cynara cardunculus* L. (cardoon or artichoke thistle) flowers that is a suitable vegetarian rennet used for cheese making (Roseiro et al., 2003).

Plant aspartic proteases include nepenthesins, found in carnivorous pitcher plants such as nepenthesin-1 from *Nepenthes gracilis* Korth (Kadek et al., 2014) and a homologue, HvNEP-1, from barley (*Hordeum vulgare* L.) (Bekalu et al., 2021) as well as nepenthesin-like aspartic proteases from *A. thaliana* (Takahashi et al., 2008). The secretory glands of the lower parts of the pitcher plants produce nepenthesin which hydrolyses the proteins of insects trapped in the pitchers as a source of nitrogen (Kadek et al., 2014, Bekalu et al., 2020). Barley HvNEP-1 hydrolyses phytases used by *Fusarium* spp. to obtain orthophosphate from phytic acid that is the main storage form of organic phosphate in cereal grains. The gene coding for HvNEP-1, could be used as a resistance gene for developing fusarium head blight resistant crops (Bekalu et al., 2021). Constitutive disease resistance 1 (CDR1) from the seeds of *A. thaliana* is important for disease resistance signaling and is an atypical aspartic protease (Simões et al., 2007). The overexpression of this protease results in salicylic acid-mediated disease resistance in response to the pathogen *Pseudomonas syringae* (Simões et al., 2007, Carstens et al., 2014). Promotion of cell survival 1 (PCS1) aspartic protease from the *Arabidopsis* genome is responsible for cell fate during gametogenesis and embryogenesis by degeneration of the male and female gametophytes and cell death of developing embryos (Ge et al., 2005). The homozygous *pcs1* mutant present in germinating seeds is lethal, resulting in early abortion of the seeds, while ovules from *pcs1*/+ plants had abnormal morphology during flower opening and later degenerated (Ge et al., 2005). Promotion of cell survival 1 promotes cell survival during gametogenesis and embryogenesis, as its overexpression blocks PCD that is associated with anther dehiscence.

1.2 Plant latex

Plant latex is a non-transparent white sap stored in tissues called laticifers, that is released when plants experience physical damage such as from feeding insects (Konno, 2011). The properties of latex differ amongst plants of different species in terms of viscosity, transparency and colour. For instance, latex from celandine (*Chelidonium majus* L.) is a transparent yellow

to orange in colour (Konno, 2011), while in other plants the colour varies from white to yellow to scarlet and can change upon air exposure (Bhagyashri et al., 2015). An example is the thick white latex obtained from the branches of *Euphorbia tirucalli* L. (Figure 1.7). The white latex colour and sticky consistency is due to the presence of rubber particles and hence the latex from *Hevea brasiliensis* (Willd. ex A.Juss.) Müll.Arg. (rubber tree) is used for rubber production (Agrawal and Konno, 2009). There are three possible functions of white latex; one being that it has no function or no reason for the white colour; second being that other latex bearing plants cannot produce white latex due to chemical constraints and lastly it can serve as a visual advantage for example as a defence mechanism (Lev-Yadun, 2014). Latex becomes coagulated upon air exposure; when a plant is physically damaged, the laticifers release the stored latex and simultaneously activate coagulating proteins so that when exposed to air, a latex plug forms around the latex, concentrating the latex and evaporating the water, thus leading to coagulated latex (Salomé Abarca et al., 2019).

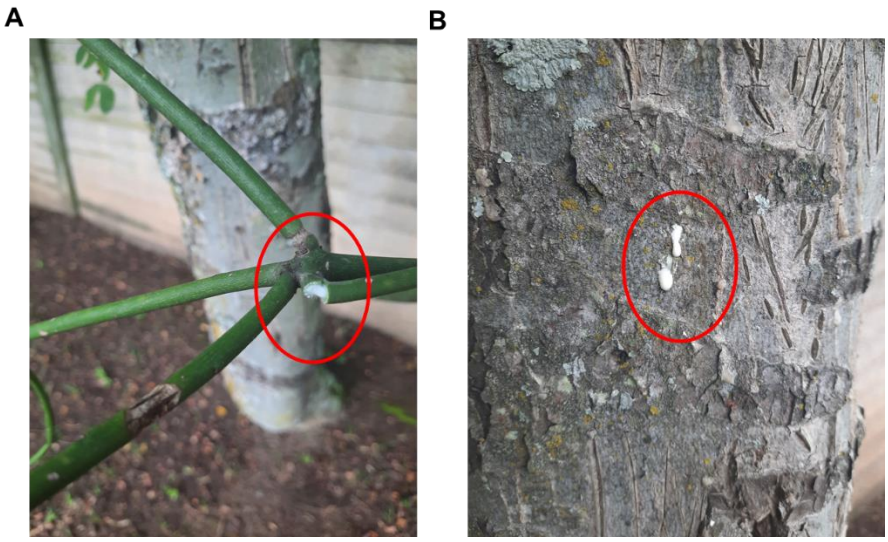

Figure 1.7: White latex from *Euphorbia tirucalli.* (A) Latex from the branches and **(B)** latex exuded from the tree stem. The red circles highlight the thick white latex exuded upon physical injury.

Latex contains different compounds and proteins such as alkaloids, terpenoids, rubber and enzymes such as proteases, protease inhibitors and chitinases (Konno, 2011). Cysteine proteases have been isolated from the latex of various plants such as papain from *C. papaya*, ficin (27 kDa) from *F. carica*, morrenain b II from *Morrenia brachystephana* and procerain (28.8 kDa) from *Calotropis procera* (Aiton) W. T. Aiton. (giant milkweed) (Nassar and Newbury, 1987, Barberis et al., 2002, Dubey and Jagannadham, 2003, Hafid et al., 2020). Serine proteases isolated from the latex include Ficin E (50 kDa) from *Ficus elastic* Roxb. (rubber fig), hevain (69 kDa) from *H. brasiliensis*, cucumisin-like protease (80 kDa) from *Euphorbia sapina* Raf., antiquorin (thrombin-like protease) from *Euphorbia antiquorum* L. (antique

spurge), carnein (80.4 kDa) from *Ipomoea carnea* (pink morning glory) (Lynn and Clevette-Radford, 1984b, Lynn and Clevette-Radford, 1986, Arima et al., 2000, Patel et al., 2007, Urs et al., 2021). The latex of *C. procera*, showed high cysteine protease inhibitory activity against papain when extracted by sodium phosphate buffer and concentrated by acetone precipitation (Abdulkadir et al., 2016). A subtilisin protease inhibitor of 11.73 kDa and pI of 4.15 was found in the latex of *H. brasiliensis* (Archer, 1983).

A high amount of alkaloids is found in the latex of the opium poppy (*Papaver somniferum*) and deters herbivores from feeding on them (Kurek, 2019). Colchicine is an alkaloid found in plants of the Liliaceae family and is used for the treatment of gout (Kurek, 2019). A diterpenoid taxol (paclitaxel) was isolated from the stem of the yew tree (*Taxus brevifolia* Nutt.) and is used as an anticancer agent (Wani et al., 1971, Kim and Kim, 2015). Plant latex is also a good source of phenolic compounds with antibacterial, antifungal and antiviral properties (Bhagyashri et al., 2015). Phenolic compounds such as cyanidin 3-sambubioside (C3S) and 5-caffeoyl quinic acid (5-CQA) present in crimson fruit (*Viburnum dilatatum* Thunb.) can prevent long-term diabetes since orally administered freeze-dried crimson fruit juice to diabetic rats showed suppressed glucose levels (Iwai et al., 2006, Lin et al., 2016). Latex feeding is fatal to insects or causes reproduction complications (Bhagyashri et al., 2015). These effects form part of a plants defence mechanism, that will be discussed in the next section.

1.3 Plant defence mechanisms

Plants are continuously attacked by various phytopathogens and feeding herbivores hence, plants have developed different methods for protection. There are two types of defence responses: a direct response that involves physical attributes such as trichomes, leaf surface wax and thorns that deter predators and herbivores (Hanley et al., 2007) or an indirect response in which plants can attract natural enemies of the insects and herbivores (Aljbory and Chen, 2018). The production of latex also plays a role in plant defence, by releasing latex upon physical injury to the plant, this latex coagulates and forms a barrier at the injury site protecting the plant (Salomé Abarca et al., 2019). Plants have the ability to distinguish the type of damage encountered, whether it is being fed on by animals/insects or mechanical damage by strong winds and hail (Furstenberg-Hagg et al., 2013). The plants examine the type of tissue damage by quality and quantity for example, caterpillars follow a certain feeding pattern by eating similar amounts of leaf tissue. Plants can detect substances in oral secretions released by insects during feeding such as fatty acid-amino conjugates (FACs) and β-glucosidase (Furstenberg-Hagg et al., 2013), that trigger a defence response within the plant. Plants also secrete proteases and protease inhibitors as a form of protection against herbivorous insects (Hartl et al., 2011) and fungi (Bekalu et al., 2021). For example, as part of a plant's defence against fungi, it secretes proteases like P69 (subtilisin-like serine protease);

C14 (cysteine protease) and cysteine protease inhibitors or cystatins (Figure 1.8) (Jashni et al., 2015). These plant protease inhibitors are small proteins that play a role in a plant's defence mechanism by forming a stable complex with the target insect of fungus protease thus blocking the active site of the protease (De Leo et al., 2002). Natural plant protease inhibitors are mostly found in plant seeds and leaves (Srikanth and Chen, 2016).

There are 12 plant protease inhibitor families including serpins, phytocystatins, Kunitz-type protease inhibitors, Bowman-Birk inhibitors, bifunctional α-Amylase/trypsin inhibitors, potato-type inhibitors, metallocarboxypeptidase inhibitors, mustard-type trypsin inhibitors, α-hairpinin inhibitors, squash trypsin inhibitors and cyclic Momordica-type trypsin inhibitors and cyclic cysteine-rich peptides with only the Kunitz-type, Bowman-Birk and squash type inhibitors contributing to a plant defence mechanism against herbivores (Hellinger and Gruber, 2019). Kunitz-type protease inhibitors generally range from 18 to 24 kDa in size however, some smaller peptide inhibitors (~8 kDa) have been identified in plants as well as animals (Bendre et al., 2018). In plants these inhibitors regulate physiological homeostasis and inhibit pathogenic proteases (Hellinger and Gruber, 2019). An example of a Kunitz-type protease inhibitor is the serine protease inhibitor ECTI, isolated from the seeds of *Enterolobium contortisiliquum* (Vell.) Morong. also known as the Pacara earpod tree (Batista et al., 1996). A Bowman-Birk inhibitor such as the sunflower trypsin inhibitor-1 (SFTI-1) from the seeds of *Helianthus annuus* L.*,* consists of only 14 amino acids (1.54 kDa) and a single disulfide bond and due to its small size, is a suitable candidate for drug development trials (Hellinger and Gruber, 2019, de Veer et al., 2021). An example of a squash type inhibitor is the *Cucurbita maxima* Duchesne. trypsin inhibitor I (CMTI-I) from the seeds of the plant and is 29 amino acids long (3.19 kDa) (Kojima et al., 1996).

Insects also have their own form of defence strategy against secreted plant proteases by producing protease inhibitors in the midgut section of their digestive tract (Wolfson and Murdock, 1995). Proteases secreted by the plant interferes with the digestive process of insects thus deterring the insects from feeding on the plants. Insects produce protease inhibitors that prevent the degradation of toxic proteases from the plant and allows them to continue feeding on the plants (Lawrence and Koundal, 2002).

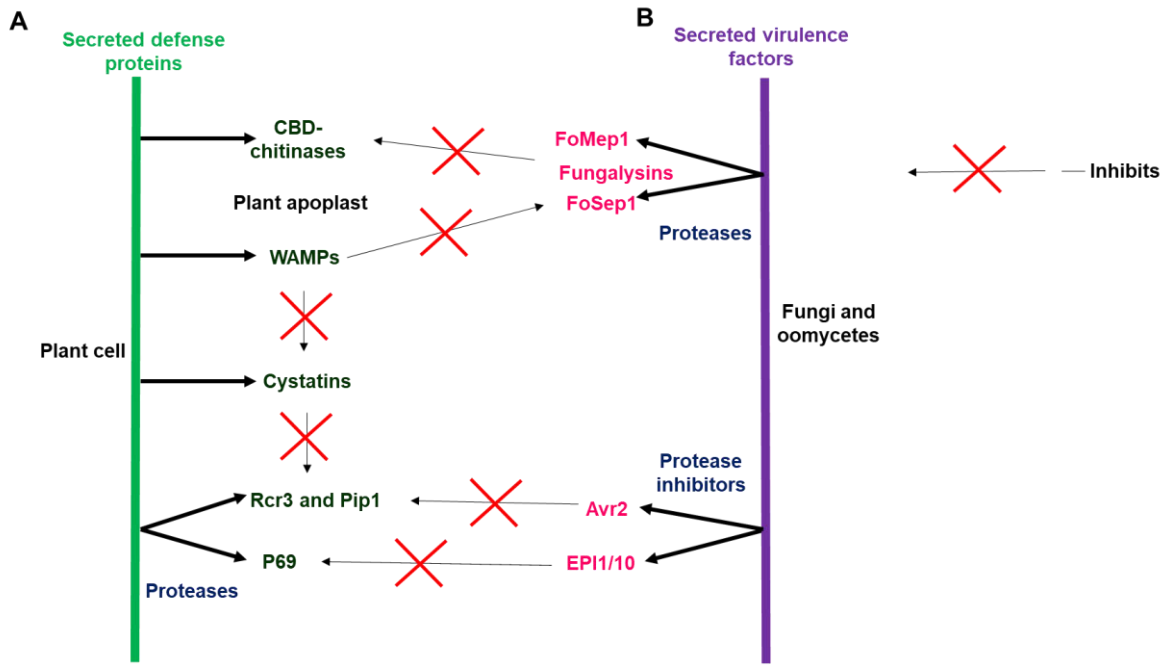

Figure 1.8: Interaction between plant proteases and fungi proteases/protease inhibitors. (A) Basal defence proteins secreted by plants and **(B)** secreted virulence factors by fungi and oomycetes. The plant secretes proteases and chitin-binding domain (CBD)-chitinases that attack pathogenic compounds. The pathogen secretes protease inhibitors that inhibit either serine or cysteine proteases. The pathogen also releases fungalysins that are either serine or metalloproteases that break down CBD-chitinases. Then the plants secrete wheat antimicrobial peptides (WAMPs) that inhibits the fungalysins. The WAMPs also inhibits cystatins that inhibit plant cysteine proteases (endogenous). The red cross shows an inhibitory effect. Figure obtained from Jashni et al. (2015).

1.4 Methods of isolation and characterisation of proteases from plant latex

Various methods are employed in the isolation, purification and characterisation of proteases from plant latex (Sequeiros et al., 2005, Tomar et al., 2008, Chanda et al., 2011, Liggieri et al., 2009, Putranto et al., 2016). The collection of latex involves making incisions on the stems or fruit, allowing the latex to flow into a test tube. The latex is either diluted in a buffer such as phosphate buffered saline (PBS) or distilled water and centrifuged or directly centrifuged to remove rubber particles to prevent coagulation. Isolation and purification methods can be a one-step method or a series of different methods. Protease isolation involves methods such as three phase partitioning (TPP), which uses *t*-butanol and ammonium sulfate to fraction out proteases from the plant tissue or a solvent precipitation method such as acetone fractionation to remove interfering compounds such as lipids, flavonoids and tannins (Wang et al., 2008). Different chromatography methods such cation-, anion-, affinity- and molecular exclusion chromatography could be used to further separate isolated proteases. The catalytic class (serine, cysteine, aspartic or metallo) that the isolated proteases belong to is done using catalytic class-specific protease inhibitors such as phenylmethylsulfonyl fluoride (PMSF) for

serine, L-trans-3-Carboxyoxiran-2-carbonyl-L-leucylagmatine (E-64) for cysteine, pepstatin for aspartic and Ethylenediaminetetraacetic acid (EDTA) for metalloproteases. Proteolytic activity can be monitored in two ways, one being a spectrophotometric or fluorometric enzyme assay and the other using zymogram gels. A zymogram gel is a gelatin-incorporated SDS-PAGE gel that shows a clear zone indicating proteolytic activity against a dark background after staining (Troeberg and Nagase, 2003). Reverse zymography is used to test for the presence of inhibitory activity, by incubating a gelatin-containing SDS-PAGE in buffer containing a protease such as papain. Inhibitory activity is present if a dark band is formed on the gel.

Various proteases have been isolated from different species belonging to many different families and have been redeemed useful in many applications, such as the food and pharmaceutical industries. Table 1.1 represents a list of some of the proteases isolated from plants, their function and methods of isolation.

Table 1.1: A summary of proteases and protease inhibitors isolated from the latex of Euphorbiaceae and Moraceae families.

Family	Species	Protease/protease inhibitor	Function/use	Isolation method
Euphorbiaceae	*Euphorbia tirucalli*	Euphorbains t1-t4[a] (serine proteases) Presence of cysteine protease[b]	-	Molecular exclusion chromatography and anion exchange chromatography[a]
	Euphorbia/Pedilanthus tithymaloides L.	Pedilanthin[c] (protease)	Anti-inflammatory	Ammonium sulfate precipitation and cation exchange chromatography
	Euphorbia nivulia	Antigenic glycosylated cysteine protease[d]	Medicine and agricultural industry	Acetone precipitation and anion exchange chromatography
	Euphorbia prunifolia	Prunifoline[e] (serine protease)	Food and biotechnological industry	Acetone precipitation and anion exchange chromatography
	Euphorbia cyparissias L.	Euphorbains y-1, -2 and -3[f] (serine proteases)	-	Molecular exclusion and anion exchange chromatography
	Euphorbia pulcherrima Willd. ex Klotzsch	Euphorbain P[g] (serine protease)	-	Anion exchange and molecular exclusion chromatography
	Euphorbia milii Des Moul.	Miliin[h] (serine protease)	Possible use in food industry	Cation exchange chromatography
	Euphorbia hirta L.	Hirtin[i] (serine protease)	Industrial and therapeutic applications	Anion exchange and molecular exclusion chromatography
	Euphorbia sapina	Cucumisin-like protease[j]	-	Anion exchange chromatography
	Euphorbia antiquorum L.	Thrombin-like protease[k]	Induces platelet aggregation and converts fibrinogen to fibrin	Heat treatment, ammonium sulfate precipitation and affinity chromatography
	Hevea brasiliensis	Hevain[l]	-	Molecular exclusion and anion exchange chromatography
	Hevea brasiliensis	Subtilisin protease inhibitor[m]	Possibly to restore lost latex from the tree	Ammonium sulfate precipitation, molecular exclusion and anion exchange chromatography

Table 1.1 (continued)

Moraceae	*Ficus sycomorus* L.	Thermostable peroxidase[n]	Peroxidase enzyme	Heat treatment, anion exchange and molecular exclusion chromatography
	Ficus benjamina	Cysteine protease[o]	Possible parasite control	Ammonium sulfate precipitation and cation exchange chromatography
	Ficus benghalensis L.	Benghalensin[p] (serine protease)	Structure function studies	Anion exchange chromatography
	Ficus microcarpa L. fil.	Microcarpain[q] (cysteine protease)	-	Acetone precipitation, molecular exclusion and anon exchange chromatography
	Ficus carica	FPIII[r] (serine protease)	Dairy industry	Anion and cation exchange chromatography and molecular exclusion chromatography

[a] (Lynn and Clevette-Radford, 1985) [b] (Mahajan et al., 2016), [c] (Bhowmick et al., 2008), [d] (Badgujar and Mahajan, 2013a), [e] (Mahajan and Adsul, 2015), [f] (Lynn and Clevette-Radford, 1984c), [g] (Lynn and Clevette-Radford, 1984a), [h] (Yadav et al., 2006b), [i] (Patel et al., 2012), [j] (Arima et al., 2000), [k] (Urs et al., 2021), [l] (Lynn and Clevette-Radford, 1984b), [m] (Archer, 1983), [n] (Saleh, 2011), [o] (Wanderley et al., 2018), [p] (Sharma et al., 2009), [q] (Mnif et al., 2014), [r] (Hamed et al., 2020)

1.5 Genus *Euphorbia*

The spurge family Euphorbiaceae is the most diverse group of flowering plants with at least 2000 species (Mavundza et al., 2022) of which some produce a toxic milky latex upon injury. These plants can grow as small shrubs or as big as 20-meter-tall trees. Many plants of this genus are used as traditional medicines to treat various ailments such as migraines and gonorrhea (Mavundza et al., 2022). There are 35 *Euphorbia* species that are used as traditional medicine in Southern Africa (Mavundza et al., 2022). In the present study the latex obtained from *Euphorbia tirucalli* L.*, Euphorbia. triangularis* Desf. ex A.Berger. plants and *C. papaya* leaves and fruit were analysed for the presence of proteases and protease inhibitors.

1.5.1 *Euphorbia tirucalli*

This succulent plant is commonly known as the pencil cactus, the milk bush plant or firestick plant (Binckley and Zahra, 2021). It originated in eastern tropical Africa and is now found in other parts of Africa and is used as an ornamental plant in tropical and subtropical regions. This plant can grow as small shrubs or 12-meter-tall trees and has small clusters of leaves at the branch ends with round green fruits (Figure 1.9). The milky latex from this plant is very toxic and can cause blindness, skin blisters and stomach irritation if swallowed (Binckley and Zahra, 2021).

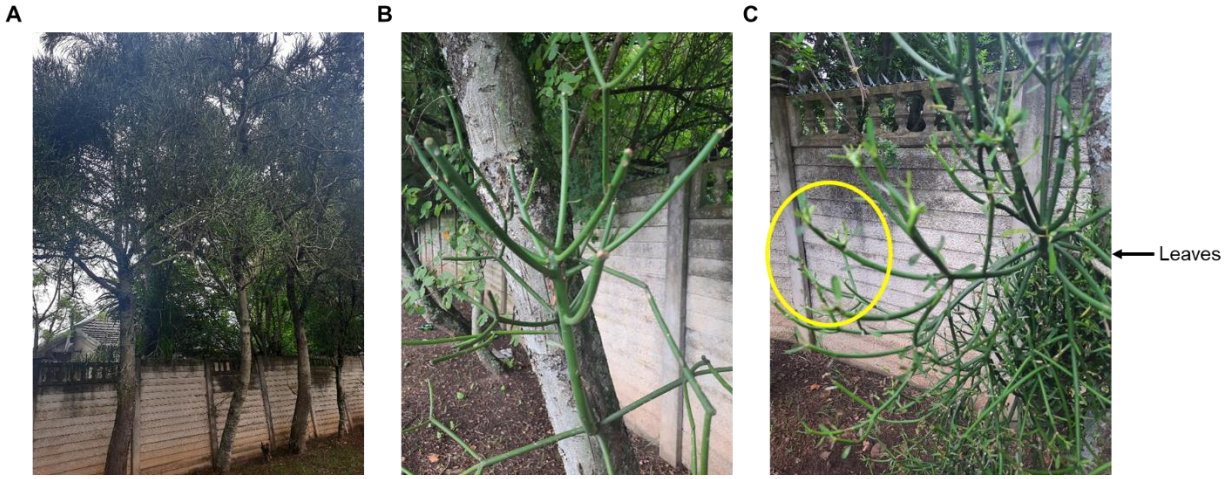

Figure 1.9: *Euphorbia tirucalli plant.* (A) Tall pencil tree plant, **(B)** Thin green branches, **(C)** Small green leaves that grow on the ends of the branches. The yellow circle highlights the small green leaves.

Different parts of the *E. tirucalli* plant are used for the treatment of snakebites with the leaves of the plant being the most used for bandaging the wound site from a snakebite (Dharmadasa et al., 2016). The latex of the plant is used to treat warts by direct application onto the skin (Njoroge and Bussmann, 2007), in a mixture *(in natura*) for treating toothaches or the branches used to brew tea for the treatment of cancer (Coelho-Ferreira, 2009). Four 74 kDa serine

proteases, named euphorbains t_1-t_4 were detected in the latex of *E. tirucalli* (Lynn and Clevette-Radford, 1985).

1.5.2 *Euphorbia triangularis*

This spiny, large succulent tree with three/five angled branches is commonly known as the river euphorbia or chandelier-tree (Ndlovu, 2018). This plant can be a small shrub or grow into an 18-meter-tall tree (Figure 1.10). It thrives on rocky hillsides, bushveld areas and coastal regions. This plant produces greenish yellow flowers that grow in clusters that develop into red globe-shaped fruits (Ndlovu, 2018).

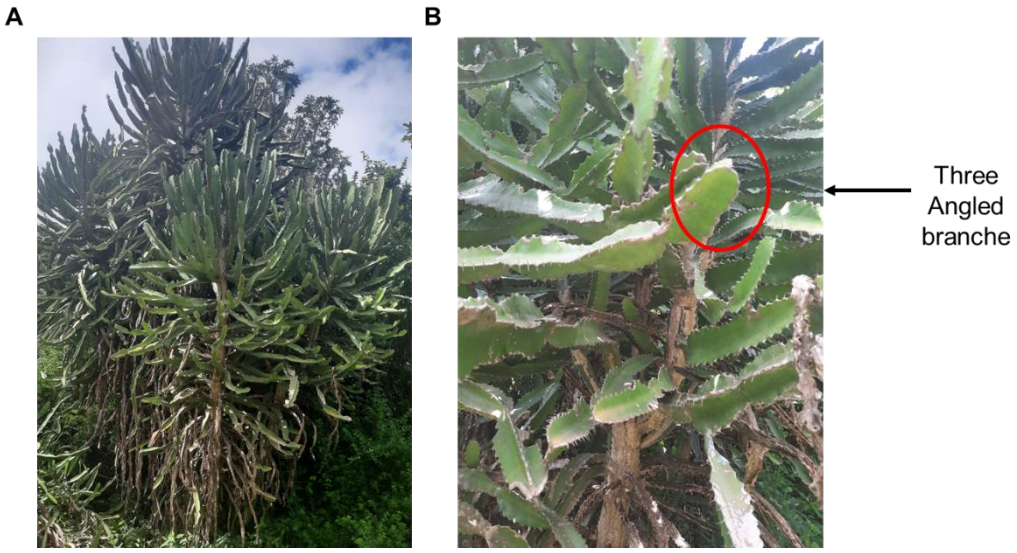

Figure 1.10: ***Euphorbia triangularis plant.*** **(A)** Large succulent tree, **(B)** Three angled branches, with small thorns on the ridges of the branches. The red circle highlights the three angled branches with thorns.

There are no reports of proteases and/or protease inhibitors isolated from *E. triangularis,* however mono- and diesters of 12-desoxy-phorbol were detected in the plant latex that where classified as tumor promoting compounds (Gschwendt and Hecker, 1969).

1.6 *Carica papaya* as a source for papain isolation

Papain is a cysteine protease present in the latex of unripe papaya (*C. papaya*) fruit. The proteases present in the papaya fruit include papain, chymopapain, glycyl endopeptidase and caricain, with papain the least abundant (Barrett et al., 1998).

In a previous study papain was isolated in a one-step method using TPP from the latex of papaya fruit (Hafid et al., 2020). The isolated papain showed milk clotting activity for cheese production and for possible use as a meat tenderising agent in the food industry. Papain has also been isolated by TPP from fresh and dried peels of papaya fruits, with the most proteolytic

activity present in the dried peels (Chaiwut et al., 2010). Papain is also used in food preservation by lowering bacterial growth (Shouket et al., 2020) and can be chemically modified using succinic anhydride for use in the production of detergents (Khaparde and Singhal, 2001).

1.7 Rationale

Proteases are used in many applications ranging from milk clotting agents in the food industry to dehairing skins in the leather-processing industry. Research has shown that plant proteases can be used as alternatives to harmful chemicals and used as therapeutic agents. In the past, various plants have been used for medical treatment of different ailments. These treatments were not scientifically verified, but have been beneficial where medical treatment was not readily accessible. Plant proteases from the latex of the Euphorbiaceae family can be used as milk clotting agents and other applications in the biotechnology industry such as beer brewing and the leather and detergent industry. In previous studies (Table 1.1), serine proteases have been identified in the latex of *Euphorbia tirucalli* which is also reported to contain cysteine proteases. However, there are no reports on the purification and characterisation of *E. tirucalli* cysteine proteases and information on the enzymatic characterisation of the serine proteases is incomplete. To the author's knowledge there are no reports on proteases isolated and characterised from *Euphorbia triangularis* which is indigenous to South Africa. Several of the reported isolation methods are also quite cumbersome or not very efficient and consequently, three phase partitioning was explored as a possible protein isolation method early in the purification procedures. Since gelatin-containing zymograms offer a useful technique to illustrate proteolytic activity, a suitable positive control preparation is required. The 23.4 kDa plant cysteine protease, papain, is commercially available for this purpose, but is observed at a size greater than 97.4 kDa on gelatin-containing zymograms. Hence papain was isolated from the latex of *C. papaya* by two methods to determine if a freshly prepared sample would contain gelatinolytic activity at the expected size of 23.4 kDa on a gelatin-containing zymogram.

1.8 Aims and objectives

AIM 1

To isolate and characterise proteases present in the latex of *E. tirucalli*

Objectives of Aim 1

1. To identify proteolytic activity in latex preparations of *E. tirucalli* with gelatin-containing SDS-PAGE (zymography)

2. To optimise the conditions for isolating proteases from the latex of *E. tirucalli* using three phase partitioning (TPP)
3. To analyse *E. tirucalli* proteins isolated by TPP using reducing and non-reducing SDS-PAGE and gelatin-containing zymograms
4. To study the effect of pH on the proteolytic activity of the proteases isolated from *E. tirucalli* latex in gelatin-containing zymograms
5. To determine the effect of catalytic class-specific inhibitors on the proteolytic activity of the proteases isolated from *E. tirucalli* latex in gelatin-containing zymograms
6. To explore molecular exclusion chromatography as a means to separate *E. tirucalli* latex proteases
7. To compare the activity of the separated *E. tirucalli* latex proteases against a synthetic fluorogenic peptide substrate, Z-Phe-Arg-AMC to the activity of trypsin and papain
8.
9. To determine the milk-clotting ability of *E. tirucalli* latex

AIM 2

To isolate and characterise proteases present in the latex of *E. triangularis*

Objectives of Aim 2

1. To identify proteolytic activity in latex preparations of *E. triangularis* with gelatin-containing SDS-PAGE (zymography)
2. To optimise the conditions for isolating proteases from the latex of *E. triangularis* using three phase partitioning (TPP)
3. To explore using acetone fractionation for the isolation of proteases from the latex of *E. triangularis*
3. To analyse *E. triangularis* proteins isolated by TPP and acetone fractionation using reducing and non-reducing SDS-PAGE and gelatin-containing zymograms
4. To determine the effect of catalytic class-specific inhibitors on the proteolytic activity of the proteases isolated from *E. triangularis* latex in gelatin-containing zymograms
5. To separate the identified three active *E. triangularis* serine proteases by *p*-aminobenzamidine affinity chromatography
6. To compare the activity of the separated *E. triangularis* latex proteases against a synthetic fluorogenic peptide substrate, Z-Phe-Arg-AMC to the activity of trypsin
7.
8. To study the effect of pH on the proteolytic activity of the proteases isolated from *E. triangularis* latex in gelatin-containing zymograms

9. To test for the presence of protease inhibitors in the TPP isolated fraction of *E. triangularis* by reverse zymography
10. To determine the milk-clotting ability of *E. triangularis* latex

AIM 3

To isolate papain from the latex of *C. papaya* for use as a control protease in gelatin-containing zymograms

Objectives for Aim 3

1. To explore using a combination of pre-precipitation with 60% ammonium sulfate and TTP for the isolation of papain from the latex of green *C. papaya* fruit
2. To analyse the ammonim sulfate-TPP purification of papain using SDS-PAGE, gelatin-containing zymography and activity against Z-Phe-Arg-AMC
3. To investigate the recognition of isolated *C. papaya* and *E. tirucalli* proteases by anti-cysteine protease (papain) and anti-serine protease antibodies in dot blots
4. To explore using CM-cellulose cation exchange chromatography to purify papain from *C. papaya* latex
5. To analyse the CM-cellulose cation exchange chromatography purification of papain using SDS-PAGE, gelatin-containing zymography and a western blot with rabbit anti-papain antibodies
6. To compare the effect of E-64 on the hydrolysis of azocasein by commercial papain and the papain fraction isolated by CM-cellulose cation exchange chromatography
7. To determine the milk-clotting ability of *C. papaya* latex

Chapter 2

Materials and Methods

2.1 Materials

All general reagents were obtained from Sigma (St. Louis, MO, USA) and Merck (Darmstadt, Germany) and were of the highest purity available. The sources of specialised reagents and equipment are detailed in the respective sections that follow.

2.1.1 Methods

2.2.1 Latex collection from *Euphorbia tirucalli and Euphorbia triangularis*

Euphorbia tirucalli can either be a small shrub or a tree that can grow from 4 to 12 m tall. It has thin pencil-like green branches with leaves only forming at the branch tips (Mwine et al., 2013). Latex was obtained from incisions made on the stem of *Euphorbia tirucalli* growing in Pietermaritzburg, KwaZulu-Natal, South Africa. A voucher specimen (NU0087104) has been deposited at the Bews Herbarium (University of KwaZulu-Natal, Pietermaritzburg campus, South Africa). *Euphorbia triangularis* is a spiked, succulent tree that can grow up to 18 m tall. It has three-angled branches with small spikes along the edges (Ndlovu, 2018). Latex was obtained from incisions on the *Euphorbia triangularis* stem and branches growing in the Botanical gardens, University of KwaZulu-Natal, Pietermaritzburg, KwaZulu-Natal, South Africa. A voucher specimen (NU0090999) has been deposited at the Bews Herbarium (University of KwaZulu-Natal, Pietermaritzburg campus, South Africa). In each case, the latex was immediately processed by the addition of phosphate buffered saline (PBS) (137 mM NaCl, 2.68 mM KCl, 6.46 mM Na_2HPO_4, pH 7.2) to an equal volume of the latex and centrifuged (6000 x *g*, 15 min, 4°C). The supernatant was stored at -20°C until further use.

2.2.2 Protein fractionation using three phase partitioning (TPP)

Three phase partitioning (Dennison and Lovrien, 1997, Eyssen et al., 2021) was used to fractionate active proteases present in the processed latex. This simple and efficient method, involves the addition of ammonium sulfate and *t*-butanol to separate proteins from the *t*-butanol and aqueous phases into the interfacial phase (middle layer) that is then concentrated by centrifugation. Tertiary butanol is totally miscible in water and by the addition of ammonium sulfate, the aqueous and *t*-butanol phases are formed (Dennison and Lovrien, 1997). The proteins present in the aqueous phase separate into the middle (interfacial) layer depending on the amount of ammonium sulfate added. Three phase partitioning separates low molecular weight pigments and lipids into the upper organic phase and proteins and carbohydrates into the lower *t*-butanol phase (Gagaoua and Hafid, 2016, Eyssen et al., 2021) and can be a one-step method into purifying and separating meat tenderising and milk clotting enzymes

(Gagaoua and Hafid, 2016). An advantage of using TPP for plant proteases is the separation of contaminants such as pigments of low molecular weight into the upper organic phase and carbohydrates and proteins into the lower aqueous phase (Gagaoua and Hafid, 2016, Eyssen et al., 2021). Three phase partitioning has the advantage of concentrating and stabilising proteins while also enhancing proteolytic activity (Gagaoua and Hafid, 2016).

To latex supernatant (8 mL of *E. tirucalli* or 4 mL of *E. triangularis*), 30 % (v/v) *t*-butanol was added and mixed in before 10 % (w/v) ammonium sulfate was added and dissolved under magnetic stirring. The protein pellet that formed at the interface between the upper *t*-butanol and lower aqueous phases during centrifugation (6000 x *g*, 15 min, 4°C) was collected and re-dissolved in 400 µL PBS. The remaining *t*-butanol and aqueous phases were mixed and the ammonium sulfate concentration increased by 10 % (w/v) in successive steps to reach 20, 30 and 40 % (w/v) respectively. After the addition of ammonium sulfate for each step, the protein pellet formed at the interface between the upper *t*-butanol and lower aqueous phases during centrifugation (6000 x *g*, 15 min, 4°C) was collected and re-dissolved in 400 µL PBS.

2.2.3 Protease fractionation by acetone precipitation

Plants contain different compounds such as phenolics (flavonoids and tannins) and lipids (Wang et al., 2008) that can interfere with the isolation and purification of proteins. As a consequence, acetone fractionation was compared to TPP to possibly remove any interfering compounds and/or separate active proteases. Proteins are insoluble in acetone at very low temperatures which allows for protein precipitation (Crowell et al., 2013) as well as the concentration of proteins (Simpson and Beynon, 2010). This method was adapted from Sequeiros et al. (2005) with the modifications detailed below. At -21°C, 1 mL of cold acetone was added to 2 mL *E. triangularis* latex and allowed to settle at -21°C for 1 h. Following centrifugation (8000 x *g*, 30 min, -21°C) the pellet was discarded and 1.5 mL of the supernatant was collected. Cold acetone (stored o/n at -20C) equivalent to three times the volume of the supernatant was added before centrifugation (8000 x *g*, 30 min, -21°C). The supernatant was discarded and the pellet re-dissolved in 2 mL PBS.

2.2.4 *Euphorbia tirucalli* protease separation by molecular exclusion chromatography

Molecular exclusion chromatography (MEC) is used to separate proteins based on size by using two phases: a mobile phase (eluting buffer) and a stationary phase (resin). Different resins are used for MEC such as Sephadex (ranging from G-10 to G-75) for buffer exchange and desalting of proteins. The Sephadex resin is made by crosslinking dextran with epichlorohydrin. The G-10 resin has the smallest exclusion limit of >0.7 kDa, while G-75 has the largest exclusion limit of >80 kDa. Sephadex G-50 has an exclusion limit of >30 kDa. The

resins are available in different sizes such as fine and superfine which has the smallest bead size that allows for higher separation efficiency, while the coarse and medium sizes are used for large scale separations where low operating pressures and high flow rates are required. Sephacryl S-200 resin is often used for protein separation because the hydrophilicity additionally lowers non-specific adsorption and increases the recovery rate of proteins. A Sephacryl S-200 resin can be used to separate proteins over a broad range of 5 kDa to 250 kDa with high resolution. The column was calibrated using Bio-Rad's gel filtration standard (CN #1511901) which contained a mixture of molecular weight marker proteins: -thyroglobulin (670 kDa), gamma-globulin (158 kDa), ovalbumin (44 kDa), myoglobulin (17 kDa) and vitamin B12 (0.00135 kDa) (Figure 2.1) for which myoglobulin and vitamin B12 contained visible coloured markers. The purpose of the calibration curve was to estimate the size of a protein that elutes at a certain volume from the column. This Sephacryl S-200 column was used to separate the proteases present in the 40% TPP fraction. A Sephacryl S-200 column (120 mL bed volume) was equilibrated with one column volume of MEC buffer (50 mM Tris-HCl buffer pH 8 containing 300 mM NaCl). The 40% TPP pellet was dissolved in a volume of the MEC buffer equivalent to between 2 to 5% of the column volume, clarified by filtration and loaded onto the column. Separation was carried out using the AKTAprime plus (GE Healthcare Bio-Sciences AB, Sweden) liquid protein chromatography system. Once the sample was loaded, 180 mL of MEC buffer was loaded and 1 mL samples were collected at 1 mL/min at 0.2 MPa. All buffers were degassed and filtered before use on the AKTAprime plus.

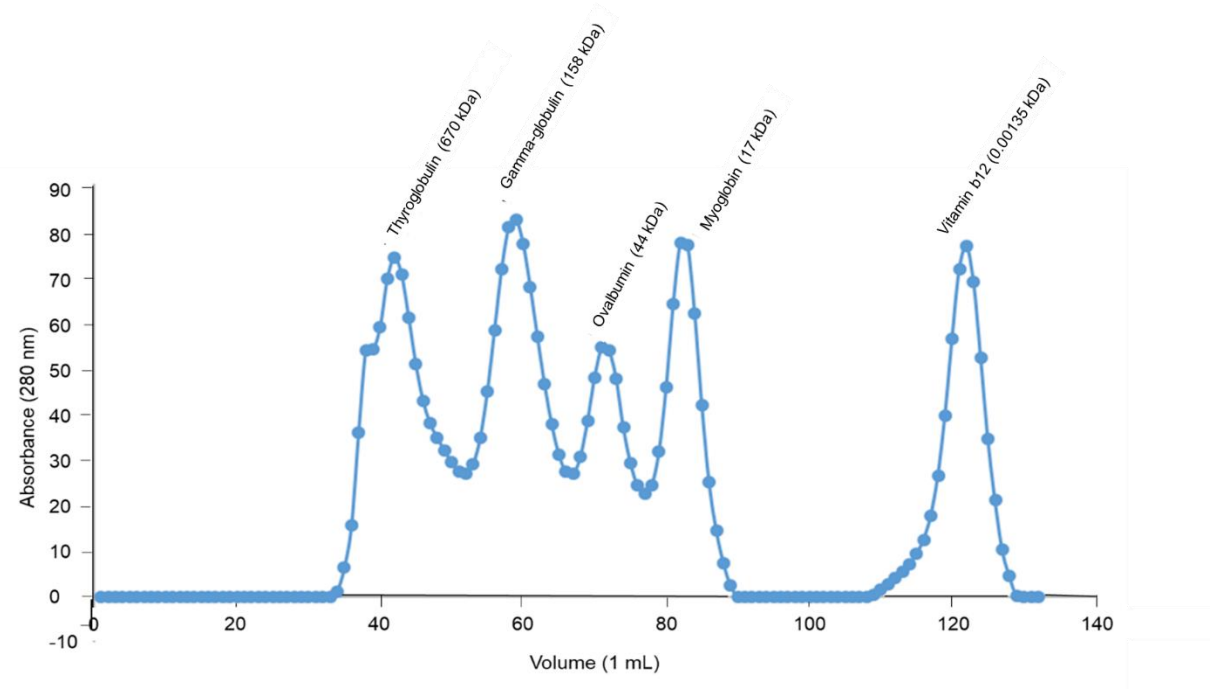

Figure 2.1: Sephacryl S-200 calibration curve obtained using the Bio-Rad's gel filtration standard. The standard contained a mixture of molecular weight marker proteins: - thyroglobulin (670 kDa), gamma-globulin (158 kDa), ovalbumin (44 kDa), myoglobulin (17 kDa) and vitamin B12 (0.00135 kDa). Myoglobulin and vitamin B12 contained coloured visible markers. Samples were collected at a rate of 1 mL/min and the absorbance at 280 nm was measured.

2.2.5 *p*-aminobenzamidine affinity chromatography for serine protease purification from 40% TPP fraction of *Euphorbia triangularis* latex

Affinity chromatography is used to separate proteins based on the reversible interactions between the protein and the ligand bound to the column matrix (Magdeldin and Moser, 2012). The serine protease-specific inhibitor, *p*-aminobenzamidine was chosen as an affinity ligand for the purification of the serine proteases identified in the latex of *E. triangularis* latex. This affinity matrix is routinely used for the purification of trypsin and trypsin-like serine proteases (Evans et al., 1982, Monroe et al., 1988). A 1 mL *p*-aminobenzamidine column (Sigma, CN GE17-5143-02) was used on the AKTAprime plus to isolate the proteases present in the 40% TPP fraction from *E. triangularis*. The column was equilibrated with 5 mL of binding buffer (0.05 M Tris-HCl, 0.5 M NaCl, pH 7.4). Once the sample was loaded onto the column, it was washed with 5 to 10 mL of binding buffer or until no protein was present in the eluent. Protein was eluted with 5 to 10 mL of eluting buffer (0.05 M glycine-HCl, pH 3) and 1 mL samples were collected. To the collection tubes, 200 µL of 1 M Tris-HCl, pH 9; was added to neutralise the pH and prevent denaturation of proteins at low pH. All buffers were degassed and filtered before use on the AKTAprime plus chromatography system.

2.2.6 Protein determination

Protein determination was carried out using the Bicinchoninic acid (BCA) assay for low concentrations of protein (Smith et al., 1985) and the Bradford assay for higher concentrations of protein (Bradford, 1976). The BCA assay is a copper-based colorimetric assay that quantifies small amounts of protein. Under alkaline conditions, the BCA assay relies on the formation of a Cu^{2+}-protein complex, followed by reduction of Cu^{2+} to Cu^{1+} (Smith et al., 1985). The higher the amount of protein present in solution, the higher the amount of Cu^{2+} reduced. The change in colour from green to purple at 562 nm is due to the chelation of two molecules of BCA to one Cu^{+} ion (Otieno et al., 2016). The number of peptide bonds as well as the presence of the side chains of cysteine, tryptophan and tyrosine increase the amount of bicinchoninic- Cu^{+} complexes formed (Wiechelman et al., 1988). Protein determination was performed using the BCA protein assay kit (ThermoFisher scientific, CN 23227). Bovine serum albumin (BSA) 0.025 mg/ml - 2 mg/mL was used as a protein standard. A standard curve was generated for the microplate procedure by assaying (in triplicate) 25, 125, 250, 500, 750, 1000, 1500 and 2000 µg/mL BSA (Figure 2.2A). To 50 mL of solution A, 1 mL of solution B was added to make the working reagent. To, working reagent (1 mL) was added to each 50 µL sample and samples were incubated at 37°C for 30 min before 200 µL of sample was loaded into a microplate (ThermoFisher scientific 96–Well Plates, CN 15041) and the absorbance read at 562 nm.

The Bradford assay is a dye binding assay that depends on the differential colour change of Coomassie brilliant blue G-250 in response to different concentrations of protein (Becker et al., 1996). When protein binding occurs, the maximum absorbance of an acidic solution for Coomassie brilliant blue G-250 shifts from 465 to 595 nm. Since the dye-albumin complex solutions extinction coefficient is constant over a 10-fold concentration range, then Beer's law can be applied (Becker et al., 1996). Beer's law is applied for an accurate measurement of protein concentration by the selection of a suitable ratio of dye volume to sample concentration. Ovalbumin was used for this assay as it is a generally used calibration protein for the Bradford assay (Pike, 1990). The Bradford standard curve (Figure 2.2B), was produced by measuring the absorbance of ovalbumin standards (1 mg/mL) in 20 µg intervals ranging from 0-100 µg (in triplicate). To 100 µL of standard protein, 900 µL of Bradford reagent [Coomassie brilliant blue G-250 (0.3 g), 2% (v/v) perchloric acid] was added and the absorbance measured at 595 nm.

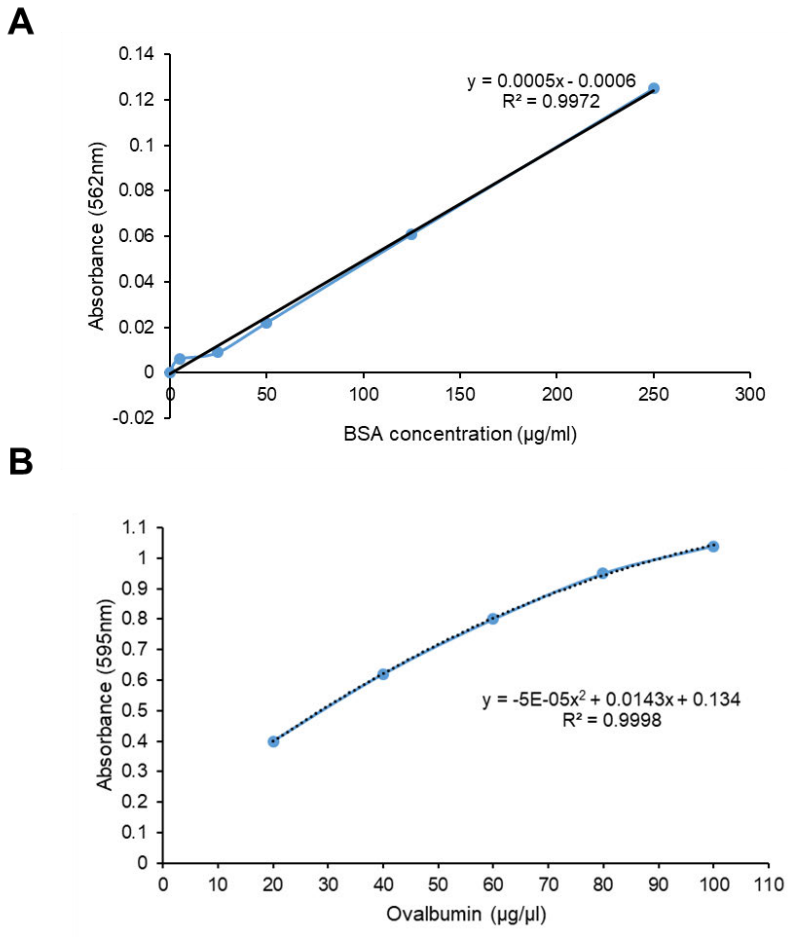

Figure 2.2: Standard curves obtained using the BCA™ assay protein kit and the Bradford protein assay. (A) Bovine serum albumin standards (5 to 250 µg/mL) were added to the BCA reagent and the resulting absorbance values measured at 595 nm after incubation at 37°C for 30 min. The equation of the trendline is y = 0.0005x - 0.0006 (correlation coefficient of 0.9972). **(B)** Ovalbumin solutions (0-100 µg) were added to the Bradford dye and the absorbance at 595 nm was measured. The equation of the trendline is y = -5E-05x^2 + 0.0143x + 0.134 (correlation coefficient of 0.9998). Each data point represents the mean absorbance (n=3).

2.2.7 Azocasein assay

Azocasein was found to be a suitable substrate to measure the activity of proteolytic enzymes (Langner et al., 1973). Azocasein is a chromogenic derivative of casein where the histidine and tyrosine residues in casein are derivatised by diazotised sulfanilic acid or sulfanilimide in an alkaline medium. The protease degrades azocasein, which releases peptides that are soluble in trichloroacetic acid (TCA), while the non-hydrolsed substrate is precipitated. The soluble peptides are yellow in colour due to the azo-groups and their absorbance can be measured at 366 nm (Langner et al., 1973, Charney and Tomarelli, 1947).

The azocasein assay (Barrett and Kirschke, 1981) was performed using papain as a standard protease for calibration. To 50 mL of 6% (w/v) azocasein [6% (w/v), Sigma, CN A2765], 54 g of Urea (Merck, CN SAAR6375040EM) was added and the solution stirred with heat until the

urea was dissolved. The azocasein/urea solution was made up to 150 mL with cysteine assay buffer [100 mM Na-acetate, 1 mM EDTA, 0.02% (w/v) NaN_3, pH 5]. Azocasein was incubated with 2 mg/mL papain (Roth, CN 8933.1) for several days at room temperature. A sample (200 µL) of the resulting mixture was precipitated in 5% (w/v) TCA (1 mL) and this was treated as the 100% hydrolysate. This mixture was diluted in 5% (w/v) TCA, that gave further points on the calibration curve (Figure 2.3) of absorbance (366 nm) against % hydrolysate.

The plant protease sample (200 µL) was mixed with 200 µL of cysteine assay buffer and incubated at 37 °C for 5 min. After incubation, 400 µL of azocasein/urea was added. A sample (200 µL) was immediately taken out and 1 mL of 5% (w/v) TCA was added. This sample served as the blank for the reaction. After 2 h, a further 200 µL was taken out and 1 mL 5% TCA (w/v) was added. The sample was centrifuged at (12 000 x *g*, 5 min, RT). The absorbance was measured at 366 nm in glass cuvettes, with blacked out sides that prevents transmission of light around the sample.

The equation used to calculate % hydrolysate was as follows:

$$\%\ Hydrolysis\ (\%\ H) = \frac{A366 - 0.0223}{0.0436}$$

The units of activity were defined as 1 unit = 1 µg of azocasein digested in 1 min (Schwartz and Barrett, 1980). The following equation was used:

$$Units = \frac{(\%\ H\ x\ 10^{-2})\ x\ 2000\ \mu g\ azocasein}{time}$$

Units/mL = 5 x units

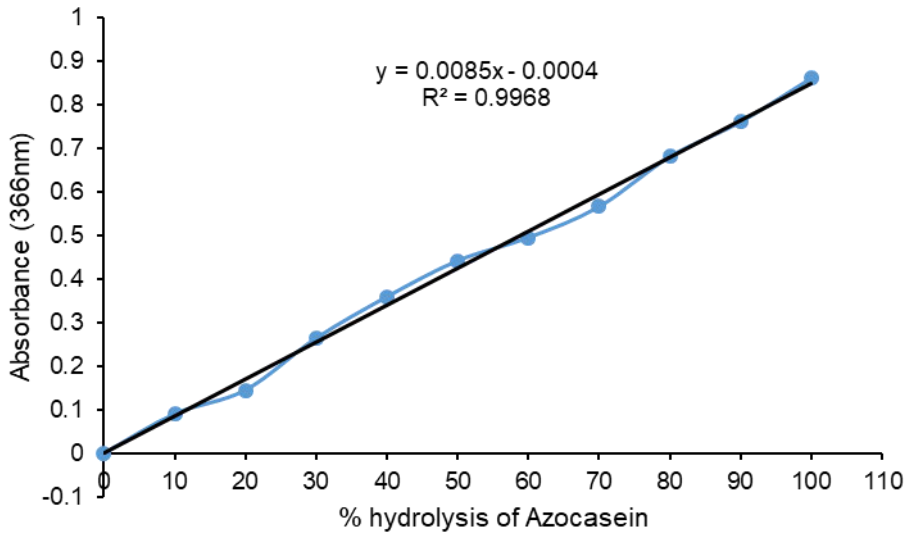

Figure 2.3: Calibration curve of azocasein digested by 2 mg/mL papain. Azocasein was digested by papain for several days and the calibration curve was created by measuring dilutions of the 100% hydrolysate at 366 nm. The equation of the trendline is given by y = 0.0085x – 0.0004 (correlation coefficient of 0.9968). The units of activity were expressed as units/mL.

2.2.8 Analysis of samples by reducing and non-reducing SDS-PAGE

Protein analysis was carried out using sodium dodecyl sulfate polyacrylamide gel electrophoresis (SDS-PAGE) according to the principles of Laemmli (1970) that separates proteins based on their molecular weight in an electric field. The anionic detergent, SDS, binds to proteins in a ratio of 1.4 g of SDS to 1 g of protein, thereby giving them a uniform negative charge (Reynolds and Tanford, 1970, Al-Tubuly, 2000). Proteins will therefore have a similar charge to mass ratio and the rate at which an SDS-bound protein migrates in a gel will depend on its size hence, determining its molecular weight. When an electric field is applied, the glycine in the running or tank buffer enters the low pH of 6.8 in the stacking gel buffer. As a result, the glycine anions (trailing ions) become weakly ionised and have a low mobility. The chloride ions (leading ions) become completely ionised hence having a high mobility. The glycine anions and the chloride ions in the buffer create a gradient that concentrates the proteins at the interface between the running and stacking gels. As a consequence, all the proteins in samples are lined up together and the proteins that are closer to the gel enter the separating gel first. The chloride ions in the stacking gel move faster than the SDS-bound proteins and creates an ion front. The glycine ions move from the running buffer and creates a front behind the proteins. The proteins are sandwiched between the chloride and glycine ions when a voltage gradient is formed. Furthermore, at the interface between the stacking and running gels, the percentage of acrylamide is increased and the pore size of the running gel decreases. The decrease in the pore size of the running gel separates the proteins based on molecular weight as the charge to mass ratio for all proteins in each sample are equal.

Under reducing conditions, 2-mercaptoethanol disrupts the intra- and intermolecular disulfide bonds which unfolds the proteins allowing them to remain in a reduced state. SDS binds better to proteins ensuring the negatively charged polypeptide chains migrate based on size. SDS is used for protein solubility as it disrupts the hydrophobic interactions within the protein (Luche et al., 2003).

The BioRad Mini PROTEAN Tetra vertical slab electrophoresis gel system was assembled according to the manufacturer's instructions. The protein samples were prepared by adding an equal volume of reducing treatment buffer [125 mM Tris-HCl, 4% (w/v) SDS, 20% (v/v) glycerol, 10% (v/v) 2-mercaptoethanol, pH 6.8] and boiled at 100°C for 5 min or half the volume of non-reducing buffer [125 mM Tris-HCl, 4% (w/v) SDS, 20% (v/v) glycerol, pH 6.8]. To the samples 1 % (w/v) bromophenol was added. Electrophoresis was carried out using a 4% stacking gel and a 12.5% separating gel in a running buffer [250 mM Tris-HCl, 192 mM glycine, 0.1% (w/v) SDS, pH 8.3] at 80V for approximately 2 h. The calibration curve (Figure 2.4) was produced by plotting the log molecular weight of each protein contained in the molecular weight marker against relative mobility (the distance travelled by each protein divided by the distance travelled by the dye front). The molecular weight marker used consisted of phosphorylase B (97.4 kDa), BSA (68 kDa), ovalbumin (45 kDa), carbonic anhydrase (30 kDa), soybean trypsin inhibitor (SBTI) (20.1 kDa) and lysozyme (14.4 kDa). After electrophoresis, proteins were visualised by staining with Coomassie blue R-250 [0.125% (w/v) Coomassie blue R-250, 50% (w/v) methanol, 10% (w/v) acetic acid]. In order to detect smaller amounts of proteins, a silver staining method was used (section 2.2.11). The gel images were captured using a GENE Sys version 1.2.4.0 gel documentation system, G: BOX chemi XR5 system (Syngene, Cambridge, UK).

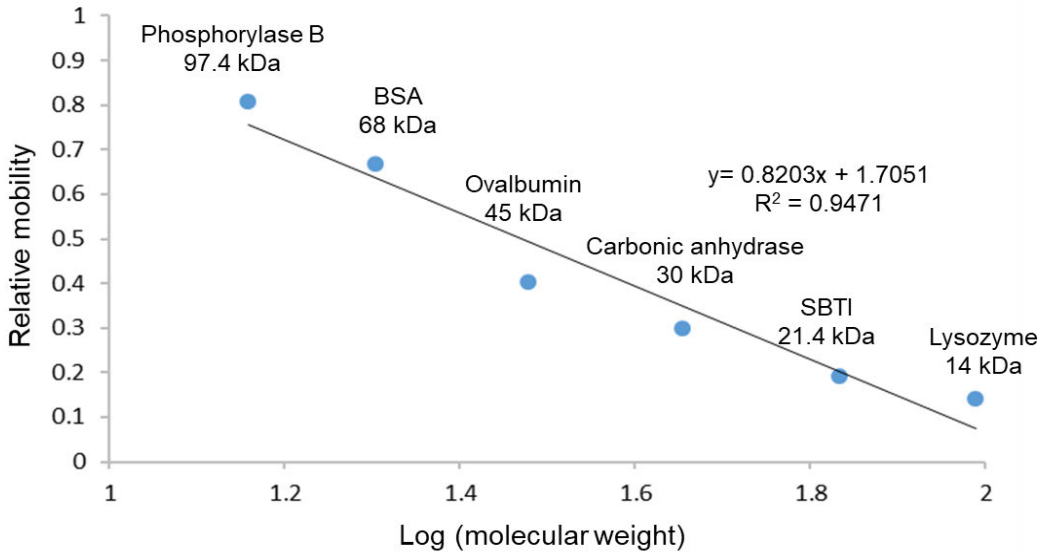

Figure 2.4: Standard curve for protein molecular weight determination by SDS-PAGE. The molecular weight marker used for SDS-PAGE consisted of phosphorylase B (97.4 kDa), bovine serum albumin (BSA, 68 kDa), ovalbumin (45 kDa), carbonic anhydrase (30 kDa), soybean trypsin inhibitor (SBTI, 21.5 kDa) and lysozyme (14 kDa). The equation of the trendline is given by y= -0.8203x + 1.7051, with a correlation coefficient of 0.9471.

2.2.9 Tris-tricine SDS-PAGE analysis

Proteins were analysed using a discontinuous Tris-tricine SDS-PAGE system as per Schägger and Von Jagow (1987). Tris-tricine SDS-PAGE is used to separate proteins of low molecular weight, i.e. smaller than 30 kDa (Schägger, 2006). Separation is performed by using an anode (composed of Tris-HCl, tricine and SDS) and a cathode (Tris-HCl) buffer, where the glycine used in the Laemmli tank buffer is replaced with tricine. Tricine acts as a trailing ion that allows for better stacking and destacking of small proteins, leading to better resolution.

The BioRad Mini PROTEAN Tetra vertical slab electrophoresis gel system was assembled according to the manufacturer's instructions. The protein samples were prepared by adding an equal volume of reducing treatment buffer [125 mM Tris-HCl, 4% (w/v) SDS, 20% (v/v) glycerol, 10% 2-mercaptoethanol, pH 6.8] and boiled at 100°C for 5 min. To the samples 1 % (w/v) bromophenol blue was added. Electrophoresis was done using a 10% separating gel and 4% stacking gel in a Tris-tricine buffer system [200 mM Tris-HCl, pH 8.9] as the anode buffer and [100 mM Tris-HCl, 100 mM Tricine, 0.1%(w/v) SDS, pH 8.25] as a cathode buffer, and run at 80V until the proteins reached the separating gel, thereafter ran at 100V for approximately 1.5 h. Commercial Pierce™ Unstained Protein molecular weight marker (Thermo Scientific™, CN 26610) was used to determine protein size. The calibration curve (Figure 2.5) was produced by plotting the log molecular weight of each protein contained in the molecular weight marker against relative mobility (the distance travelled by each band

divided by the distance travelled by the dye front). After electrophoresis, gels were silver stained (section 2.2.11). The gel images were captured using a GENE Sys version 1.2.4.0 gel documentation system, G: BOX chemi XR5 system (Syngene, Cambridge, UK).

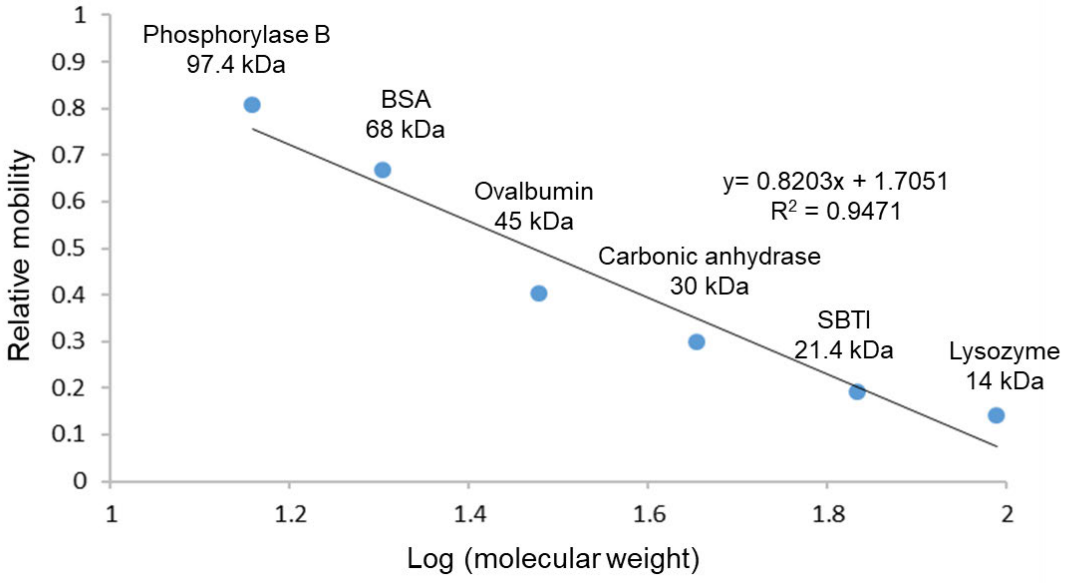

Figure 2.5: Standard curve for protein molecular weight determination by Tris-tricine SDS-PAGE. The Pierce™ Unstained Protein molecular weight marker was used for calibration. The equation of the trendline is given by y = -1.3358x + 2.095, with a correlation coefficient of 0.9588.

2.2.10 Proteolytic activity analysis by gelatin-containing SDS-PAGE

Zymography is a method used to determine proteolytic activity and involves the incorporation of gelatin as a general protein substrate into the SDS-PAGE running/separating gel (Heussen and Dowdle, 1980). Gelatin-containing SDS-PAGE is conducted under non-reducing conditions with SDS as the denaturing agent. Denaturation by SDS inactivates the proteases during electrophoresis, after which the proteases are renatured and proteolytic activity restored by incubation in Triton X-100 that replaces the SDS (Jones, 2014). Following incubation in a suitable buffer containing an activator (cysteine in the case of cysteine proteases) and staining, proteolytic activity is observed as clear zones on the gel. Gelatin, [1 % (w/v)] was added to the running gel buffer before the gels were cast. After electrophoresis at 80V, the gels were washed with 2.5% (v/v) Triton X-100 to replace the SDS for 2 x 30 min. The gels were rinsed twice with distilled water and incubated in 100 mM Na-acetate buffer, pH 5 containing 100 mM Na_2EDTA, 0.02% (w/v) NaN_3 and 40 mM cysteine-HCl at 37°C for 16 h. The gels were rinsed in distilled water and stained with 0.1% (w/v) amido black (methanol:acetic acid:dist. H_2O in a ratio of 30:10:60) for 1 h and destained in destaining solution (methanol:acetic acid:dist. H_2O in a ratio of 30:10:60) until clear zones of proteolytic

digestion of the gelatin were observed. Zymogram gels were analysed by the DNr Bio-imaging MiniBIS Pro from Lasec (Jerusalem, Israel).

2.2.11 Visualisation of proteins on SDS-PAGE gels by silver staining

Silver staining is a sensitive method used to detect small amounts of proteins in the nanogram range by depositing metallic silver onto the surface of the gel. Silver ions from the silver nitrate reagent bind to carboxyl, amine, sulfhydryl and imidazole groups of proteins. These silver ions are reduced by formaldehyde into metallic silver resulting in a brown-black colour. Thiosulfate is added as a reducing agent that sensitises the proteins before metallic silver is deposited and prevents non-specific background staining (Blum et al., 1987, Gharib et al., 2009). The method of Nesterenko et al. (1994) was used for silver staining as it provides quick staining in 30 min. All steps were carried out in scrupulously clean glassware on an orbital shaker at room temperature. The following reagents were made: 50% (v/v) acetone in dist. H_2O, 50% (w/v) trichloroacetic acid (TCA) in dist. H_2O, 20% (w/v) $AgNO_3$ in dist. H_2O and 10% (w/v) $Na_2S_2O_3.5H_2O$ in dist. H_2O. The working solutions were all freshly made to a volume of 60 mL before use. After electrophoresis (Section 2.2.8), the gel was incubated for 5 min in fixing solution [60 mL 6.77 M acetone stock, 1.5 mL 3.06 M TCA stock, 25 µL 37% (v/v) 12.7 M formaldehyde (HCHO] and rinsed in dist. H_2O (3 x 5 s). The gel was subsequently incubated in acetone stock for 5 min, rinsed in dist. H_2O (3 x 5 s) and incubated in pre-treatment solution [100 µL 0.63 M $Na_2S_2O_3.5H_2O$ stock in 60 mL dist. H_2O] for 1 min and the rinse step repeated. The gel was soaked in impregnation solution [800 µL 1.18 M $AgNO_3$ stock, 600 µL 37% (v/v) 12.7 M HCHO, 25 µL 0.63 M $Na_2S_2O_3.5H_2O$ stock in 60 mL dist. H_2O] for 8 min. Following the rinse step, the gel was incubated in developing solution [1.2 g Na_2CO_3, 25 µL 37% (v/v) 12.7 M HCHO, 25 µL 0.63 M $Na_2S_2O_3.5H_2O$ stock in 60 mL dist. H_2O] for 20 s or until the bands were clearly observed. The developing solution was discarded, and the reaction stopped by incubation in stopping solution [1% glacial acetic acid in dist. H_2O] for 30 s. The gels were rinsed and stored in dist. H_2O. The gel images were captured using a GENE Sys version 1.2.4.0 gel documentation system, G: BOX chemi XR5 system (Syngene, Cambridge, UK).

2.2.12 Assay for pH stability of latex proteolytic activities

The *E. triangularis* latex preparation was tested over a pH range using constant ionic acetate-MES-Tris (AMT) buffer, pH 4 to 9 (Ellis and Morrison, 1982). Constant ionic strength buffers allow for accurate measurement of proteolytic activity at different pH values by keeping the concentration of all ions in solution constant as ionic strength affects the proteolytic activity of an enzyme either by changing its stability or the solubility of the enzyme (Eun, 1996). Using gelatin containing SDS-PAGE gels (Section 2.2.10), a 1:1 dilution of the processed latex and a 1:10 dilution of the 40% TPP pellet of *E. triangularis* in AMT buffers [100 mM acetate, 100 mM MES, 200 mM Tris, 4 mM Na_2EDTA] titrated with HCl or NaOH to a range of pH-values

from pH 4 to 9, with, and without, 40 mM cysteine-HCl at 37°C for 16 h. The gels were stained with 0.1% (w/v) Amido black (methanol:acetic acid:dist. H_2O in the ratio of 30:10:60).

2.2.13 Determination of the catalytic class of protease using catalytic class-specific inhibitors

Catalytic class-specific inhibitors were used to determine the class of the proteases present in the 40% TPP fraction of *E. tirucalli* and *E. triangularis*. Different dilutions (in PBS) of the 40% TPP pellet in PBS was analysed on a 12.5% non-reducing gelatin-containing SDS-PAGE gel (Section 2.2.10). Each sample (in duplicate) was incubated at 37°C for 15 min with the respective inhibitors before gel electrophoresis. Inhibitors (final concentrations) used according to Beynon and Salvesen (2001) were: 10 mM ethylenediamine tetra-acetic acid (EDTA, VWR chemicals, CN BDH4616) for metalloproteases; 1 µM pepstatin (Sigma, CN P5318) for aspartic proteases; 10 µM trans-epoxysuccinyl-L-leucylamido(4-guanidino)butane (E-64, Melford) for cysteine proteases; 100 µM soybean trypsin inhibitor (SBTI, Melford, CN T1203), 1 mM phenylmethylsulfonyl fluoride (PMSF, Sigma, CN P7626), 100 µM tosyl phenylalanyl chloromethyl ketone (TPCK, Sigma, CN T-4376) and 100 µM tosyl-L-lysyl-chloromethane hydrochloride (TLCK, Sigma, CN T-7254) for serine proteases. After gel electrophoresis and incubation in Triton X-100, the gels were cut in strips according to the pre-electrophoresis incubation with the respective inhibitors. The gel strips were incubated in 6 mL 100 mM Na-acetate buffer, pH 5 containing 100 mM Na_2EDTA, 0.02% (w/v) NaN_3 and 40 mM cysteine-HCl and the respective inhibitors at the final concentrations specified above. Gels were stained with 0.1% (w/v) Amido black (methanol:acetic acid:dist. H_2O in a ratio of 30:10:60). Inhibitor stocks and concentrations were prepared as per (Zollner, 1992, Beynon and Salvesen, 2001) with the exception of SBTI which was made up in 100 mM phosphate buffer pH 7.2 containing 150 mM NaCl as per Hermanson (2013).

2.2.14 Reverse zymogram to detect protease inhibitors

Reverse zymography is a method used to detect the presence of protease inhibitory activity in a sample. The protease inhibitor-containing sample is electrophoretically separated in a gelatin-containing SDS-PAGE gel and after electrophoresis the gel is incubated in a buffer containing a protease (Figure 2.6). The method used was adapted from Hanspal et al. (1983) with the modification of using 600 µg/mL (instead of 400 µg/mL) of papain from papaya latex (Roth, CN 8933.1), or 14.2 µg/µL (instead of 14.2 µg/mL) of trypsin and AMT buffer, pH 8 instead of 100 mM glycine-NaOH buffer, pH 8.3 for incubation with trypsin from porcine pancreas (Sigma, CN T-4799). To test for the presence of cysteine protease inhibitors, chicken egg white cystatin (Sigma, CN C-0408) and a 1:1 dilution of the 40% TPP sample for *E. triangularis* were loaded in separate wells on a gelatin-containing SDS-PAGE gel. The gel was

incubated in AMT buffer pH 6, containing 600 µg/mL papain at 37°C for 16 h and stained with 0.1% (w/v) Amido black (Section 2.2.13).

To test for the presence of serine protease inhibitors, 0.5 mM SBTI and a 1:1 dilution of the 40% TPP sample for both plants were loaded in separate wells on a gelatin-containing SDS-PAGE gel. The gel was incubated in AMT buffer pH 8, containing 14.2 µg/µL of trypsin at 37°C for 16 h and stained with 0.1% (w/v) Amido black.

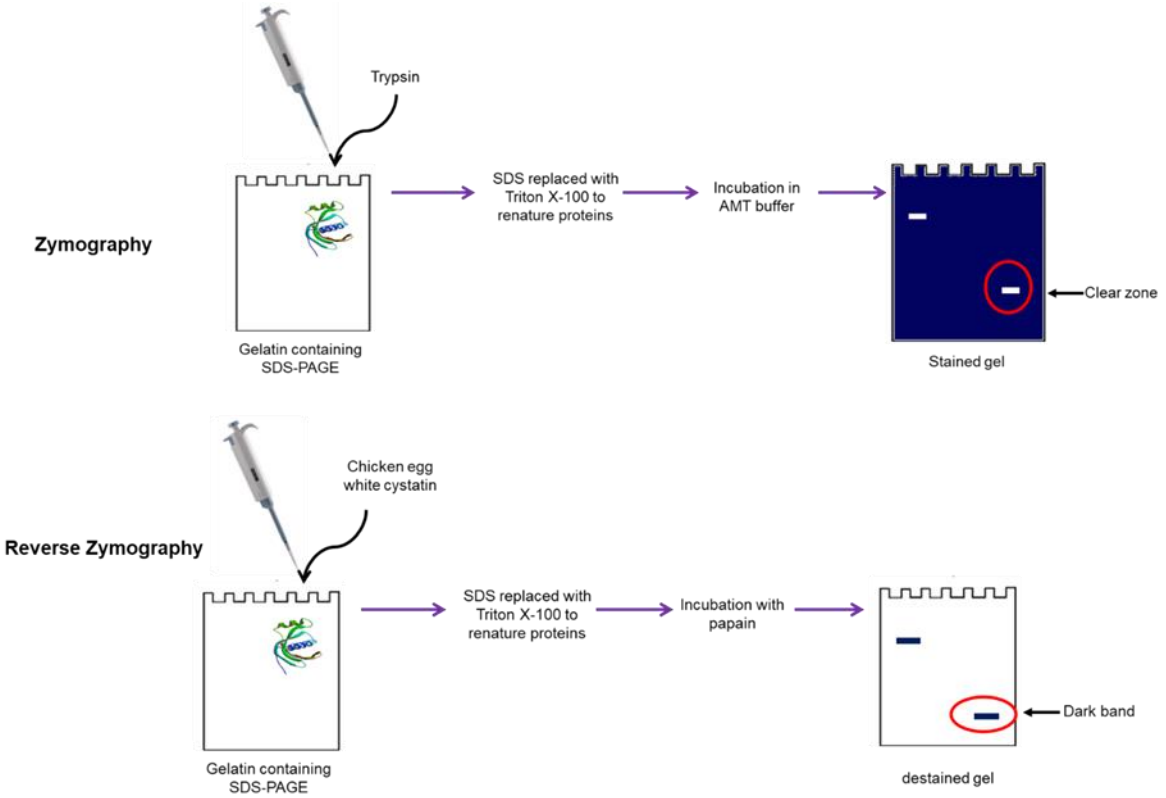

Figure 2.6: Schematic diagram showing the method of gelatin zymography and reverse zymography. Zymography is used to determine proteolytic activity by first separating a protease-containing sample on a gelatin-containing SDS-PAGE gel. After electrophoresis the gel is incubated in Triton X-100 to replace the denaturant SDS that inactivated the protease during electrophoresis. The gel is incubated in a suitable buffer, stained in Amido black and destained several times until clear zones of proteolytic activityare observed on a blue background. Reverse zymography uses the same principle as zymography, however, a protease inhibitor (chicken egg white cystatin, 13 kDa) or sample to be tested for the presence of an inhibitor is separated on the gelatin-containing SDS-PAGE gel. The gel is then incubated in buffer containing a suitable protease that digests the gelatin throughout the gel, except for the area where the inhibitor was present, indicated as a dark area on a clear background after staining.

2.2.15 Isolation of papain from *Carica papaya* fruit using TPP

Green unripe papayas were collected and vertical incisions made to collect the latex in a beaker over ice (Figure 2.7). The isolation and purification of papain was carried as per Hafid et al. (2020). In order to remove insoluble materials from the collected latex (4 mL), dist. H_2O was added to the latex at a ratio of 1:0.5 (latex to dist. H_2O) and centrifuged (2500 x *g*, 10 min, 4°C). To the supernatant 20% (w/v) ammonium sulfate was added and centrifuged as stated above. To the second supernatant 60% (w/v) ammonium sulfate was added and centrifuged as stated above. The pellet was dissolved in 7.2 mL of dist. H_2O (volume of initial + volume of dist. H_2O added at the start x 1.2) and dialysed overnight using dialysis membrane (molecular mass cut off, 14 kDa, Sigma, CN D9652) in 30 mM sodium phosphate buffer, pH 6.5 containing 2 mM cysteine-HCl at 4°C. After dialysis, the sample was subjected to TPP using 40% (w/v) ammonium sulfate and 30% (v/v) *t*-butanol at a ratio of 1:0.75 (*t*-butanol to dialysed sample) and allowed to incubate for 45 min before centrifugation at (4000 x *g*, 10 min, 4°C). The aqueous and interfacial phases were used for protein analysis. The interfacial phase was dissolved in 800 µl of 50 mM phosphate buffer, pH 7.5, before dialysis overnight against 30 mM sodium phosphate buffer, pH 6.5 containing 2 mM cysteine-HCl at 4°C.

Figure 2.7: Green unripe papayas from which latex was collected by making vertical incisions.

2.2.16 Isolation of papain from *Carica papaya* fruit using ion exchange chromatography

Ion exchange chromatography is used to separate molecules such as proteins, amino acids and peptides based on their overall charge. Proteins carry either a positive or a negative charge or no net charge (at the isoelectric pH or pI). The pH of the buffer determines the charge of the protein. If the pH is greater than the pI of the protein, the protein will be negatively charged and will bind to a positively charged anion exchange resin such as diethylaminoethyl cellulose (DEAE-C). If the pH is lower than the pI of the protein, the protein will be positively charged and will bind to a negatively charged cation exchange resin such as SP Sepharose Fast Flow. The proteins are either eluted from the column by a salt gradient or a change in

pH. The isolation and purification of papain was as per Monti et al. (2000) with some modifications. Green unripe papayas collected, vertical incisions made on the surface of the papayas and the latex collected in a beaker over ice. In order to remove insoluble material from the collected latex (4 mL), 0.4 M sodium acetate buffer, pH 5 containing 0.4 M NaCl, was added to the latex at a ratio of 1:0.5 (latex to buffer) and centrifuged (2500 x *g*, 10 min, 4°C). A CM-cellulose cation exchange column (18 mL) was packed and equilibrated with 3 column volumes of 0.4 M sodium acetate buffer, pH 5 containing 0.4 M NaCl. The latex sample (0.5 mL) was filtered through a 0.45 µm sterile syringe filter (Millipore, CN SLHV004SL) and loaded onto the column. The column was washed with 2 column volumes of the same buffer to collect the unbound fraction. Thereafter, 1 mL samples were collected by elution using a salt gradient (0.4-1 M in the same buffer) at a flow rate of 0.5 mL/min. The absorbance of the samples was measured at 280 nm.

2.2.17 Analysis of enzymatic activity of proteases using synthetic substrates

Enzyme activity was measured against peptidolytic substrates: benzyloxycarbonyl-Arg-Arg-7-amido-4-methylcoumarin hydrochloride (Z-Arg-Arg-AMC, Sigma, CN C5429) for serine protease activity and Z-Phe-Arg-AMC (Sigma, CN C9621) in the presence of a reductant (Cys) for cysteine protease activity. Control enzyme preparations for serine protease activity (25 µL of a 1 ng/mL stock of trypsin) or latex-derived samples (50 µL of 20 µg/mL preparations) were added to 10 µM substrate diluted in 100 mM Tris buffer, pH 8 containing 1 mM $CaCl_2$, 50 mM NaCl, in separate reactions. Control enzyme preparations for cysteine protease activity (25 µL of a 1 ng/mL stock of papain) or latex-derived samples (50 µL of 20 µg/mL preparations) were added to 100 mM Na-acetate buffer, pH 5 containing 100 mM Na_2EDTA, 0.02% (w/v) NaN_3 with 40 mM cysteine-HCl and activated at 37 °C for 15 min. Thereafter, substrate was added and incubated at 37 °C for 10 min. The samples were read at 30 cycles using a FLUOstar Omega microplate reader (BMG LABTECH, Offenburg, Germany) with excitation at 360 nm and emission at 463 nm.

2.2.18 Enzymatic activity of proteases using casein as a substrate

Protease activity was assayed using 1% (w/v) casein as the substrate, made up in 50 mM sodium phosphate buffer, pH 7, containing 250 mM EDTA, 1 mM DTT and enzyme concentrations of 0.2 mg/mL. Prior to measuring the activity, 0.2 ml of sample was incubated at 37°C for 15 min with 1 mL of substrate. Thereafter, 1.8 ml of 5% trichloroacetic acid (TCA) was added to stop the reaction. The sample was centrifuged (4500 x *g*, 15 min, RT) and the absorbance read at 280nm. For the blank, the enzyme was inactivated by TCA, then the substrate was added. The amount of enzyme required to increase the absorbance by 0.01 min^{-1} is defined as a unit of activity (Gagaoua *et al.,* 2015).

2.2.19 Detection of proteases using protease-specific antibodies in dot blots

A dot blot can be used to detect the presence of a protein using antibodies. This involves immobilising the protein on a membrane such as nitrocellulose of polyvinylidene fluoride (PVDF), blocking unoccupied sites with a protein before detection by primary and enzyme-labelled secondary (detection) antibodies and an appropriate substrate. The primary antibody is specific for the protein of interest, while the secondary antibody is coupled to an appropriate enzyme such as horseradish peroxidase (HRP) and is primary antibody species specific. If the secondary antibody recognises and binds to the primary antibody, the antibody-coupled enzyme catalyses a chemical reaction with the substrate, H_2O_2 and a chromogen such as 4-chloro-1-naphthol (for HRP) that produces a precipitating coloured product on a nitrocellulose membrane. HRP catalyses the oxidation of 4-chloro-1-naphthol in the presence of H_2O_2, resulting in a coloured product formed as a by-product of this reaction. On a small piece of nitrocellulose membrane, 0.5 µl of sample was dotted and allowed to air dry. The unoccupied sites on the membrane were blocked in 10 mL of 5% (w/v) non-fat milk powder prepared in Tris buffered saline (TBS) (20 mM Tris, 200 mM, NaCl, pH 7.4) for 1 h. The membrane was washed with TBS (3 times for 5 min each). For cysteine protease detection, primary antibodies used were in-house preparations of 10 and 100 µg/ml chicken anti-papain IgY and rabbit anti-papain IgG. Serine proteases were detected using 10 and 100 µg/ml chicken anti-oligopeptidase IgY and affinity purified chicken anti-oligopeptidase peptide IgY. The membranes were incubated in 10 mL of the respective primary antibodies, diluted in 0.5% (w/v) BSA in TBS (BSA-TBS), for 2 h at room temperature with gentle agitation. The membranes were washed twice with TBS for 5 min each before incubation in rabbit anti-chicken IgY (Sigma, CN A9792) or goat anti-rabbit IgG (Sigma, CN A9037) antibodies conjugated to HRPO (both at dilutions of 1:10000 in BSA-TBS) for 1 h at room temperature with gentle agitation. The membranes were washed 3 times for 5 min each with TBS before incubation in substrate-chromogen solution [0.06% (w/v) 4-chloro-1-naphthol, 0.1% (v/v) methanol, 0.0015% (v/v) H_2O_2 in TBS], in the dark until dots were visible.

2.2.20 Western blot detection of proteases using protease-specific antibodies

The proteins electrophoresed on a 10% reducing Tris-tricine SDS-PAGE gel (Section 2.2.9) were transferred onto a nitrocellulose membrane (45 micron, Merck, CN N8142) using a wet blotter (Bio-Rad, Hercules, USA), in blotting buffer [45 mM Tris-HCl, 173 mM glycine, 0.1% (w/v) SDS], at 200 mA for 16 h. A pre-stained broad range molecular weight protein marker (Bio Labs, CN P7712S) was used so that the marker was visible on the nitrocellulose after protein transfer. The unoccupied sites on the membrane were blocked in 10 mL of 5% (w/v) non-fat milk powder prepared in TBS for 1 h at room temperature with gentle agitation. The membrane was washed with TBS (3 times for 5 min each) before incubation with 10 mL rabbit

anti-papain IgG (100 µg/mL BSA-TBS) for 2 h at room temperature with gentle agitation. The membrane was washed twice with TBS for 5 min each before incubation in goat anti-rabbit IgG conjugated to HRPO (Sigma, CN A9037) at a dilution of 1:2500 in BSA-TBS for 1 h at room temperature with gentle agitation. The membranes were washed 3 times for 5 min each with TBS and incubated in substrate-chromogen solution [0.06% (w/v) 4-chloro-1-naphthol, 0.1% (v/v) methanol, 0.0015% (v/v) H_2O_2 in TBS], in the dark until dark bands were visible.

2.2.21 Milk clotting assay to determine milk clotting by crude latex

A milk clotting assay was used to determine if the crude latex of *E. tirucalli* and *E. triangularis* were able to clot milk. Casein is an important protein found in milk and forms about 80% of the total nitrogen in milk (Sarode et al., 2016). Casein is a phosphorylated and glycosylated complex produced by the mammary glands. It is made of three polypeptide chains (αs_1, αs_2, and ß) that are held together by non-covalent interactions (Sarode et al., 2016). Kappa-casein is a milk protein that plays an important role by controlling the amount of clotting that occurs. The κ-casein hydrophilic domain encloses the α_s-caseins and β-caseins located within the micelle. The α_s-caseins and β-caseins are exposed to calcium by the hydrolysis of the κ-casein domain, which results in the milk separating into two phases, a solid curd and a liquid phase (Pontual et al., 2012). Low fat milk powder was dissolved in assay buffer with 10 mM $CaCl_2$ to a concentration of 12% (w/v), pH 6.4. Controls used were 1 mg/mL papain from papaya latex (Roth- 8933.1) and pepsin from porcine mucosa (Sigma- P7012). To 1 mL of substrate (after incubation at 37 °C for 5 min), 100 µL of crude latex was added. The samples were monitored for 40 min and the time taken to clot was recorded. The amount of enzyme required to clot 10 mL of sample in 40 min at 37°C is defined as one milk-clotting unit. The following equation was used: MCA (U/mL) = 2400 x V/(t x v), where V is the volume of milk (mL), t is the clotting time in seconds and v is the volume of enzyme (mL) (Gagaoua et al., 2015).

Chapter 3

Results

3.1 Isolation and characterisation of proteases from the latex of *Euphorbia tirucalli*

The milky, white latex collected from incisions made on the *E. tirucalli* stem was diluted in PBS and debris removed by centrifugation before any further analysis was conducted, the results of which will be presented in the ensuing sections.

3.1.1 Analysis of processed *E. tirucalli* latex dilutions using SDS-PAGE and gelatin SDS-PAGE

The processed *E. tirucalli* latex was analysed by reducing and non-reducing SDS-PAGE, followed by Coomassie blue staining to determine the protein composition and by gelatin-containing SDS-PAGE to determine if active proteases are present in the latex (Figure 3.1). Under reducing conditions the processed latex contained proteins of approximate sizes of 45, 40, 33 and 28 kDa (Figure 3.1A), while under non-reducing conditions proteins of 75, 70, 53, 37, 32, 28 and 25 kDa were observed (Figure 3.1B). Figure 3.1C shows the presence of two active proteases of approximate sizes of 75 and 37 kDa (high and low molecular weight proteins), indicated by the red and yellow boxes respectively.

The 70 and 75 kDa proteins observed in panel B showed activity as a single broad band at 75 kDa on the zymogram (panel C). A similar observation is made for the 32 and 37 kDa protein bands (panel B) that show activity as a broad area of activity at 37 kDa on the zymogram shown in panel C. Upon further dilution (1:10), two separate bands of activity of similar size can be distinguished (panel C). The sizes of the proteins shown in panels B and C differ even though both were separated under non-reducing conditions because the sizes of proteins separated on a gelatin-containing gel are approximated since their migration is restricted by the co-polymerised gelatin. This difference is also observed for the papain control sample where the 23.3 kDa protease shows activity corresponding to a larger size on the zymogram gel (Figure 3.1C).

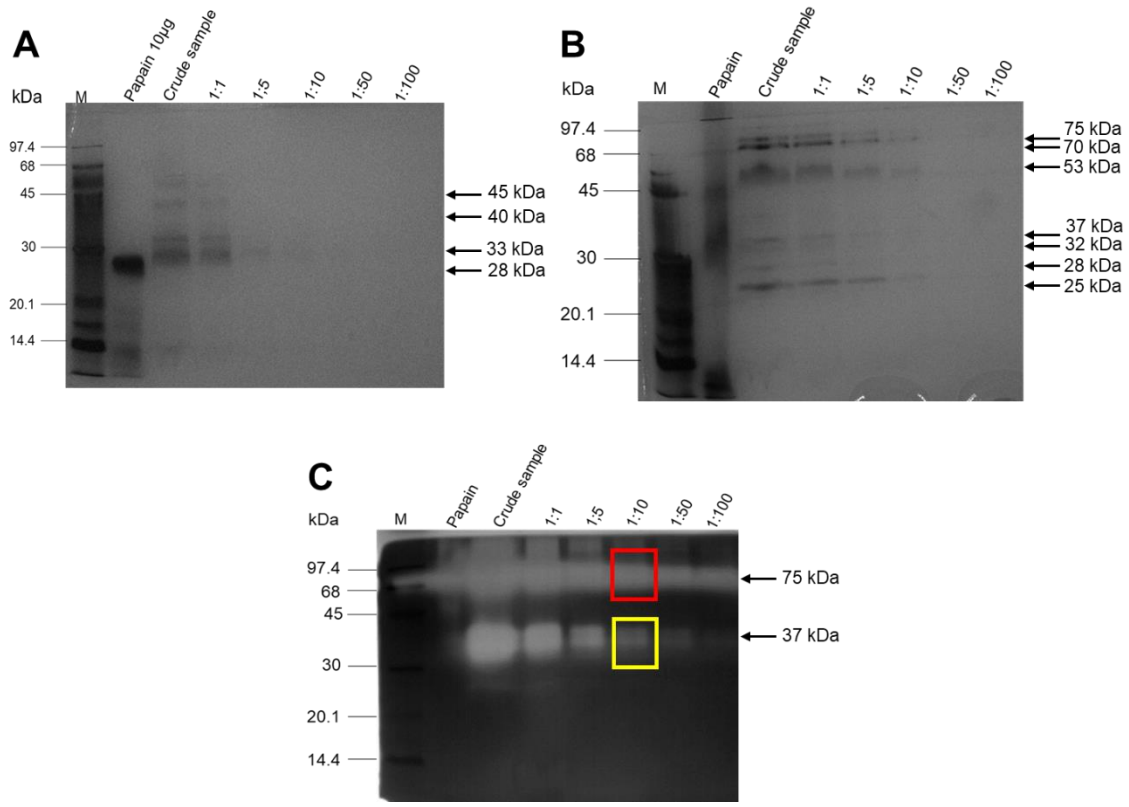

Figure 3.1: Analysis of dilutions of processed *E. tirucalli* latex by SDS-PAGE and gelatin-zymography. Samples (25 µg of crude latex or papain, 10 µg in panels A and B or 8 ng in panel C) were analysed on Coomassie R-250-stained **(A)** reducing, **(B)** non-reducing 12.5% SDS-PAGE and **(C)** non-reducing 1% (w/v) gelatin-containing 12.5% SDS-PAGE zymogram stained with 0.1% (w/v) Amido black. The zymogram was incubated in 100 mM Na-acetate buffer, pH 5 containing 100 mM Na_2EDTA, 0.02% (w/v) NaN_3 containing 40 mM cysteine-HCl after replacing the SDS with Triton X-100. The red and yellow boxes shows the high and low molecular weight proteins respectively. Lane M, molecular weight marker as per section 2.2.8.

3.1.2 Three phase partitioning (TPP) isolation of active proteases from processed *E. tirucalli* latex

Three phase partitioning was investigated as a method to separate the high and low molecular weight proteolytic activities, present in the processed *E. tirucalli* latex, from contaminating proteins (Figure 3.2). As the percentage ammonium sulfate used in TPP was increased from 10% to 20-40%, the latex proteins present in the interfacial (third) phase were concentrated as indicated by the presence of prominent 28, 33, 37 and 45 kDa protein bands following analysis on reducing SDS-PAGE (Panel A). The 28 and 37 kDa proteins were particularly prominent in the 20% TPP fraction. Only the high (75 and 70 kDa) and low (37 and 32 kDa) molecular weight proteins seem to be present in the 40% TPP fraction when analysed by non-reducing SDS-PAGE (Panel B, green box) when compared to the crude latex proteins shown in Figure 3.1B that also contained 53, 28 and 25 kDa protein bands. Analysis of the TPP-fractionated samples on a gelatin-containing zymogram showed that the 37 and 75 kDa proteins have proteolytic activity (Panel C). This indicates that TPP fractionation removed non-

active proteins present in the processed latex. An oversight was made with the amount of crude sample loaded as 25 µg in Figure 3.1 clearly showed the bands however, 15 µg was loaded thereafter.

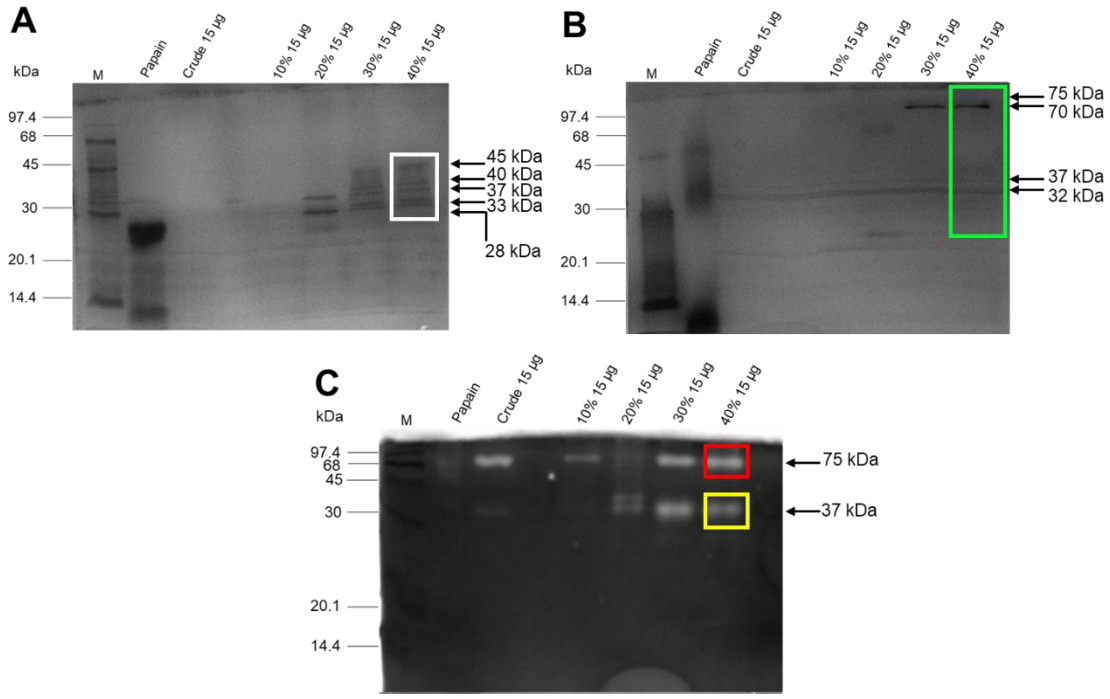

Figure 3.2: Analysis of Three Phase Partitioning (TPP) conducted on processed *E. tirucalli* latex. Reducing **(A)** and non-reducing **(B)** Coomassie R-250 stained 12.5% SDS-PAGE gels, **(C)** non-reducing 12.5% SDS-PAGE zymogram containing 1% (w/v) gelatin stained with 0.1% (w/v) Amido black. Zymogram incubated in 100 mM Na-acetate buffer, pH 5 containing 100 mM Na_2EDTA, 0.02% (w/v) NaN_3 and 40 mM cysteine-HCl, after replacing SDS with Triton X-100. Papain at 10 µg for A and B and 8 ng for C. The TPP samples at 15 µg for A, B and C. The white box shows proteins identified under reducing conditions, the light green box shows proteins identified under non-reducing conditions, the red and yellow boxes shows the high and low molecular weight proteolytic activities respectively. Lane M, molecular weight marker as per section 2.2.8.

3.1.3 Effect of pH on the proteolytic activity of the TPP fractionated *E. tirucalli* sample

The re-dissolved 40% TPP interfacial pellet of *E. tirucalli* was incubated in constant ionic strength AMT buffers ranging from pH 4 to 9 (Figure 3.3), with and without 40 mM cysteine. The high molecular weight protein, showed proteolytic activity from pH 4 to 9, in the presence and absence of cysteine. The low molecular weight protein, showed proteolytic activity from pH 5 to 8 in the presence of cysteine, while no proteolytic activity was observed in the absence of cysteine. This suggests that the low molecular weight protein might be a cysteine protease as it is only active in the presence of cysteine.

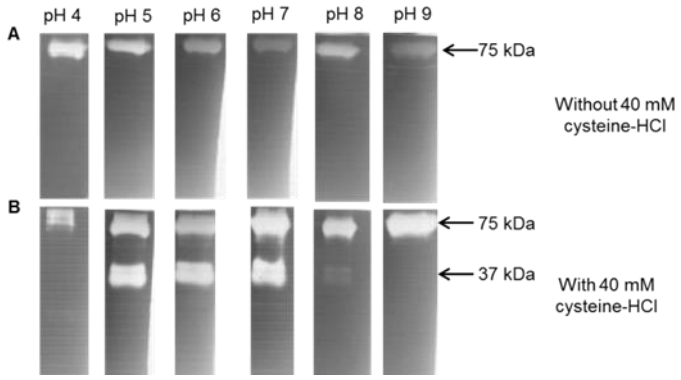

Figure 3.3: Gelatinolytic activity of proteases from the 40% TPP sample of *E. tirucalli* over a pH range from 4 to 9. Proteolytic activity analysed on non-reducing 12.5% zymogram gels containing 1% (w/v) gelatin – redissolved 40% TPP interfacial pellet samples (8 µg). Arrows show the two molecular weight protease activity bands 75 and 37 kDa. Gels were incubated in AMT buffer (pH 4-9) with and without 40 mM cysteine-HCl after replacing SDS with Triton X-100. Gels were stained with 0.1% (w/v) Amido black. Lane M, molecular weight marker as per section 2.2.8.

3.1.4 Effect of protease catalytic class-specific inhibitors on high and low molecular weight *E. tirucalli* proteases

In order to determine to which catalytic class the active proteases present in the *E. tirucalli* 40% TPP fraction belong, the sample was incubated with various class-specific protease inhibitors (Figure 3.4). This information would also inform further purification steps. Samples were appropriately diluted to aid visualisation of bands of activity on the zymograms. In the presence of EDTA (metalloprotease inhibitor) and pepstatin (aspartic protease inhibitor), both the 75 and 37 kDa protease activities were present, indicating that they are neither metalloproteases nor aspartic proteases. In the presence of E-64 (cysteine protease inhibitor), the 37 kDa protease activity band is not present, indicating that it is a cysteine protease. The serine protease inhibitors PMSF and SBTI completely inhibited the 75 kDa protease activity band, while TLCK and TPCK showed partial inhibition hence indicating that the 75 kDa protease is a serine protease.

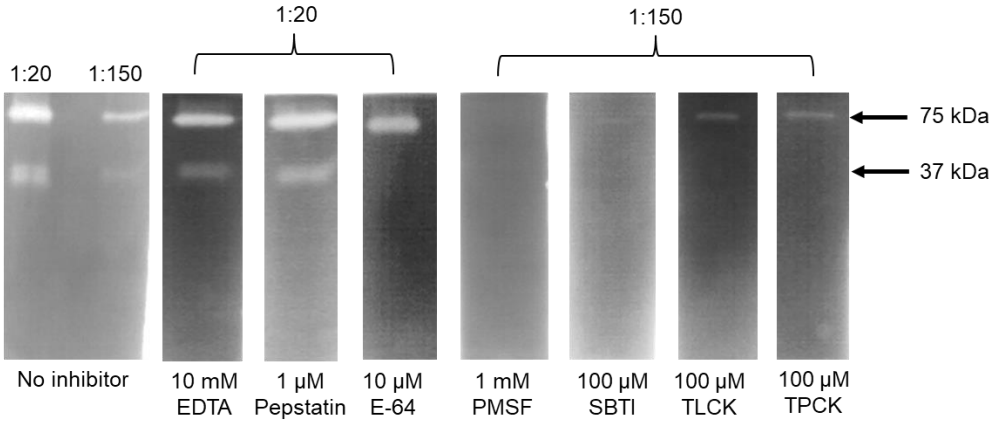

Figure 3.4: Classification of proteases from the *E. tirucalli* 40% TPP fraction using catalytic class-specific inhibitors. Proteolytic activity analysed on non-reducing 12.5% zymogram gels containing 1% (w/v) gelatin. Prior to loading of samples, the inhibitors were added to the 40% TPP fraction and incubated at 37°C for 15 min. Arrows show the high (75 kDa) and low (37 kDa) molecular weight protease activity bands. Gels were incubated in 100 mM Na-acetate buffer, pH 5 containing 40 mM cysteine-HCl and inhibitor at the indicated concentration. Gels were stained with 0.1% (w/v) Amido black. Sample dilutions are shown above the lanes.

3.1.5 Separation of active *E. tirucalli* proteases by Sephadex S-200 molecular exclusion chromatography and testing protease activity using substrate specific assays

Molecular exclusion chromatography using a Sephadex S-200 column was used to separate the proteases present in the *E. tirucalli* 40% TPP fraction by size. Figure 3.5A shows the four peaks of protein eluted from the column that were analysed by reducing and non-reducing SDS-PAGE and on a gelatin-containing zymogram. Panels C and D show the separation of the high and low molecular weight proteases in that the 75 kDa serine protease eluted in peak 2, while the 37 kDa cysteine protease eluted in peak 3. Peaks 1 and 4 did not show the presence of any proteins or any protease activity. For ease of reference, the 75 kDa serine protease is named *E. tiru* SP (*E. tirucalli* latex serine protease) and 37 kDa cysteine protease is named *E. tiru* CP (*E. tirucalli* latex cysteine protease).

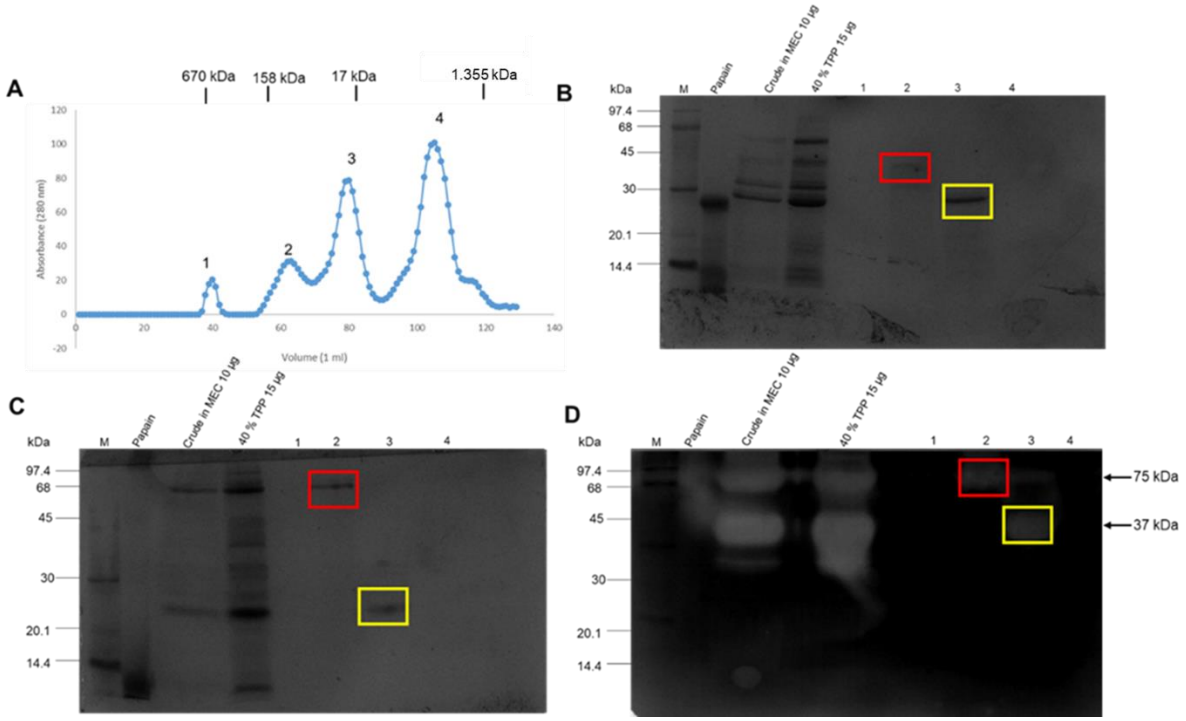

Figure 3.5: Separation of active *E. tirucalli* proteases from the 40% TPP pellet by molecular exclusion chromatography and analysis by reducing, non-reducing and gelatin-containing SDS-PAGE. (A) Elution profile of proteases on a Sephadex S-200 column (120 mL, 1 mL/h) in 50 mM Tris-HCl buffer pH 8, containing 300 mM NaCl. Silver stained reducing **(B)** and non-reducing **(C)** 12.5% SDS-PAGE gel and **(D)** non-reducing gelatin-containing zymogram. Following renaturation of the separated proteases, the zymogram was incubated in 100 mM Na-acetate buffer, pH 5 containing 100 mM Na_2EDTA, 0.02% (w/v) NaN_3 and 40 mM cysteine-HCl for 16 h at 37°C and stained with 0.1% (w/v) Amido black. Fractions from MEC shown in (A): peaks 1 (0.5 µg), 2 (2 µg), 3 (6 µg), 4 (0.3 µg); papain control 10 µg in panels B and C and 8 ng in panel D; lane M, molecular weight marker as per section 2.2.8. The red and yellow boxes show the high (75 kDa) and low (37 kDa) molecular weight proteins respectively. (A) The molecular weights of the calibration proteins are indicated at the top.

To further test the activity of the isolated *E. tirucalli* proteases following purification, the eluted samples (peaks 2 and 3) were subjected to a fluorescence enzyme assay using specific substrates (Figure 3.6). The activity of the 75 kDa serine protease, *E. tiru* SP was minimal in comparison to the trypsin control sample, while the activity of the papain control sample was extremely high in comparison to the 37 kDa cysteine protease *E. tiru* CP. The slight activity observed in Figure 3.6 is in accordance with the activity observed on the zymogram gel shown in Figure 3.5D. The standard deviation for all samples were low, indicating that the data is clustered around the mean.

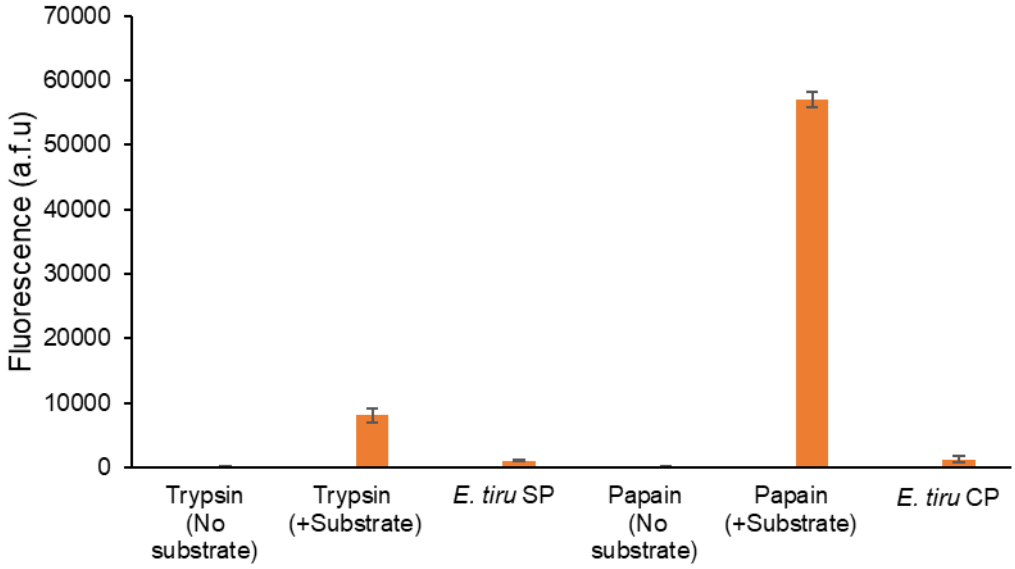

Figure 3.6: Bar graph showing activity of *E. tirucalli* proteases separated by Sephadex S-200 MEC against Z-Arg-Arg-AMC for serine proteases and Z-Phe-Arg-AMC for cysteine proteases. To triplicate 25 ng/mL protease samples 10 µM of substrate was added and fluoresence was measured at (Ex_{360nm} Em_{463nm}) using a FLUOstar Omega microplate reader for 30 cycles. Error bars are shown on the graph (n=3).

The purification profile of *E. tiru* SP and *E. tiru* CP from the 40% TPP fraction is summarized in Table 3.1. The TPP fraction had the highest protease recovery of 160.60% and a 8.2 fold purification in the interfacial pellet. The 8.2 fold purification for TPP shows that most non-active proteases were removed from the crude latex. *E. tiru* SP and *E. tiru* CP had a low protease recovery of only 6.17 and 4.19%, this is expected as protein samples eluted from MEC are much diluted.

Table 3.1: Purification of *E. tiru* SP and *E. tiru* CP from the crude latex of *E. tirucalli*

Step[a]	Total protein (mg)[c]	Total activity (U)[d]	Specific activity (U/mg)	Purification (fold)	Yield (%)
Crude latex[b]	225.4	45.08	0.2	1	100
TPP	44.2	72.4	1.64	8.2	160.6
E. tiru SP	6.87	2.78	0.4	2	6.17
E. tiru CP	5.4	1.89	0.35	1.75	4.19

[a] TPP, three phase partitioning; MEC, molecular exclusion chromatography
[b] Processed crude latex
[c] Protein concentration was determined using the Pierce™ BCA Protein Assay Kit and the Bradford assay
[d] Enzyme activity was determined using casein where one unit of activity is defined as the amount of enzyme that increases the absorbance by 0.01 min^{-1}

3.2 Isolation and characterisation of proteases from the latex of *Euphorbia triangularis*

The thick milky white latex was collected from incisions made on the stem and leaves of *E. triangularis*, diluted in PBS and any debris was removed by centrifugation before further analysis was conducted.

3.2.1 Analysis of processed *E. triangularis* latex dilutions using SDS-PAGE and gelatin SDS-PAGE

The processed *E. triangularis* latex was analysed by reducing and non-reducing SDS-PAGE, followed by Coomassie blue staining to determine the protein composition and by gelatin-containing SDS-PAGE to determine if active proteases are present in the latex. Under reducing conditions, the processed latex was shown to contain proteins of approximate sizes of 45, 38, 31, 25, 22 and 17 kDa (Figure 3.7A), while under non-reducing conditions two proteins of greater than 97.4 kDa and a further two proteins at 68 and 22 kDa were observed (Figure 3.7B). Gelatin-containing zymography analysis shown in Figure 3.7C reveals the presence of three active proteases of approximate sizes of >97.4, 68 kDa and 38 kDa indicated by the blue boxes.

The 38 kDa protein observed on the zymogram shown in panel C, is not observed on the non-reducing SDS-PAGE shown in panel B. The sizes of the proteins shown in panels B and C differ even though both were electrophoresed under non-reducing conditions because the protein sizes on a gelatin zymogram gel are approximated since their migration is restricted by the co-polymerised gelatin. This difference is also observed for the papain control sample where the 23.3 kDa protease shows activity corresponding to a larger size on the zymogram gel (Figure 3.7C). It is possible that the proteolytic activity of the two proteins that are larger than 97.4 kDa observed in panel B is observed as a single broad digestion area express activity together in panel C when the sample was diluted at 1:10.

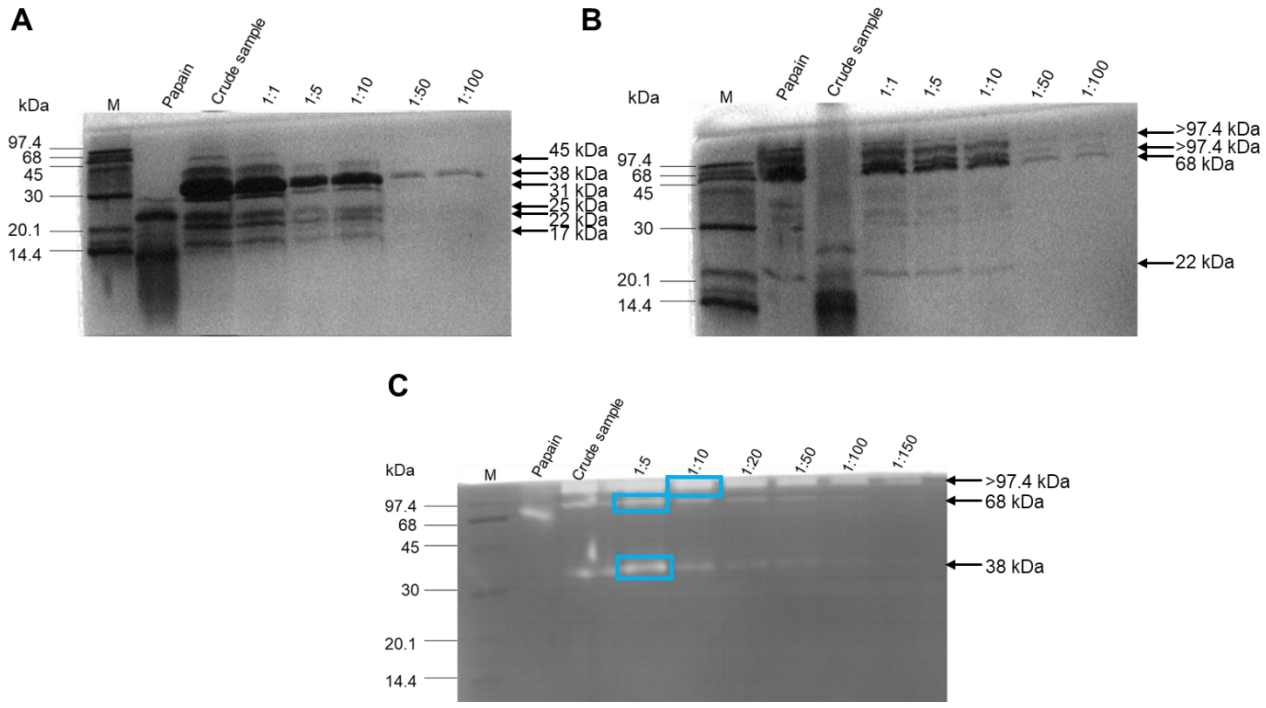

Figure 3.7: Analysis of dilutions of processed *E. triangularis* latex by SDS-PAGE and gelatin-zymography. Samples (10 µg of papain or crude latex, 10 µg of other samples in panels A and B or 8 ng of all samples in panel C) were analysed on silver stained **(A)** reducing, **(B)** non-reducing 12.5% SDS-PAGE gels and **(C)** non-reducing 1% (w/v) gelatin-containing 12.5% SDS-PAGE zymogram, stained with 0.1% (w/v) Amido black. The zymogram was incubated in 100 mM Na-acetate buffer, pH 5 containing 100 mM Na_2EDTA, 0.02% (w/v) NaN_3 containing 40 mM cysteine-HCl after replacing the SDS with Triton X-100. The blue boxes show the observed active proteases. Lane M, molecular weight marker as per section 2.2.8.

3.2.2 Three phase partitioning (TPP) isolation of active proteases from processed *E. triangularis* latex

Three phase partitioning was investigated as a method for separating the proteins present in the processed *E. triangularis* latex (Figure 3.8). As the percentage ammonium sulfate used in TPP was increased from 10% to 20-40%, the latex proteins present in the interfacial (third) phase were concentrated as indicated by the presence of prominent 22, 38, 68 and >97.4 kDa protein bands following analysis on non-reducing SDS-PAGE (Panel B). The 30 and 40% TPP fractions contain the same molecular weight proteins (Panel B) and when compared to the crude latex shown in Figure 3.8B, no protein bands were visible, however, the crude latex in Panel A (red box) shows a single protein band. In panel B, the 22 kDa is more prominent than observed in Figure 3.7B and the 38 kDa protein that is observed in Figure 3.8B in the 30 and 40% TPP fractions, but was not clearly observed in Figure 3.7B, indicating that TPP possibly concentrated this protein present in the processed latex. Analysis of the TPP-fractionated samples on a gelatin-containing zymogram showed that the 38, 68 and >97.4 kDa proteins have proteolytic activity (Panel C) in only three fractions (20%-40%). The 22 kDa protein band

in Panel B does not show proteolytic activity in Panel C, thus indicating that TPP fractionation removed non-active proteins present in the processed latex.

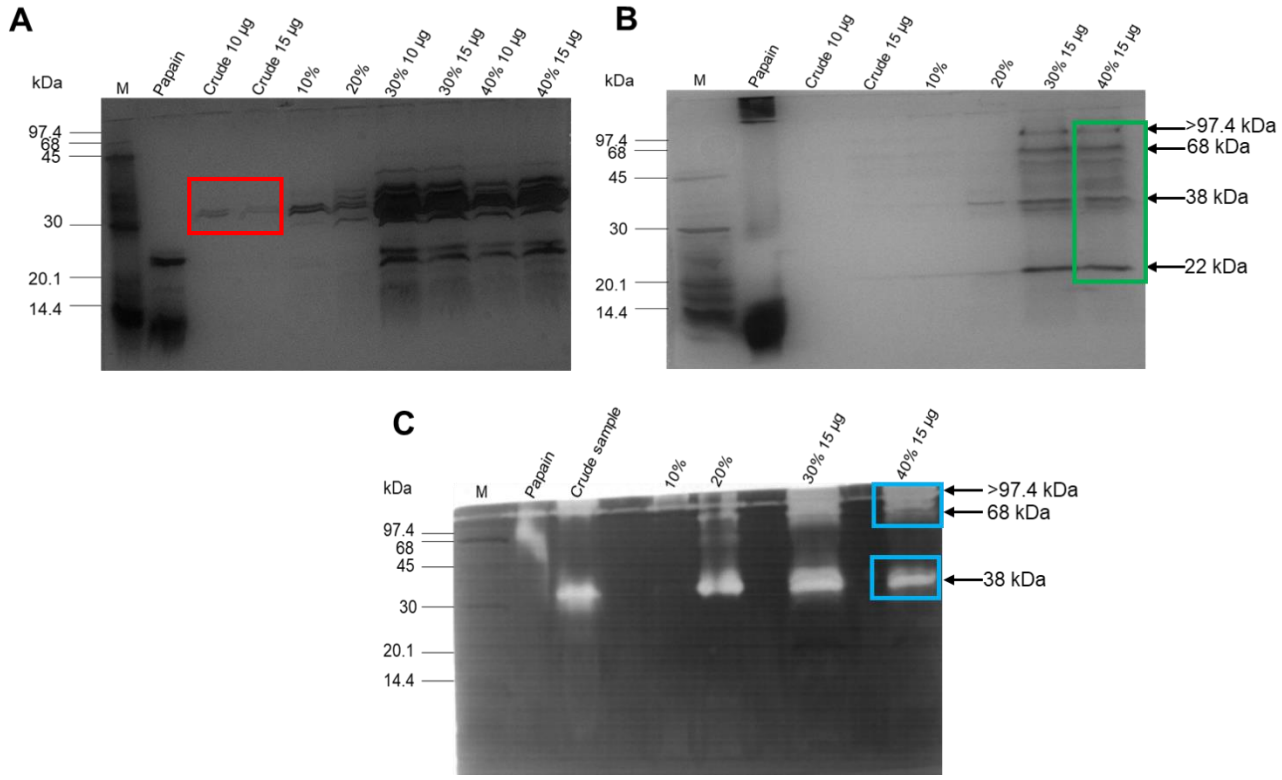

Figure 3.8: Analysis of Three Phase Partitioning (TPP) conducted on processed *E. triangularis* latex. Samples (10 µg of papain, 10 and 15 µg crude latex, 10 and 15 µg of other samples in panels A, B and C, 8 ng of papain in panel C) were analysed on silver stained **(A)** reducing, **(B)** non-reducing 12.5% SDS-PAGE gels and **(C)** non-reducing 1% (w/v) gelatin-containing 12.5% SDS-PAGE zymogram, stained with 0.1% (w/v) Amido black. Gelatin containing zymogram incubated in 100 mM Na-acetate buffer, pH 5 containing 100 mM Na_2EDTA, 0.02% (w/v) NaN_3 and 40 mM cysteine-HCl after replacing the SDS with Triton X-100. The red box shows proteins identified under reducing conditions, the green box shows proteins identified under non-reducing conditions and the blue boxes show the three molecular weight proteins. Lane M, molecular weight marker as per section 2.2.8.

Three phase partitioning did not adequately separate the three high molecular weight proteins from one another, hence acetone fractionation was done on the 40% TPP sample of *E. triangularis* latex. Pellet 2 is the soluble pellet formed after addition of acetone to crude latex. The latex proteins present in pellet 2 were concentrated as indicated by the presence of prominent 17, 22, 31, 38 and 45 kDa protein bands following analysis on reducing SDS-PAGE in Figure 3.8A, when compared to the crude sample. Analysis of the TPP-fractionated (Figure 3.8C) and acetone fractionation samples (Figure 3.9B) on a gelatin-containing zymogram showed the same proteolytically active proteins of sizes 38, 68 and >97.4 kDa respectively. The proteolytic activity of the >97.4 and 68 kDa proteins show combined activity in panel B while the 38 kDa protein shows a single band of activity. In comparison of the 40% TPP sample in Figure 3.8C to the acetone fractionation pellet in Figure 3.9B, the same three proteolytically

molecular weight proteins are observed. This indicates that acetone fractionation had the same effect on the crude *E. triangularis* latex as TPP.

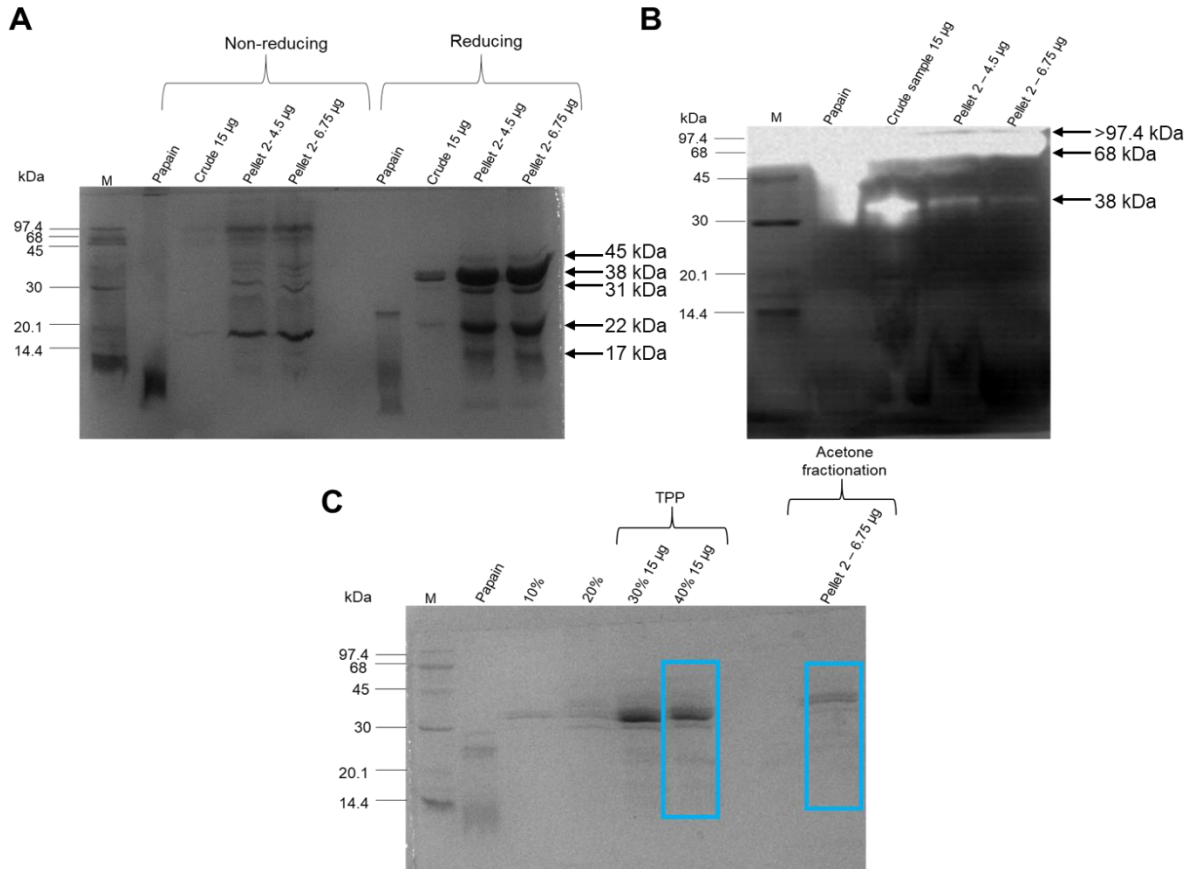

Figure 3.9: Analysis of acetone fractionation conducted on processed *E.triangularis* latex. Samples (10 µg of papain,15 µg crude latex, 4.5 µg and 6.75 µg of pellet 2 in panels A, B and C, 8 ng of papain in panel C) were analysed on silver stained **(A)** reducing and non-reducing 12.5% SDS-PAGE gels, **(B)** non-reducing 1% (w/v) gelatin-containing 12.5% SDS-PAGE zymogram, stained with 0.1% (w/v) Amido black. **(C)** Reducing Coomassie R-250 stained 12.5% SDS-PAGE gel. Gelatin containing zymogram incubated in 100 mM Na-acetate buffer, pH 5 containing 100 mM Na_2EDTA, 0.02% (w/v) NaN_3 and 40 mM cysteine-HCl after replacing SDS with Triton X-100. The blue boxes show proteins identified in the 40% TPP fraction and in the acetone fractionation pellet respectively. Lane M, molecular weight marker as per section 2.2.8.

3.2.3 Effect of protease class-specific inhibitors *E. triangularis* proteases

In order to determine to which catalytic class the active proteases present in the *E. triangularis* 40% TPP fraction belong, the sample was incubated with various class-specific protease inhibitors (Figure 3.10). This information would also inform further purification steps. In the presence of EDTA (metalloprotease inhibitor), pepstatin (aspartic protease inhibitor), E-64 (cysteine protease inhibitor) all three of the >97.4, 68 and 38 kDa protease activities were present, indicating that none of the activities belong to these classes of proteases. In the presence of PMSF, SBTI and TPCK (serine protease inhibitors), complete inhibition of all three protease activities by PMSF, partial inhibition by SBTI and TPCK could be observed, indicating that all three proteases are serine proteases. The control trypsin, has high activity that is

partially inhibited by SBTI and artifactual activity is observed across all lanes at the top of the gels.

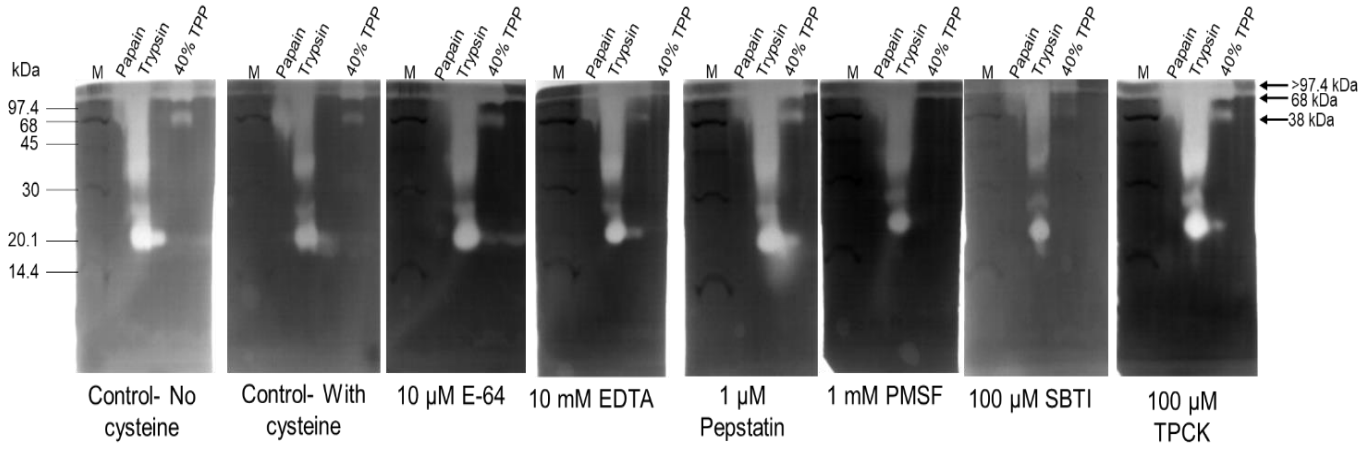

Figure 3.10: Classification of proteases from the *E. triangularis* 40% TPP fraction using catalytic class-specific inhibitors. Proteolytic activity analysed on non-reducing 12.5% zymogram gels containing 1% (w/v) gelatin. Prior to loading of samples, the inhibitors were added to the 40% TPP fraction and incubated at 37°C for 15 min. Papain at 8 ng, trypsin at 6ng and 40% TPP redissolved interfacial pellet at 8 µg. Arrows show the three molecular weight protease activity bands >97.4, 68 and 38 kDa. Gels were incubated in 100 mM Na-acetate buffer, pH 5 containing 40 mM cysteine-HCl and inhibitor after replacing SDS with Triton X-100. Gels were stained with 0.1% (w/v) Amido black. Lane M, molecular weight marker as per section 2.2.8.

3.2.4 Separation of three active *E. triangularis* proteases by *p*-aminobenzamidine affinity chromatography and testing protease activity using substrate specific assays

Para-aminobenzamidine affinity chromatography was used to separate the serine proteases present in the *E. triangularis* 40% TPP fraction based on reversible protease-inhibitor interaction. Protein that did not bind to the affinity matrix eluted in two peaks (Figure 3.11A), while elution by lowering the pH resulted in four peaks of bound protein eluting from the column (Figure 3.11B). Analysis by reducing SDS-PAGE showed separation of the 38 and 22 kDa proteins in the unbound 2 fraction and only a 38 kDa protein in the bound fractions (Figure 3.11C). Non-reducing SDS-PAGE showed protein bands of 38, 68, 80 and >97.4 kDa in the unbound fraction while the bound fractions show three protein bands, 38, 68, >97.4 kDa (Figure 3.11D). The three protein bands showed proteolytic activity by analysis on a gelatin-containing zymogram gel (Figure 3.11E). Analysis of the bound fractions on a gelatin-containing zymogram (Panel E), show broad areas of activity at 68 and >97.4 kDa. The proteins eluted in unbound fraction 2 are the same proteins observed in the crude latex (Panels C and D). The active proteases present in the crude latex are the same active protease found in the bound fractions, indicating that the serine proteases were not separated. It is possible that all three serine proteases have similar affinity for the para-aminobenzamidine affinity matrix. For ease of reference, the 97.4 kDa protease is named *E. laris* SP1 (*E.*

triangularis serine protease 1), the 68 kDa protease *E. laris* SP2 (*E. triangularis* serine protease 2) and the 38 kDa protease *E. laris* SP3 (*E. triangularis* serine protease 3).

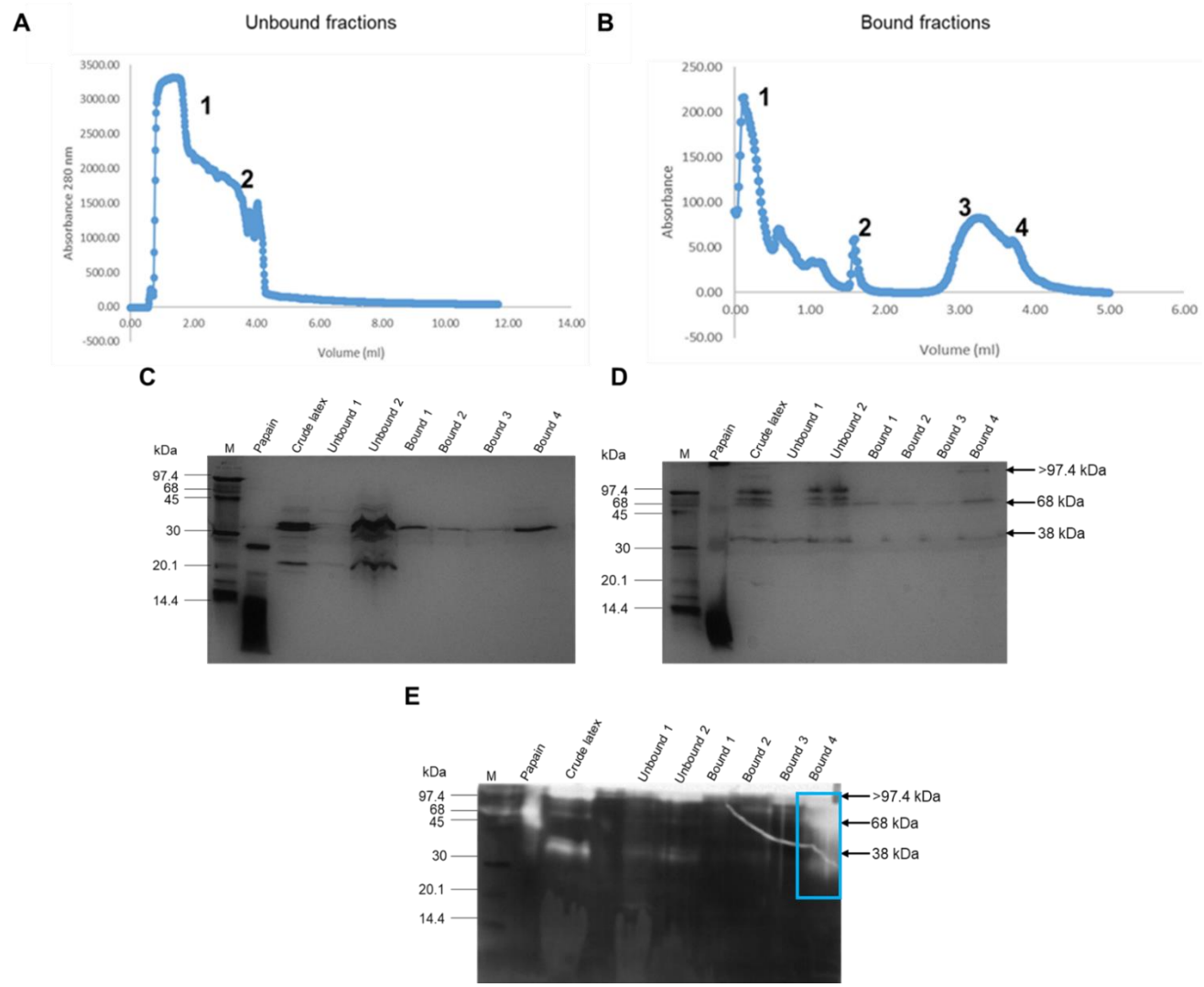

Figure 3.11: Separation of redissolved 40% TPP interfacial pellet of *E. triangularis* proteins by *p*-benzamidine affinity chromatography and analysis by reducing, non-reducing and gelatin-containing SDS-PAGE. (A) Elution profile of the redissolved 40% TPP interfacial pellet on a *p*-aminobenzamidine column (1 mL, 1 mL/min in 50 mM Tris-HCl, 0.5M NaCl, pH 7.4). **(A)** Elution profile of unbound fractions. **(B)** Elution profile of bound fractions eluted using 50 mM glycine-HCl buffer, pH 3. Silver stained reducing **(C)** and non-reducing **(D)** 12.5% SDS-PAGE gel and **(E)** non-reducing 12.5% gelatin-containing zymogram. Following renaturation of the separated proteases, the zymogram was incubated in 100 mM Na-acetate buffer, pH 5 containing 100 mM Na_2EDTA, 0.02% (w/v) NaN_3 and 40 mM cysteine-HCl) for 16 h at 37°C and stained with 0.1% (w/v) Amido black. Fractions from affinity chromatography shown in (A): unbound 1 (0.4 µg) and unbound 2 (5 µg); (B) bound 1 (0.3 µg), 2 (0.5 µg), 3 (0.6 µg) and 4 (0.8 µg); papain control 10 µg in panels C and D and 8 ng in panel E; lane M, molecular weight marker as per section 2.2.8. The blue box shows the three active proteases, *E laris* SP1, *E. laris* SP2 and *E. laris* SP3.

To further test the activity of the >97.4, 68 and 38 kDa *E. triangularis* proteases following affinity chromatography, all unbound and bound protein fractions were subjected to a fluorescence enzyme assay using peptide substrates (Figure 3.12). The activity of all the bound fractions were slightly higher than the activity of the trypsin control sample, while the

activity of unbound fractions 1 and 2 was extremely high in comparison to the trypsin control sample. The slight activity observed for all bound fractions in Figure 3.12 is in accordance with the activity observed on the zymogram gel shown in Figure 3.11E, however, the activities observed in Figure 3.12 (unbound 1 and 2) are not in accordance with the activity observed in Figure 3.11E. The unbound 1 and 2 fractions show less activity on the gelatin containing zymgogram gel (Figure 3.11E) as compared to the high activity shown in Figure 3.12.

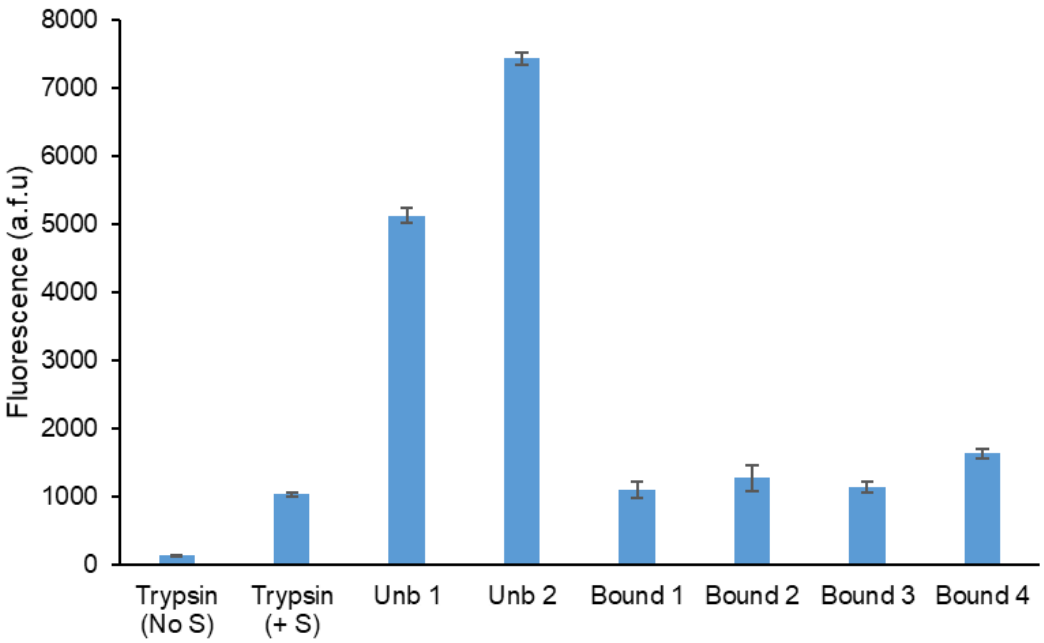

Figure 3.12: Assay for hydrolysis of Z-Arg-Arg-AMC by *E. triangularis* proteases from *p*-aminobenzamidine affinity chromatography. To triplicate 25 ng/mL protease samples, 10 µM of Z-Arg-Arg-AMC substrate was added and the fluorescence measured (using Ex_{360nm} and Em_{463nm}) using a FLUOstar Omega microplate reader for 30 cycles. Error bars are shown on the graph (n=3). S refers to the substrate and Unb to the fraction that did not bind to the column.

The purification profile of *E. laris* SP1, *E. laris* SP2 and *E. laris* SP3 from the 40% TPP fraction is summarized in Table 3.2. The bound 4 fraction from affinity chromatography had the highest purification fold of 13.5 in comparison to TPP of 8.55. This suggests that TPP and affinity chromatography removed non-active proteins from the 40% TPP fraction. Three chase partitioning showed to have the highest protease recovery of 196.35% followed by affinity chromatography of 78.93%.

Table 3.2: Purification of *E. laris* SP1, *E. laris* SP2 and *E. laris* SP3 from the crude latex of *E. triangularis*.

Step[a]	Total protein (mg)[c]	Total activity (U)[d]	Specific activity (U/mg)	Purification (fold)	Yield (%)
Crude latex[b]	168.71	33.74	0.2	1	100
TPP	38.52	66.25	1.71	8.55	196.35
AC	9.87	26.63	2.70	13.5	78.93

[a] TPP, three phase partitioning; AC, affinity chromatography bound fraction 4
[b] Processed crude latex
[c] Protein concentration was determined using the Pierce™ BCA Protein Assay Kit
[d] Enzyme activity was determined using casein where one unit of activity is defined as the amount of enzyme that increases the absorbance by 0.01 min^{-1}

3.2.5 Effect of pH on the proteolytic activity of the TPP fractionated *E. triangularis* sample

The re-dissolved 40% TPP interfacial pellet of *E. triangularis* was incubated in constant ionic strength AMT buffers ranging from pH 4 to 9 (Figure 3.13), with and without 40 mM cysteine before analysis on gelatin-containing. The proteins, *E. laris* SP1, *E. laris* SP2 and *E. laris* SP3 showed proteolytic activity from pH 4 to 9, in the presence and absence of cysteine. The yellow box placed on some of the panels, shown in Fig. 3.13, highlights that the >97.4 kDa and 68 kDa proteins did not separate very well in some instances on non-reducing gelatin SDS-PAGE. The 38 kDa band was observed at a higher size (slower electrophoretic mobility) than shown in Figure 3.11E, possibly due to incubation with AMT buffers prior to analysis on non-reducing gelatin SDS-PAGE. However, the same observation was not made when the gelatinolytic activity of the *E. tirucalli* proteases were analysed in constant ionic strength AMT buffers (Figure 3.3).

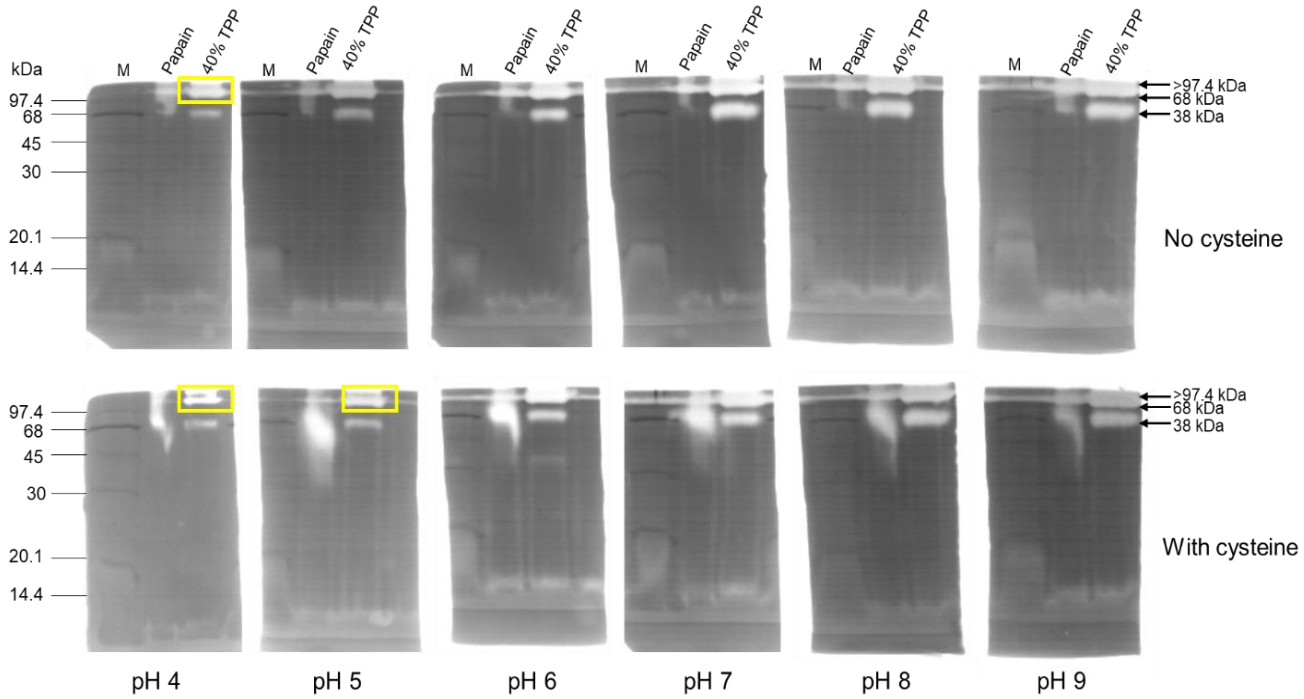

Figure 3.13: Gelatinolytic activity of proteases from the 40% TPP sample of *E. triangularis* over a pH range from 4 to 9. Proteolytic activity analysed on non-reducing 12.5% zymogram gels containing 1% (w/v) gelatin – of papain (8 ng) and redissolved 40% TPP interfacial pellet samples (8 µg). Arrows show the three molecular weight protease activity bands >97.4, 68 and 38 kDa. Gels were incubated in AMT buffer (pH 4-9) with and without 40 mM cysteine-HCl after replacing SDS with Triton X-100. Gels were stained with 0.1% (w/v) Amido black. Lane M, molecular weight marker as per section 2.2.8.

3.2.6 Testing for the presence of protease inhibitors in the 40% TPP sample of *E. triangularis* by reverse zymography

A 22 kDa protein band, present in the 40% TPP fractionated *E. triangularis* preparation, that showed no activity on a zymogram gel (Fig. 3.8B) could be a protease inhibitor. Reverse zymography was therefore used to test for the presence of protease inhibitors by separating 40% TPP fractionated *E. triangularis* proteins on a gelatin-containing zymogram gel and then incubating the zymogram in AMT buffer containing either papain or trypsin.

To test for the presence of a cysteine protease inhibitor, chicken egg white cystatin (13 kDa), a cysteine protease inhbitor, was used as a positive control (Figure 3.14A) for incubation of the zymogram in papain. Chicken egg white cystatin should show a dark band at 13 kDa, indicating that papain was inhibited, however no dark band was observed, suggesting that a higher concentration of chicken egg white cystatin should be used. There were no dark bands present in the 40% TPP sample and hence, no cysteine protease inhibitors were present.

The presence of a serine protease inhibitor was tested using the control SBTI (20.1 kDa), a serine protease inhibitor (Figure 3.14B) for incubating the zymogram in trypsin. A dark band at 20.1 kDa should be onserved for SBTI, indicating that trypsin was inhibited by SBTI. A dark

smear was observed for SBTI instead of a single dark band at 20.1 kDa. The smear resulted from either a too high concentration of SBTI used or the commercial SBTI preparation not being homogenous. There were no dark bands present in the 40% TPP sample hence, no serine protease inhibitors were present.

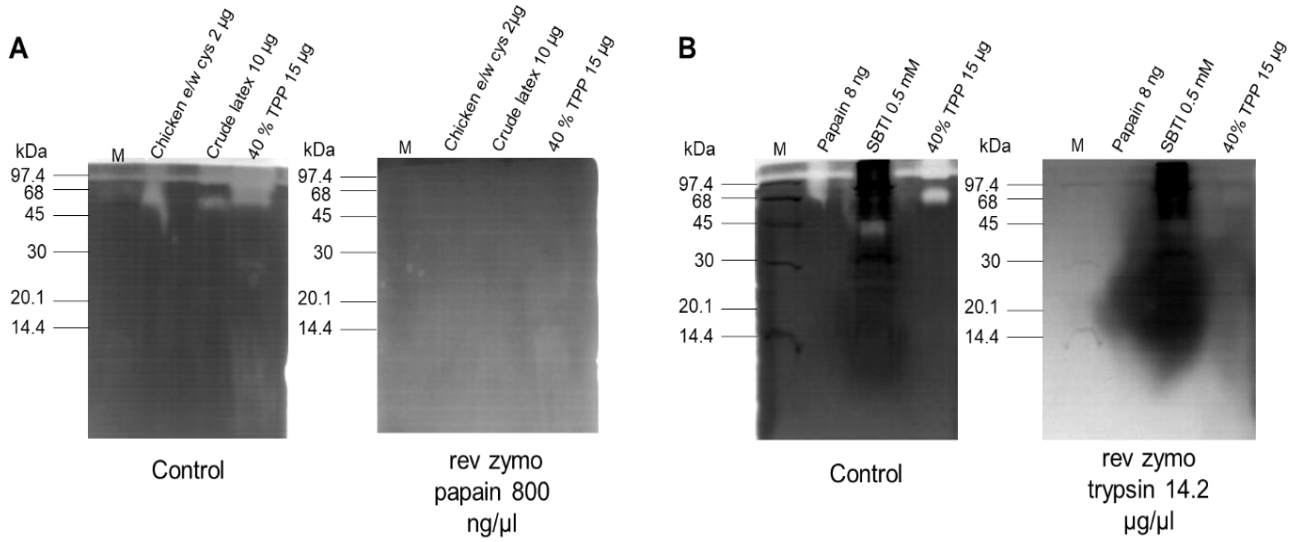

Figure 3.14: Reverse zymography of the 40% TPP sample from *E. triangularis* for detection of cysteine and serine protease inhibitors. Inhibitory activity was analysed by separating samples on non-reducing 12.5% zymogram gels containing 1% (w/v) gelatin, followed by replacing SDS with Triton X-100. **(A)** Cysteine protease inhibitor detection: incubation in AMT buffer pH 6, containing 40 mM cysteine-HCl without (control) or with 800 ng/µL papain. **(B)** Serine protease inhibitor detection: incubation in AMT buffer pH 8, containing 40 mM cysteine-HCl without (control) or with 14.2 µg/µL trypsin (without trypsin for the control). Gels were stained with 0.1% (w/v) Amido black and destained several times in metanol/acetate destain. Lane M, molecular weight marker as per section 2.2.8.

3.3. Isolation of papain from the latex of *Carica papaya*

Papain is a cysteine protease present in the latex of unripe papaya fruits. When commercially available papain preparations are separated on gelatin-containing zymogram gels, the proteolytic activity after renaturation and incubation in an appropriate buffer system is not observed at the expected size of 23.3 kDa, but a size larger than 97.4 kDa (Figure 3.1C). Possible reasons for this could be that the co-polymerised gelatin slows down the migration of the protein during electrophoresis or some inherent property of commercially produced papain. Papain was therefore isolated from the latex of unripe papaya fruit by TPP after extraction using 60% ammonium sulfate as per Hafid et al. (2020).

Analysis on non-reducing SDS-PAGE showed no protein bands thus, a higher concentration of sample should be loaded (Figure 3.15A). Analysis by reducing SDS-PAGE showed a single protein band of 26 kDa in the aqueous phase, in comparison to the commercial papain which was observed at 26 kDa (Figure 3.15A). Although papain has a size of 23.3 kDa, the estimated

size is close to the original size. The interfacial pellet showed a smear of protein indicating an impure sample which resembled the crude latex before any purification was performed. In order to confirm that the single protein band is papain, it was analysed by dot blot with rabbit anti-papain IgG antibodies (Figure 3.16B, sample D), which showed a purple dot positively identifying the isolated protein band as papain.

Analysis on a gelatin-containing zymogram gel shows activity for papain in the aqueous phase at a high molecular weight as is the case for commercial papain (Figure 3.15B). Due to low sample yield from the interfacial pellet, the sample was subjected to a fluorescence enzyme assay using substrate Z-Phe-Arg-AMC (Figure 3.15C). Enzyme activity was observed in both the interfacial pellet and aqueous phase samples. Since a pure sample (Figure 3.15A) was obtained from purification by TPP, the sample can be concentrated for future purification and analysed by gelatin containing zymogram gel to test if it shows at 23.3 kDa.

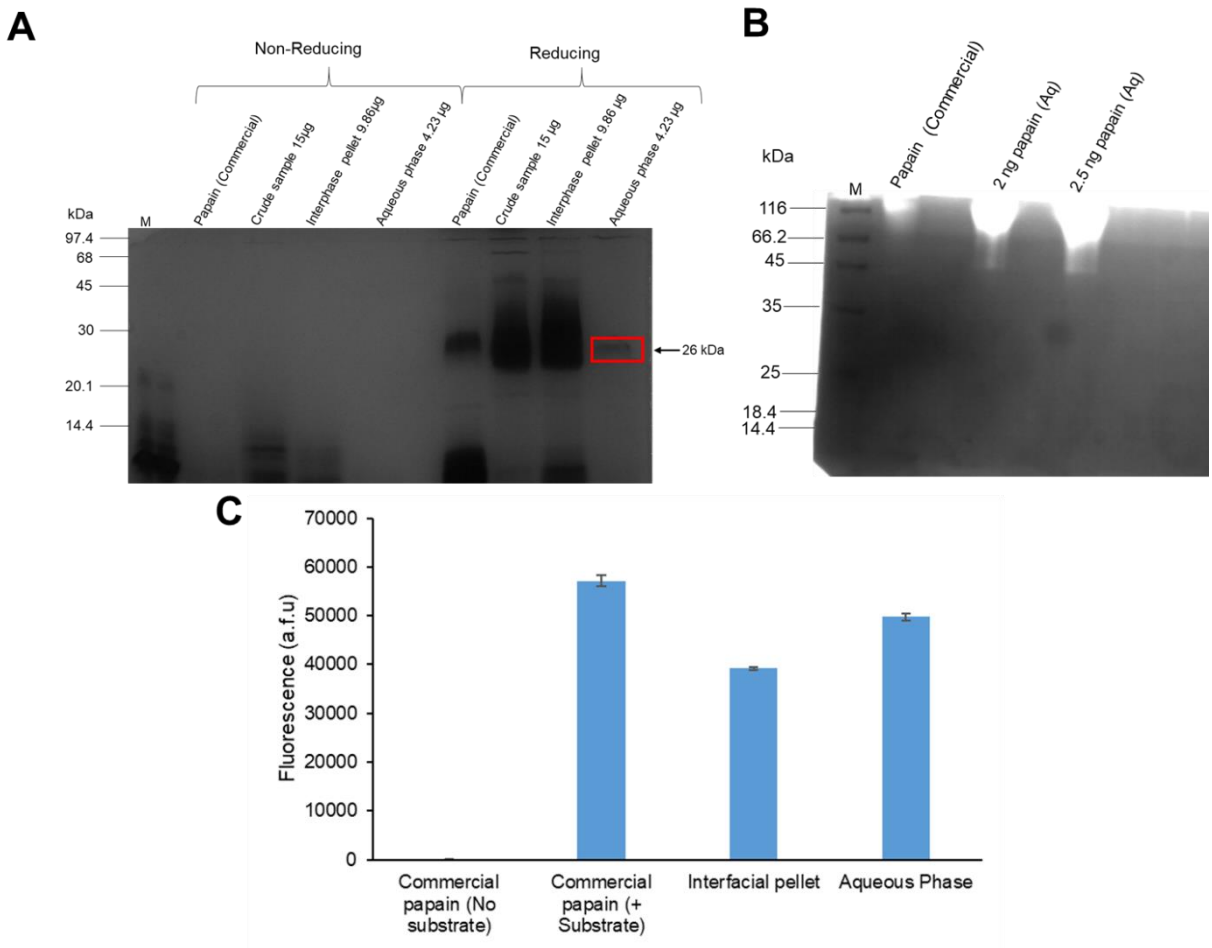

Figure 3.15: Analysis of papain isolated from latex of unripe *Carica papaya* fruit. (A) Samples (10 µg commercial papain,15 µg crude latex, 9.86 µg TPP interfacial pellet and 4.23 µg TPP aqueous phase) were analysed under non-reducing and reducing conditions on a 12.5% SDS-PAGE gel and silver-stained. The red box highlights isolated papain from the TPP aqueous phase .**(B)** Samples (8 ng commercial papain, 2 and 2.5 ng TPP aqueous phase) were analysed on a non-reducing 1% (w/v) gelatin-containing 10% tris-tricine SDS-PAGE zymogram. After replacing SDS with Triton X-100, the gel was incubated in 100 mM Na-acetate buffer, pH 5 containing 100 mM Na_2EDTA, 0.02% (w/v) NaN_3 and 40 mM cysteine-HCl and stained with 0.1% (w/v) Amido black. Panel A, lane M, molecular weight marker as per section 2.2.8 and panel B molceular weight marker as per section 2.2.9. **(C)** To triplicate 25 ng/mL protease samples, 10 µM of substrate Z-Phe-Arg-AMC was added and the fluorescence measured (using Ex_{360nm} and Em_{463nm}) using a FLUOstar Omega microplate reader for 30 cycles. Error bars are shown on the graph (n=3).

3.3.1 Dot blot analysis of the *E. tirucalli* proteases and papain isolated from *C. papaya* fruit using anti-cysteine and anti-serine protease antibodies

The isolated serine and cysteine proteases, *E. tiru* SP and *E. tiru* CP were subjected to dot blot analysis to determine cross-reactivity with rabbit anti-papain IgG and chicken anti-serine oligopeptidase IgY. Dot blot analysis showed that *E. tiru* CP was not recognised by either the chicken anti-papain IgY or rabbit anti-papain IgG primary antibodies (Figure 3.16A and B) and *E. tiru* SP was not recognised by either the chicken anti-serine oligopeptidase or chicken anti-

serine oligopeptidase peptide primary antibodies (Figure 3.16C and C) at either 10 and 100 µg/mL of primary antibody.

Papain (interfacial pellet) isolated from the papaya fruit was recognised by the chicken anti-papain IgY and rabbit anti-papain IgG primary antibodies (Figure 3.16A and B, block 4). This suggests that the protein concentration of *E. tiru* CP was too low to be recognised by the primary antibodies and the same can be stated for *E. tiru SP* (Figure 3.16A-D).

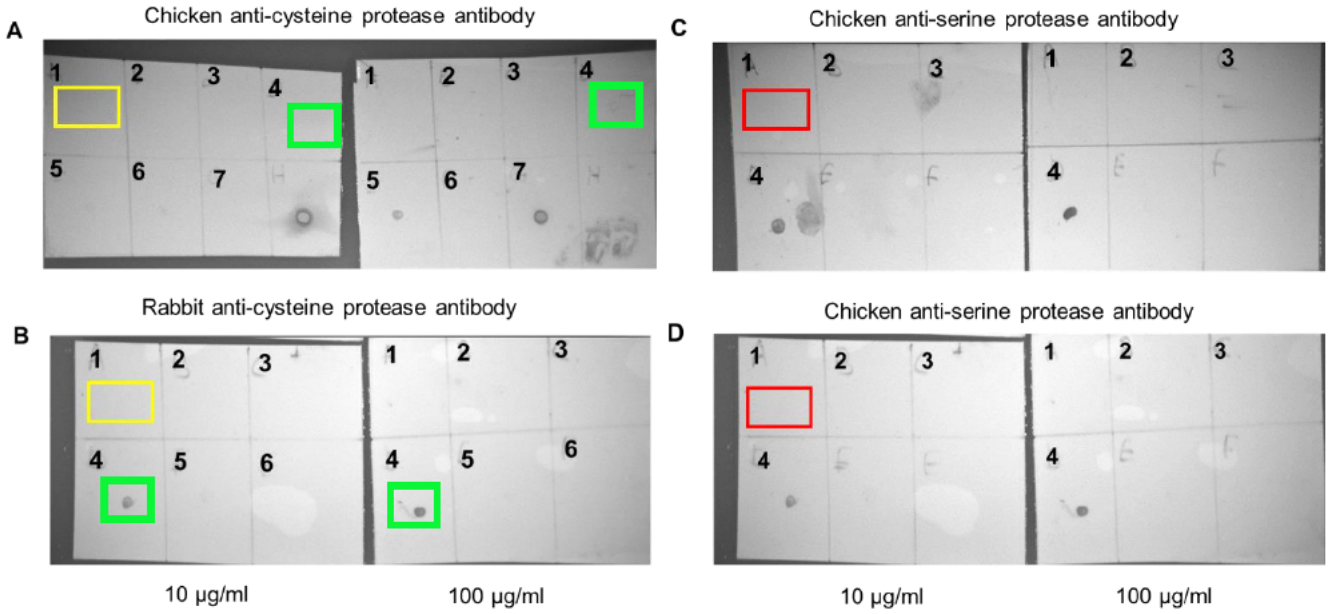

Figure 3.16: Dot blot analysis of purified *E. tirucalli* and *C. papaya* proteases with anti-cysteine and serine protease antibodies. The following samples were dotted on nitrocellulose: Panels **(A)** and **(B)** 1, *E. tiru* CP; 2, commercial papain; 3, TPP aqueous phase papain; 4, TPP interfacial pellet papain; 5, primary antibody control; 6, secondary antibody control and 7, pre-immune IgY control and incubated in **(A)** chicken anti-papain IgY and **(B)** rabbit anti-papain IgG. Panels **(C)** and **(D)** 1, *E. tiru* SP; 2, trypsin; 3, primary antibody control and 4, secondary antibody control and incubated in **(C)** chicken anti-serine protease and **(D)** anti-serine protease peptide primary antibodies. Primary antibodies were used at 10 and 100 µg/mL as indicated. Rabbit anti-chicken IgY and goat anti-rabbit IgG secondary antibodies conjugated to horse radish peroxidase at a dilution of 1:10000. The red and yellow boxes indicate where the *E. tiru* SP and *E. tiru* CP proteases were dotted respectively and the green boxes indicate the TPP interfacial pellet papain.

3.3.2 Isolation of papain from the latex of *Carica papaya* by CM-cellulose cation exchange chromatography

Papain isolated from the latex of unripe papayas, as described by Hafid et al. (2020) using TPP, showed the same result as shown in Figure 3.1C by gelatin containing zymogram analysis (Figure 3.15B). An alternative method of papain isolation using ion exchange chromatography was carried out by the method of Monti et al. (2000) with some modifications. Ion exchange chromatography using a CM-cellulose cation exchange column was used to isolate papain from the latex of *Carica papaya*. Figure 3.17A shows the five peaks of protein

eluted from the column that were analysed by reducing and non-reducing tris-tricine SDS-PAGE and on a gelatin-containing zymogram. Analysis by reducing tris-tricine SDS-PAGE, showed the presence of a protein band at 26 kDa in the unbound fraction and three other proteins bands of sizes between 14.4 and 25 kDa (Figure 3.17B). Sample 5 from column chromatography showed a single protein band at 26 kDa, while the other samples did not show any protein bands (Figure 3.17B). Analysis by non-reducing tris-tricine SDS-PAGE showed the presence of a few protein bands in the unbound sample, while the samples eluted from the cation exchange column did not show any protein bands (Figure 3.17C), indicating that a higher concentration of sample should be loaded. Analysis on a gelatin-containing zymogram gel showed proteolytic activity in the unbound and eluted sample 5 (Figure 3.17D). Sample 5 showed proteolytic activity at the same size as that shown in Figure 3.1C, indicating that a change in the isolation method did not change the size of proteolytic activity in a gelatin containing zymogram gel. Further analysis of sample 5 on a western blot showed that the isolated papain was detected by rabbit anti-papain IgG (Figure 3.17E).

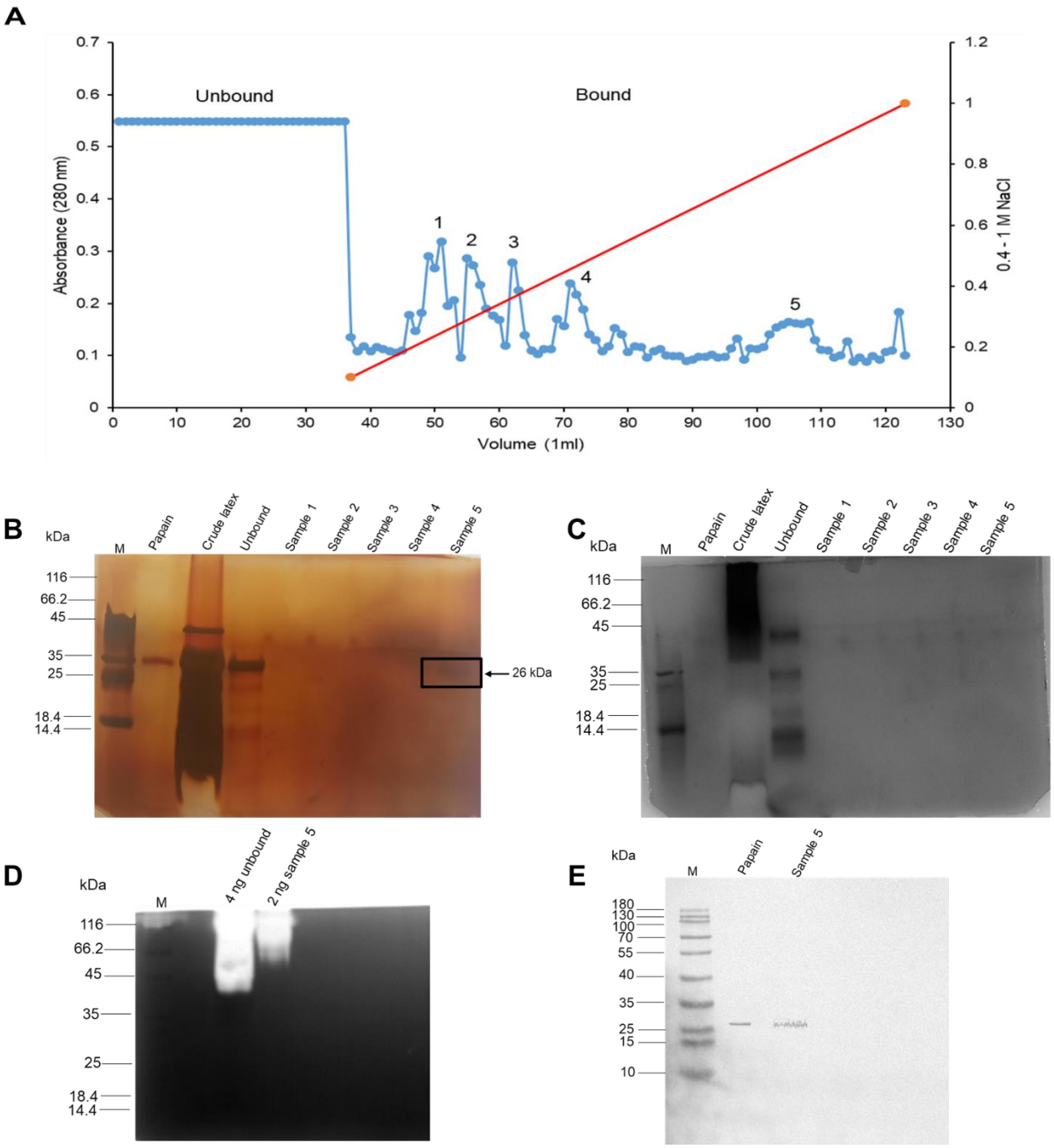

Figure 3.17: Analysis of papain isolated from *Carica papaya* unripe fruit by cation exchange chromatography and analysis by reducing, non-reducing and gelatin-containing tris-tricine SDS-PAGE. (A) Elution profile of proteases on a CM-cellulose cation exchange column (18 mL, 0.5 mL/min) in 0.4 M sodium acetate buffer, pH 5 containing 0.4 M NaCl using a salt gradient of 0.4-1 M NaCl. Silver-stained reducing **(B)** and non-reducing **(C)** 10% tris-tricine SDS-PAGE gel and **(D)** non-reducing gelatin-containing zymogram. Following renaturation, the zymogram was incubated in 100 mM Na-acetate buffer, pH 5 containing 100 mM Na_2EDTA, 0.02% (w/v) NaN_3 and 40 mM cysteine-HCl for 16 h at 37°C and stained with 0.1% (w/v) Amido black. **(E)** Western blot of eluted sample 5 incubated in rabbit anti-papain IgG (100 µg/mL), detected by goat anti-rabbit IgG conjugated to HRPO at a dilution of 1:2500. Fractions from ion exchange chromatography shown in (A): peaks 1 (6 µg), 2 (8 µg), 3 (6 µg), 4 (5 µg), 5(10 µg); papain control, 10 µg: crude latex, 15 µg: unbound, 10 µg in panels B and C and papain, 8 ng, unbound, 4 ng and 2 ng peak 5 in panel D; 10 µg papain and sample 5 in panel E; lane M, molecular weight marker as per section 2.2.9 for panels B-D and as per section 2.2.19. The black box indicated isolated papain at 26 kDa.

To test the activity of the isolated papain against a cysteine protease inhibitor following ion exchange chromatography, sample 5 was subjected to an azocasein assay following incubation with cysteine protease inhibitor, E-64 (Figure 3.18). Commercial papain was used as a control and following incubation showed a decrease in activity from 30 Units/mL to about 6 Units/mL. Sample 5 showed decreased activity after incubation with E-64, from 25 Units/mL to about 3 Units/mL. The activity of sample 5 is in accordance with the proteolytic activity shown in Figure 3.16D. The standard deviation was low for the data, indicating that the data was clustered around the mean.

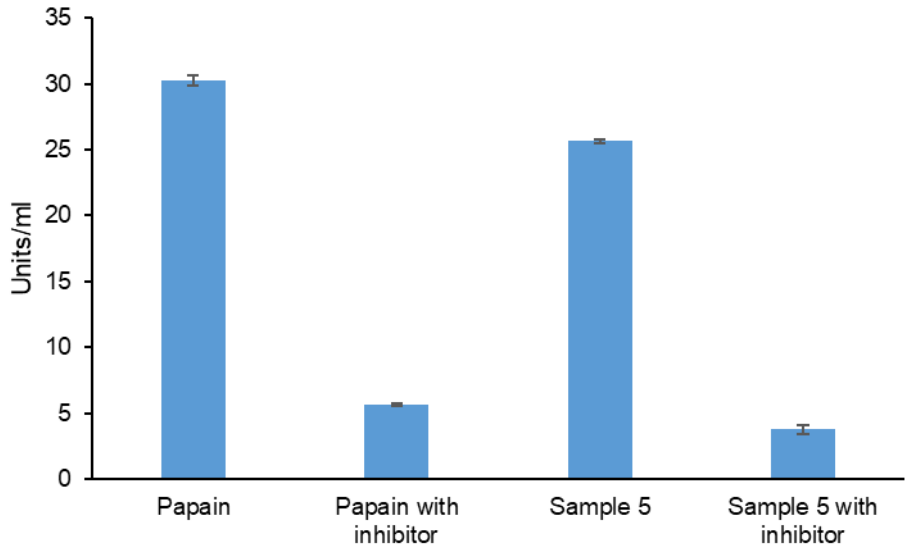

Figure 3.18: E-64 inhibition of azocasein hydrolysis by papain isolated from *Carica papaya* latex by CM-cellulose cation exchange chromatography. Triplicate samples (1 mg/mL commercial papain, as a control; 10 µg sample 5 were incubated without or with 10 µM E-64 before azocasein substrate was added. Absorbance was measured at 366 nm of the TCA soluble hydrolysis products. The units of activity were calculated according to the equation in section 2.2.7. Error bars are showed on the graph (n=3).

3.3.3 Evaluation of milk clotting ability of crude *E. tirucalli, E. triangularis* and *Carica papaya* latex

The milk clotting-, or coagulation-activity of the crude *E. tirucalli*, *E. triangularis* and *C. papaya* latex samples was tested and compared to plant (papain) and animal (pepsin from porcine mucosa) protease controls (Figure 3.19). Milk clotting was carried out at room temperature and the crude latex sample of all the tested plants showed low clotting activity in comparison to papain and pepsin (in the presence of calcium chloride). Without the addition of calcium chloride, the milk clotting ability of the crude latex in all plants was lower than in the presence of calcium chloride. The milk clotting ability of pepsin and papain in the absence of calcium chloride also decreased when compared to that in the presence of calcium chloride. Thus, the presence of calcium chloride increases the milk clotting ability of crude latex of all the tested plants (*E. tirucalli*, *E. triangularis* and *C. papaya*). The standard deviation was low for the data, indicating that the data was clustered around the mean.

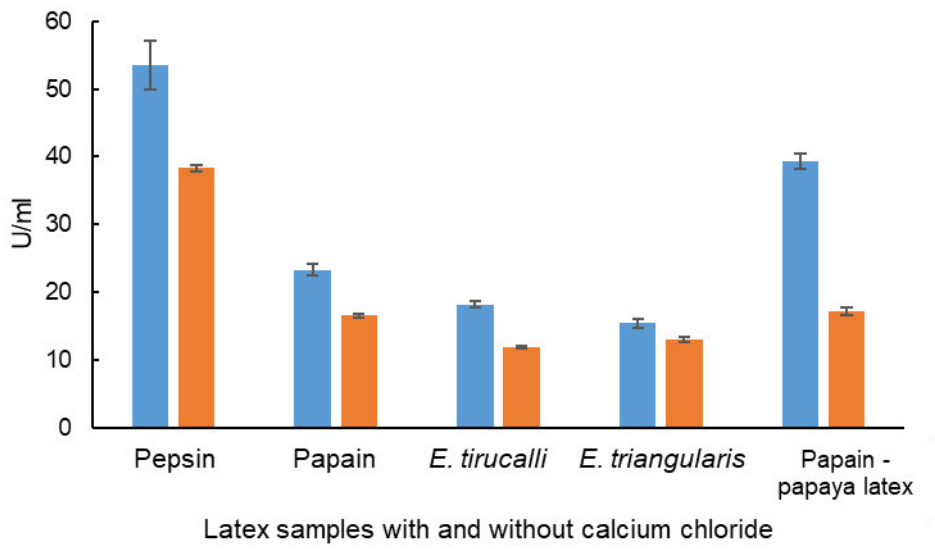

Figure 3.19: Milk clotting assay with *E. tirucalli*, *E. triangularis* and *C. papaya* crude latex samples. The crude latex was added to 12% (w/v) non-fat milk powder made up in assay buffer (100 mM Na-acetate buffer, pH 6.4 containing 100 mM Na2EDTA, 0.02% (w/v) NaN3, 10 mM calcium chloride) and the time it took to clot at room temperature was recorded as per the equation in Section 2.2.20 (Gagaoua et al., 2015). Triplicate samples of papain or pepsin (1 mg/mL) or 15 µg of *E. tirucalli*, *E. triangularis* and *C. papaya* crude latex samples were used. Error bars are shown on the graph (n=3). Blue bars represent results with calcium and orange bars without calcium.

Chapter 4

Discussion

Plant proteases are involved in various roles in a plants life cycle from developmental processes, plant growth, homeostasis, and responses to biotic and abiotic stress (van der Hoorn and Klemenčič, 2021). These plant proteases have been used in the food processing industries as milk clotting agents and as meat tenderizers (Shah and Mir, 2019), for use as therapeutic agents for the treatment of different diseases (Silva-López and Gonçalves, 2019) and biotechnological applications such as wastewater treatment (Troncoso et al., 2022). Plant proteases are produced in various regions of a plant however our main interest is on plant proteases found in plant latex. In the present study, *E. tiru* SP and *E. tiru* CP from *E. tirucalli*; *E. laris* SP1, *E. laris* SP2 and *E. laris* SP3 from *E. triangularis* and papain from the latex of *C. papaya* were isolated.

The collected latex needs to be processed before any analysis or isolation of proteases can be conducted as the rubber particles need to be removed to prevent coagulation of the latex. In this study, PBS, pH 7.2 was added in a ratio of 1:1 to the latex of *E. tirucalli* and *E. triangularis*, and centrifuged to obtain “crude latex” that was stored at 20°C. In other studies, latex from *E. tirucalli* and *E. cyparissias* was collected and immediately centrifuged for one hour with no addition of buffer, to separate the rubber from the latex (Lynn and Clevette-Radford, 1984c, Lynn and Clevette-Radford, 1985). The latex of *E. milii* was collected in 0.01 M acetate buffer, pH 4.5 containing 0.01 M sodium tetrathionate and frozen at 20°C for 36 hours, before insoluble gum and debris was removed by centrifugation (Yadav et al., 2006a). The supernatant was dialysed against sodium acetate and centrifuged before any further analysis. Latex coagulates quickly upon air exposure which presents a problem where large amounts of latex is required. Yadav et al. (2006a) circumvented this problem by adding sodium tetrathionate to the collection buffer to prolong the coagulation time. The relatively simple method used in the present study to obtain crude *Euphorbia* latex preparations was suitable for further purification of proteases. Similarly, in this study, the latex of *C. papaya* was diluted in distilled water in a ratio of 1:0.5, latex to distilled water and then centrifuged before further analysis as reported by Hafid et al. (2020) Other workers either used the *C. papaya* latex immediately for papain isolation or stored it at -8°C under nitrogen atmosphere before further analysis (Monti et al., 2000).

Three phase partitioning, followed by molecular exclusion chromatography were used to isolate and separate two active proteases from the latex of *E. tirucalli*: a serine protease *E.*

tiru SP and a cysteine protease *E. tiru* CP. Three phase partitioning is a simple, cost-effective, non-chromatographic method used to isolate and purify proteases from various sources, including plants (Dennison and Lovrien, 1997). This method removes contaminating particles and non-active proteins from the crude sample and results in the isolated protease structure being more flexible and hence showing enhanced activity. Non-polar compounds such as lipids and low-molecular mass pigments are contained in the *t*-butanol phase (upper organic phase), while the proteins and proteases are precipitated into the interfacial phase (Dennison and Lovrien, 1997, Eyssen et al., 2021). In the present study *E. tiru* SP and *E. tiru* CP proteases were isolated using a 1:0.4 ratio of the crude latex to *t*-butanol and 40 % ammonium sulfate with a purification fold of 2 and 1.75 respectively. Three phase partitioning removed non-active proteins from the crude latex of *E. tirucalli* and the isolated proteases were partitioned into the interfacial phase. Three phase partitioning has been used to isolate proteases from various plants such as the latex of *Calotropis procera*, pineapple crowns and the leaves of *Moringa oleifera* (Rawdkuen et al., 2010, Gul et al., 2022, Abdoulaye et al., 2023). Different ratios of the crude extract to *t*-butanol were used, from 1:0.5 to 1:0.75, together with relatively high concentrations of ammonium sulfate (65-70%), but a lower concentration of 35% in the latter case. In all these instances the respective proteases were partitioned into the interfacial phase. In this instance, using a 1:0.5 ratio of crude latex to *t*-butanol and 65% ammonium sulfate resulted in a 6.92-fold increase in the purity of the protease in the interfacial phase (Rawdkuen et al., 2010). Bromelain was purified from pineapple crowns in a one-step TPP method using 1:0.5 crude extract to *t*-butanol ratio and 70% ammonium sulfate (Gul et al., 2022). The 26 kDa bromelain was partitioned into the interfacial phase of TPP, and had optimal activity at pH 7 and 35°C. A protease was isolated by TPP from the leaves of *Moringa oleifera* using 35% ammonium sulfate with a 1:0.75 ratio of crude extract to *t*-butanol with a 96.20% recovery in the interfacial phase (Abdoulaye et al., 2023).

The two proteases, *E. tiru* SP and *E. tiru* CP, were separated by MEC using a S-200 Sephacryl column. In other studies, the processed crude latex was directly loaded onto various chromatography columns for purification. Milin was isolated from the latex of *Euphorbia milii* Des Moul. (crown of thorns) using a single SP-Sepharose fast flow cation exchange chromatography step (Yadav et al., 2006a). Analysis by SDS-PAGE showed a single protein band of 51 kDa and the protease had optimal activity at pH 8 and 60°C. Milin was classified as a serine protease as its activity was inhibited by PMSF and not by E-64. Serine proteases named euphorbains y-1, -2 and -3 were isolated from the latex of *E. cyparissias* (cypress spurge), firstly by Sephadex G-25 chromatography to remove low molecular weight components and pigments from the crude latex (Lynn and Clevette-Radford, 1984c).

Thereafter, the active fraction was applied to a DEAE-Sepharose CL-6B anion exchange column that separated euphorbain y-3 (68 kDa) from euphorbains y-1 and y-2. The protein peak containing euphorbains y-1 (66 kDa) and y-2 (31 kDa) was separated by molecular exclusion chromatography using a high-pressure liquid chromatography (HPLC) system. The size of euphorbain y-3 was determined on the same HPLC column and were similar to the sizes obtained by SDS-PAGE. The protein electrophoresis technology available at the time (tube, rather than gel slabs) may well explain why electrophoretograms were not presented.

These authors used the same procedure to isolate four 74 kDa active serine proteases, euphorbains t_1 – t_4, from the latex of *E. tirucalli* (Lynn and Clevette-Radford, 1985). These isolated proteases are similar to the single 75 kDa *E. tiru* SP isolated in the present study (Figure 3.1C). Although the authors stated the results of SDS-PAGE analysis, as showing 33.5 kDa band, the results were not shown. The authors deduced that this was a monomeric unit since it did not show under chromatography analysis (Lynn and Clevette-Radford, 1985). The 33.5 kDa band could correspond to the 35 kDa *E. tiru* CP, (Figure 3.1C), however an SDS-PAGE gel would provide better representation by showing the proteins present in the crude latex as well as the isolated euphorbains t_1 – t_4. The technology constraints at the time mentioned above are nevertheless appreciated. The optimum pH for the hydrolysis of a synthetic substrate, Z-Gly-p-nitrophenyl ester, by euphorbains t_1 – t_4 showed a maximum at pH 7.5, while in the present study *E. tiru* SP showed activity against Z-Arg-Arg-AMC from pH 4 to 9 (Figure 3.3).

Proteins isolated by acetone precipitation from the latex of *E. tirucalli* in a previous study, were collectively named euphorbian T, of sizes 36.5, 39, 44 and 50 kDa (Sharma et al., 2014). The SDS-PAGE gel presented, only shows the sample after acetone precipitation, and no comparative sample was shown from before purification was done. The one-step acetone precipitation method was not explained as to how much acetone was used or how the procedure was carried out to make it possible for other researchers to use the method. The catalytic class of protease that euphorbian T belongs to was not determined, but the protease showed maximum milk clotting ability at 65 °C (Sharma et al., 2014). Milk clotting ability was tested in the presence and absence of calcium (Figure 3.19) for which calcium decreased the time for milk clotting. A similar observation was made with euphorbian T, as the milk clotting time decreased as the temperature increased. *E. tiru* SP showed activity from pH 4 to 9 and *E. tiru* CP from pH 5 to 8 (Figure 3.3), while euphorbian T showed optimal activity at pH at 6 and decreased activity at highly acidic and basic pH (Sharma et al., 2014).

A cysteine protease inhibitor, tirustatin, was isolated by size exclusion chromatography using a Biogel P100 column from the stems of *E. tirucalli* (Milhm et al., 2022). Tirustatin (25.97 kDa)

had inhibitory activity against papain and was stable from pH 3 to pH 10, with maximum activity at pH 6 as well as increased inhibitory activity as the temperature increased from 30°C to 100°C (Milhm et al., 2022). Analysis of the *E. tirucalli* latex reported here, demonstrated a 25 kDa protein band in the 20% TPP fraction (Figure 3.1B) that showed no proteolytic activity (Figure 3.1C). This 25 kDa protein band should be tested for inhibitory activity using reverse zymography as was done in the present study for the 40% TPP fraction of *E. triangularis*.

A study conducted by de Freitas et al. (2010) stated that no proteolytic activity was found in the latex of *E. tirucalli* after gelatin containing zymogram analysis. Their observation contrasts with the findings of this study as proteolytic activity was observed in the crude latex of *E. tirucalli* showing two active proteases *E. tiru* CP and *E. tiru* SP of sizes 37 and 75 kDa respectively (Figure 3.1C).

This is the first report on proteases isolated from the latex of *E. triangularis* and three serine proteases *E. laris* SP1, *E. laris* SP2 and *E. laris* SP3, were detected at 97.4, 68 and 38 kDa respectively (Figure 3.7C) with a purification fold of 13.5. Three phase partitioning was compared to acetone fractionation that is routinely used and appears to be superior for protease isolation, since TPP concentrated the proteins present in the crude latex while acetone fractionatiom produced a low concentration of protein (Figure 3.9). A papain-like cysteine protease, philibertain g I of size 23.53 kDa was purified by acetone precipitation followed by cation exchange chromatography from the latex of *Philibertia gilliesii* Hook. & Arn. (Sequeiros et al., 2005). In the present study *p*-aminobenzamidine (reversible serine protease inhibitor)-affinity chromatography was done after TPP with the aim to isolate serine proteases from the TPP fraction. Three proteins (*E. laris* SP1-SP3) were indeed isolated as can be seen when comparing with the TPP fraction that showed the presence of many protein bands. However, the three proteases were not separated from one another (Figure 3.11), suggesting that they have a similar affinity for the para-aminobenzamidine affinity matrix. An alternative method of separation could be molecular exclusion chromatography using a Sephacryl S-200 resin to separate the proteins of >97.6, 68 and 38 kDa. These results observed for *E. triangularis* are similar to those reported by Sufiate et al. (2021) where the latex from *E. trigona* (African milk tree) showed three proteins: trigonin 1, 2 and 3 of sizes 36, 31 and 29 kDa respectively. Although these sizes differ from those of the *E. triangularis* proteases, analysis of their activity on a casein-containing zymogram gel showed the proteases to be of higher molecular weights. It would have been informative if these authors included a non-reducing SDS-PAGE gel for comparison to the casein zymogram gel.

Proteases isolated from other plants belonging to the genus *Euphorbia* include euphorbain p, a multi-chain 74 kDa serine protease, was isolated from the latex of *Euphorbia pulcherrima*

(poinsettia) by DEAE-Sephadex CL-6B anion exchange chromatography, eluting at 300 mM NaCl on a 0 to 1 M salt gradient , followed by Sephadex-100 and Sephacryl S-300 molecular exclusion chromatography resulting in a single active peak (Lynn and Clevette-Radford, 1984a). Hirtin, a 34 kDa serine protease, was isolated from the latex of *Euphorbia hirta* (asthma plant) by Q-Sepharose anion exchange chromatography followed by Superdex 200 gel chromatography (Patel et al., 2012). Hirtin was inhibited by PMSF and AEBSF and showed optimal activity at pH 7.2 and 50°C. A 43 kDa glycosylated cysteine protease isolated from the latex of *Euphorbia nivulia* (leafy milk hedge, holy milk hedge or dog's tongue) by acetone precipitation and DEAE cellulose chromatography, showed optimal activity at pH 6.6 and 45°C (Badgujar and Mahajan, 2013b). A cucumisin-like serine protease of 80 kDa, was isolated from the latex of *Euphorbia sapina* (accepted name *E. maculate* L. or spotted spurge) by DEAE-cellulose and DEAE-Sepharose anion exchange chromatography. EuRP-61, a 61 kDa serine protease, was isolated from the latex of *Euphorbia resinifera* (resin spurge) by ethanol precipitation followed by HiTrap SP FF cation exchange and HiTrap phenyl FF hydrophobic chromatography (Siritapetawee et al., 2020). It is therefore evident that chromatography methods are most commonly used to isolate proteases from the latex of the *Euphorbia* species. In a few cases acetone and ethanol precipitation followed by chromatographic methods were used, whereas in this study TPP was first used before any chromatography methods.

The observation of darkly stained protean bands in gelatin-zymograms of *E. triangularis* latex samples in addition to clear bands denoting proteolytic activity, prompted using reverse zymography to determine if these protein bands represent protease inhibitors. Neither cysteine nor serine protease inhibitors were detected in the latex of *E. triangularis* (Figure 3.14). This observation concurs with literature that protease inhibitors are mostly found in plant storage tissues, leaves and seeds (Ryan, 1990, Leo et al., 2002). Although an *in-silico* investigation of phytochemicals of *E. hirta* identified potential SARS-CoV-2 main protease (a cysteine protease) inhibitors, these were all small phenylpropanoid and polyketide molecules (Cayona and Creencia, 2021). In future, the leaves and seeds of *E. triangularis* could be investigated for the presence of protease inhibitors.

In this study*, E. tiru* SP and *E. tiru* CP (cysteine protease) from the latex of *E. tirucalli* and *E. laris* SP1, *E. laris* SP2 and *E. laris* SP3 from the latex of *E. triangularis* were classified as serine and cysteine protease since they were inhibited by catalytic class specific inhibitors PMSF, SBTI and TPCK for serine proteases and E-64 for cysteine proteases (Figure 3.4 and 3.10). Milin was classified as a serine protease on account of inhibition by PMSF, p-(amidinophenyl)methanesulfonyl fluoride (APMSF) and diisopropyl fluorophosphates (DFP),

however, SBTI did not inhibit milin as it had proteolytic activity of 105% (Yadav et al., 2006a). The activity of all four serine proteases, *E. tiru* SP and *E. laris* SP1-3, were inhibited by SBTI.

In this study the effect of pH on proteolytic activity of crude latex from both *E. tirucalli* and *E. triangularis* were shown on gelatin containing zymogram gels incubated separately from pH 4 to 9 in constant ionic strength AMT buffers. It is essential to use constant ionic strength buffers to test for enzyme activity over a pH range, since the ionic strength affects enzyme activity. It is often not appreciated that the ionic strength of phosphate varies greatly over its effective pH range, i.e. one pH unit below and above the pKa of 7.21 (Ellis and Morrison, 1982, Dehrmann et al., 1995). The pH optimum of 7 reported for casein hydrolysis by prunifoline isolated from *E. prunifolia* may therefore be questioned since the authors used different buffer systems to cover the pH range of 4.5 to 9.5 (acetate, phosphate and carbonate). Additionally some of the buffers were used at pH values outside their buffering capacity (Mahajan and Adsul, 2015). In future studies the effect of pH (using AMT buffers) on substrate hydrolysis would need to be tested on the purified proteases *E. tiru* SP, *E. tiru* CP and once separated, the *E. laris* SP1-3 proteases.

Since commercially available papain preparations show anomalous behaviour on gelatin-containing SDS-PAGE gels in that proteolytic activity is observed at a size greater than 97.4 kDa, instead of the expected 23.4 kDa, papain was isolated from the latex of *Carica papaya* using two different one-step methods: TPP according to Hafid et al. (2020) and CM-cellulose chromatography according to Monti et al. (2000). Although both isolation methods resulted in a 26 kDa protein observed on reducing SDS-PAGE (Figures 3.15 and 3.17), the freshly isolated papain showed the same behaviour on a gelatin zymogram as commercial papain, with clear zones of activity at >97.4 kDa (Figure 3.1C). Although Hafid et al. (2020) also used TPP for the isolation of papain that showed a single protein band at 26 kDa on reducing SDS-PAGE, they did not analyse papain on a gelatin zymogram gel, but only reported a 134% increase in activity when tested against the substrate casein. When comparing the two methods, isolation by CM-cellulose chromatography is preferred over the TPP/ammonium sulfate method as it did not require so many steps and days of overnight dialysis.

The only studies where the proteolytic activity of papain has been shown on gelatin-containing zymogram gels, were for papain mutants. In the one study a mutant form of papain was produced from a wild-type (WT) pro-papain clone to improve the thermostability of papain (Choudhury et al., 2010). Single (K174R), double (K174RV32S) or triple (K174RV32SG36S) papain mutants were produced by substituting one to three amino acids in the interdomain region. While the single mutant had almost no activity, the double and triple mutants showed enhanced activity in different enzyme assays, including a gelatin zymogram. Molecular

modelling studies confirmed that increased numbers of interdomain H-bond and salt bridge interactions in the double and triple mutants increased their thermostability and hence proteolytic activity. The 40 kDa wild type and mutant forms of pro-papain were analysed on reducing SDS-PAGE, and a gel strip from the zymogram showing gelatinolytic activity for the wild type, double and triple mutants was lined up with the 40 kDa size of the reducing SDS-PAGE gel. In the absence of molecular mass markers on the zymogram gel, it is not clear at what size the gelatinolytic activity was observed. In another study, papain mutants were made by replacing the Ile-86 of the pro-peptide region with either Phe, Val or Ala, to determine if any of these hydrophobic residues would affect the proteolytic activity of the mature protease after autocatalytic removal of the inhibitory pro-peptide. Analysis on a gelatin zymogram gel showed two major areas of activity at 66 and 30 kDa for the wild type papain and each of the mutants (Dutta et al., 2016). As in the earlier study, no molecular mass marker was shown on the zymogram and the sizes were extrapolated from the adjacent reducing SDS-PAGE gel's molecular mass markers.

In other studies, papain was isolated from the latex of green fruit and the leaves of *C. papaya* using a combination of ammonium sulfate, sodium chloride and TCA precipitation (Bala and Padma, 2019). Both the latex and the leaves where dried for several days and ground to a powder before being dissolved in a suitable buffer for isolation, while in this study liquid latex was used. Although no SDS-PAGE gels or western blots to detect the isolated papain, were presented, the authors stated that papain was confirmed in both the leaf and latex by its milk clotting ability (Bala and Padma, 2019). Papain was also isolated from the latex of green papaya fruit by an aqueous two-phase system (ATPS) using polyethylene glycol (PEG) 4000 and 6000 with 40% phosphate or 40% ammonium sulfate. This method showed high protein recovery of 96-100%, but proteolytic activity was not shown on a zymogram gel (Li et al., 2010).

Babalola et al. (2023) isolated five papain enzymes, papain A-E from the leaves of *C. papaya*, by a three-step purification method that included 70% ammonium sulfate precipitation, DEAE-cellulose and Sephadex G-25 chromatography. Papain A-E showed optimum activity at 59°C, 58°C, 59°C, 59°C and 50°C r and at pH 5.5, 6.7, 4.5, 4.5 and 5.5 respectively. Papain E showed to have the best catalytic efficiency and substrate binding affinity while papain A had the lowest activity when using casein as a substrate. Other studies have only isolated papain from different parts of the plant and have not observed the presence of other enzyme forms. A study by Esti et al. (2013) showed the isolation of papain from the ripe fruit and latex with proteolytic activity in the latex much higher than in the fruit. Fruit papain and latex papain both showed good hydrolytic activity against the substrate Bz-Phe-Val-Arg-pNA. Papain was isolated first by 45% ammonium sulfate and 10% (w/v) sodium chloride precipitation and then

by an aqueous two-phase system using PEG 6000 and ammonium sulfate from the latex of *C. papaya* (Nitsawang et al., 2006). They reported the presence of five protein bands corresponding to papain, chitinase, chymopapain, glycyl endopeptidase and caricain. The aqueous two-phase system provided a simple means of isolating pure papain that was free from any contaminants (Nitsawang et al., 2006).

The crude latex of *E. tirucalli*, *E. triangularis* and *C. papaya* showed milk clotting ability with and without the presence of calcium chloride, however, the presence of calcium decreased the time for milk clotting (Figure 3.19). Since the crude latex was used, it is not certain which active protease in the latex was responsible for milk clotting hence, *E. tiru* CP, *E. tiru* SP, *E. laris* SP1, *E. laris* SP2 and *E. laris* SP3 should be tested separately for their milk clotting ability. Milk clotting is an important process in the dairy industry, that transforms milk into cheese in three steps: coagulation, dewatering and refining (Troch et al., 2017). Coagulation occurs when the enzyme is added to milk and the peptide bond of κ casein is cleaved, leading to the destabilisation of casein micelles resulting in the aggregation of milk protein (Ben Amira et al., 2017). Dewatering is when water, the remaining component in milk, is removed with the whey and refining refers to the shape and structure of the milk protein. Milk clotting proteases belong to serine, cysteine and aspartic classes of proteases (Shah et al., 2014). Streblin, a 64 kDa serine protease was isolated from the latex of *Streblus asper* by DEAE-Sepharose anion exchange chromatography (Tripathi et al., 2011). Streblin showed stability over a wide pH range of 3-12.5 and strong milk clotting ability. The crude latex of *Calotropis gigantea* showed high milk clotting activity of 450 U/mL and showed maximum milk clotting activity in the presence of 10 mM calcium chloride (Anusha et al., 2014). Aspartic proteases cyprosins 1, 2 and 3 and cardosins (six proteases) are found in the pistils of *Cynara cardunculua* (cardoon flower) and show milk clotting activity (Cordeiro et al., 1994, Folgado and Abranches, 2020). An aspartic protease chymosin, from the abomasum of calves have been used for cheese making however, there is reduced availability of calf rennet and with the increase in demand of cheese (Nicosia et al., 2022), plants have been sourced as substitutes. A study conducted by Mahajan and Chaudhari (2014), showed that the latex of *E. tirucalli*, *E. nerifolia*, *E. nivulia* and *Pedilanthus tithymaloides* had milk clotting activity with *E. tirucalli* exhibiting the highest activity of 74 U/mg, while *Pedilanthus tithymaloides* had the lowest activity of 41.3 U/mg. Zingibain is a 33.8 kDa milk clotting cysteine protease that was isolated from the rhizomes of *Zingiber officinale* by TPP using 50% ammonium sulfate (Gagaoua et al., 2015). Zingibain showed stability at 60°C and pH 7. Milk-clotting activity was enhanced in the presence of calcium, potassium and sodium, with the same observation reported for *E. tirucalli* and *E. triangularis.* Nivulian-II is a 43.7 kDa milk clotting cysteine protease isolated from the latex of *Euphorbia nivulia* (Badgujar and Mahajan, 2014). Nivulian-II showed milk clotting activity of

138.95 U/mg in the presence of 0.01 mM calcium chloride with high stability at pH 6.3. Commercial papain showed 100% milk clotting activity at 50°C however, relatively high proteolytic activity of papain results in very poor milk coagulation (Liburdi et al., 2019).

Proteases isolated from plants have been used in various industrial applications and are not only limited to milk clotting activity. Papain from the fruit, leaves and roots of *C. papaya* have been used as a meat tenderising agent, in the dairy industry for the production of cheese, in the baking industry to reduce the amount of allergenic proteins in cereals, as a teeth whitening agent and in bioethanol production (Fernández-Lucas et al., 2017, Troncoso et al., 2022). Bromelain isolated from the stems and juices of *Ananas comosus*, has been used as a meat tenderising agent, in alcohol production, in the textile industry for protein solubilisation and in biomedicine as an anti-inflammatory agent (Arshad et al., 2014). Ficin from *Ficus carica* found application in the brewing industry for extracting proteins from barley and malt, in the food industry for milk clotting and the pharmaceutical industry for the production of bioactive peptides (Homaei and Etemadipour, 2015). Actinidin from *Actinidia deliciosa* (Kiwi fruit) is used in protein hydrolysis of chicken and fish meat and in alcohol production for solubilising protein aggregates (Morellon-Sterling et al., 2020).

Conclusions and future work

This study reported on the isolation and separation of two proteases from the latex of *E. tirucalli* (*E. tiru* SP and *E. tiru* CP), the isolation of three proteases from the latex of *E. triangularis* (*E. laris* SP1, *E. laris* SP2 and *E. laris* SP3) and the isolation of papain from the latex of *C. papaya* as well as the enzymatic characterisation of the proteases.

Three phase partitioning was shown to be a good method in the removal of non-active proteins and by concentrating the proteins present in the latex for further analysis. Although one disadvantage of TPP for plant proteases is that a much smaller interfacial pellet is produced, leaving limited sample for further analysis. As a consequence, TPP needs to be conducted on a bigger scale requiring large amounts of latex. To collect large amounts of latex, multiple trees would need to be outsourced with incisions being made once every week or two to allow for latex production. The isolated proteases from *E. triangularis* (*E. laris* SP1, *E. laris* SP2 and *E. laris* SP3) can be separated using molecular exclusion chromatography such that properties of each serine protease can be further tested. Testing the thermostability of each of these proteases for further use in the baking and detergent industries where high temperature are used, would be required. In this vein, the 20% ammonium sulfate TPP fraction of the *E tirucalli* latex needs to be tested for plant protease inhibitors by reverse zymography for possible use in the detergent industry by preventing thermal denaturation of the detergent proteases (Pandhare et al., 2002).

Papain was isolated by two methods of which CM-cellulose chromatography was the simplest method. Isolated papain was not observed at 23.4 kDa, but at a size greater than 97.4 kDa in a gelatin containing zymogram gel. This shows that the migration of papain through co-polymerised gelatin is not optimal. Casein zymography can be an alternative, however, it is less sensitive than gelatin zymography as there may not be sufficient hydrolysis of the substrate in the gel, resulting in the hydrolysis zone not being clear (Sijwali and Nivya, 2021). Casein zymography is preferred for the analysis of calpain-1, calapain-2 which showed clear bands of activity and MMP-11, also known as stromelysin-3 (Beurden and Hoff, 2005, Biswas and Tandon, 2019). Plant latex from *E. papillosa*, *E. selloi* and *S. glandulosum* were analysed by casein zymography, which showed similar activity of *E. papillosa* and *E. selloi* while *S. glandulosum* showed minimal activity (Sobottka et al., 2014). An alternative protease such as trypsin or collagenase type I can be used as a control for zymogram gels since the current papain control shows at a size >97.4 kDa. A previous study conducted showed that 3 ng of trypsin shows a clear active band at 24 kDa and collagenase type I showed six active bands ranging from 68 to 130 kDa over a broad range of pH values (shown in my honours project). Trypsin and collagenase would therefore be suitable alternative controls for gelatin zymogram gels.

E. tiru SP of size 74 kDa, showed stability from pH 4 to 9 with and without the presence of cysteine, while *E. tiru* CP of size 35 kDa, showed stability from pH 5 to 8 in the presence of cysteine. *E. laris* SP1, *E. laris* SP2 and *E. laris* SP3 of sizes >97.4, 68 and 38 kDa respectively showed stability from pH 4 to 9 with and without the presence of cysteine. Papain of size 26 kDa was isolated and detected by anti-papain antibodies. All proteases showed increased milk clotting ability in the presence of calcium chloride. This study therefore paved the way for using TPP in combination with chromatography methods to isolate proteases from local *Euphorbia* spp for use as milk clotting agents and meat tenderising agents in the food industry, for alcohol production, for protein solubilisation in the textile industry and to replace harmful chemicals used for tanning in the leather industry.

REFERENCES

Abdoulaye, A., Noumavo, A. D. P., Dah-Nouvlessounon, D., Ohin, M., Bayraktar, H., Bade, F., Bankolé, H., Baba-Moussa, L. & Baba-Moussa, F. (2023). Purification of *Moringa oleifera* leaves protease by three-phase partitioning and investigation of its potential antibacterial activity. *American Journal of Plant Sciences,* **14,** 64-76.

Abdulkadir, A., Umar, I., Ibrahim, S., Onyike, E. & Kabiru, A. (2016). Cysteine protease inhibitors from *Calotropis procera* with antiplasmodial potential in mice. *Journal of Advances in Medical and Pharmaceutical Sciences,* **6,** 1-13.

Agrawal, A. A. & Konno, K. (2009). Latex: A model for understanding mechanisms, ecology, and evolution of plant defense against herbivory. *Annual Review of Ecology, Evolution, and Systematics,* **40,** 311-331.

Ahn, J. W., Kim, M., Lim, J. H., Kim, G. T. & Pai, H. S. (2004). Phytocalpain controls the proliferation and differentiation fates of cells in plant organ development. *Plant Journal,* **38,** 969-81.

Aider, M. (2021). Potential applications of ficin in the production of traditional cheeses and protein hydrolysates. *JDS Communications,* **2,** 233-237.

Al-Tubuly, A. A. (2000). SDS-PAGE and western blotting. *Methods in Molecular Medicine,* **40,** 391-405.

Aljbory, Z. & Chen, M.-S. (2018). Indirect plant defense against insect herbivores: A review. *Insect Science,* **25,** 2-23.

Anusha, R., Singh, M. K. & Bindhu, O. (2014). Characterisation of potential milk coagulants from *Calotropis gigantea* plant parts and their hydrolytic pattern of bovine casein. *European Food Research and Technology,* **238,** 997-1006.

Archer, B. L. (1983). An alkaline protease inhibitor from *Hevea brasiliensis* latex. *Phytochemistry,* **22,** 633-639.

Arima, K., Uchikoba, T., Yonezawa, H., Shimada, M. & Kaneda, M. (2000). Cucumisin-like protease from the latex of *Euphorbia supina*. *Phytochemistry,* **53,** 639-44.

Arshad, Z. I., Amid, A., Yusof, F., Jaswir, I., Ahmad, K. & Loke, S. P. (2014). Bromelain: An overview of industrial application and purification strategies. *Applied Microbiology and Biotechnology,* **98,** 7283-97.

Azarkan, M., Maquoi, E., Delbrassine, F., Herman, R., M'rabet, N., Calvo Esposito, R., Charlier, P. & Kerff, F. (2020). Structures of the free and inhibitors-bound forms of bromelain and ananain from *Ananas comosus* stem and in vitro study of their cytotoxicity. *Scientific Reports,* **10,** 19570.

Babalola, B. A., Akinwande, A. I., Gboyega, A. E. & Otunba, A. A. (2023). Extraction, purification and characterization of papain cysteine-proteases from the leaves of *Carica papaya*. *Scientific African,* **19,** e01538.

Badgujar, S. & Mahajan, R. (2013a). Identification and characterization of *Euphorbia nivulia* latex proteins. *International Journal of Biological Macromolecules,* **64**.

Badgujar, S. B. & Mahajan, R. T. (2013b). Characterization of thermo- and detergent stable antigenic glycosylated cysteine protease of *Euphorbia nivulia* buch.-ham. And evaluation of its ecofriendly applications. *TheScientificWorldJournal,* **2013,** 716545-716545.

Badgujar, S. B. & Mahajan, R. T. (2014). Nivulian-ii a new milk clotting cysteine protease of *Euphorbia nivulia* latex. *International Journal of Biological Macromolecules,* **70,** 391-8.

Baeyens-Volant, D., Matagne, A., El Mahyaoui, R., Wattiez, R. & Azarkan, M. (2015). A novel form of ficin from *Ficus carica* latex: Purification and characterization. *Phytochemistry,* **117,** 154-167.

Bala, B. N. & Padma, A. S. (2019). Isolation of papain from leaf & latex of papaya (*Carica papaya*) and study of various factors affecting enzyme activity. *International Journal of Scientific Research in Biological Sciences,* **06,** 89-92.

Balakireva, A. V., Kuznetsova, N. V., Petushkova, A. I., Savvateeva, L. V. & Zamyatnin, A. A., Jr. (2019). Trends and prospects of plant proteases in therapeutics. *Current Medicinal Chemistry,* **26,** 465-486.

Balls, A. K. & Hoover, S. R. (1937). The milk-clotting action of papain. *Journal of Biological Chemistry,* **121,** 737-745.

Bandaranayake, W. M. (2006). Quality control, screening, toxicity, and regulation of herbal drugs. *In:* Ahmad, D. I., Aqil, F. & Owais, D. M. (eds.) *Modern phytomedicine: Turning medicinal plants into drugs.*

Barberis, S., Quiroga, E., Arribére, M. a. C. & Priolo, N. (2002). Peptide synthesis in aqueous–organic biphasic systems catalyzed by a protease isolated from *Morrenia brachystephana* (Asclepiadaceae). *Journal of Molecular Catalysis B: Enzymatic,* **17,** 39-47.
Barrett, A., Rawlings, N. & Woessner, J. (1998). Introduction: Cysteine peptidases and their clans. *Handbook of Proteolytic Enzymes***,** 545-66.
Barrett, A. J. & Kirschke, H. (1981). Cathepsin B, cathepsin H, and cathepsin l. *Methods in Enzymology,* **80 Pt C,** 535-61.
Barrett, A. J. & Rawlings, N. D. (1996). Families and clans of cysteine peptidases. *Perspectives in Drug Discovery and Design,* **6,** 1-11.
Basith, S., Cui, M., Hong, S. & Choi, S. (2016). Harnessing the therapeutic potential of capsaicin and its analogues in pain and other diseases. *Molecules (Basel, Switzerland),* **21,** 966.
Batista, I. F. C., Oliva, M. L. V., Araujo, M. S., Sampaio, M. U., Richardson, M., Fritz, H. & Sampaio, C. a. M. (1996). Primary structure of a kunitz-type trypsin inhibitor from *Enterolobium contortisiliquum* seeds. *Phytochemistry,* **41,** 1017-1022.
Becker, J. M., **Caldwell, G. A.** & **Zachgo, E. A.** (1996). Exercise 13 - protein assays. *In:* Becker, J. M., Caldwell, G. A. & Zachgo, E. A. (eds.) *Biotechnology (second edition).* San Diego: Academic Press.
Bekalu, Z. E., Dionisio, G. & Brinch-Pedersen, H. (2020). Molecular properties and new potentials of plant nepenthesins. *Plants,* **9,** 570.
Bekalu, Z. E., Dionisio, G., Madsen, C. K., Etzerodt, T., Fomsgaard, I. S. & Brinch-Pedersen, H. (2021). Barley nepenthesin-like aspartic protease hvnep-1 degrades *Fusarium phytase*, impairs toxin production, and suppresses the fungal growth. *Frontiers in Plant Science,* **12**.
Bekhit, A. A., Hopkins, D. L., Geesink, G., Bekhit, A. A. & Franks, P. (2014). Exogenous proteases for meat tenderization. *Critical Reviews in Food Science and Nutrition,* **54,** 1012-1031.
Ben Amira, A., Besbes, S., Attia, H. & Blecker, C. (2017). Milk-clotting properties of plant rennet and their enzymatic, rheological, and sensory role in cheese making: A review. *International Journal of Food Properties,* **44**.
Bendre, A. D., Ramasamy, S. & Suresh, C. G. (2018). Analysis of kunitz inhibitors from plants for comprehensive structural and functional insights. *International Journal of Biological Macromolecules,* **113,** 933-943.
Beurden, P. a. M. S.-V. & Hoff, J. W. V. D. (2005). Zymographic techniques for the analysis of matrix metalloproteinases and their inhibitors. *Biotechniques,* **38,** 73-83.
Beynon, R. & Salvesen, G. S. (2001). Appendix iii. Commercially available proteinase inhibitors,. *In:* R, B. & JS, B. (eds.) *Proteolytic enzymes. A practical approach.* Oxford: Oxford University Press.
Bhagyashri, A. C., Jogendra, C. H., Avinash, V., Patil, S., Jo, L. & Pharm., D. (2015). Plant latex: An inherent spring of pharmaceuticals. *World Journal of Pharmacy and Pharmaceutical Sciences,* **4,** 2278 – 4357.
Bhowmick, R., Kumari, N., Jagannadham, M. & Kayastha, A. (2008). Purification and characterization of a novel protease from the latex of *Pedilanthus tithymaloides*. *Protein and peptide letters,* **15,** 1009-16.
Binckley, S. & Zahra, F. (2021). *Euphorbia tirucalli* [Online]. Treasure Island (FL): StatPearls Publishing. Available: https://www.ncbi.nlm.nih.gov/books/NBK574526/ [Accessed 16 March 2022].
Biswas, A. K. & Tandon, S. (2019). Casein zymography for analysis of calpain-1 and calpain-2 activity. *Methods in Molecular Biology,* **1915,** 31-38.
Blum, H., Beier, H. & Gross, H. J. (1987). Improved silver staining of plant proteins, rna and DNA in polyacrylamide gels. *Electrophoresis,* **156,** 93-99.
Bobofchak, K. M., Pineda, A. O., Mathews, F. S. & Di Cera, E. (2005). Energetic and structural consequences of perturbing gly-193 in the oxyanion hole of serine proteases. *Journal of Biological Chemistry,* **280,** 25644-50.
Bradford, M. M. (1976). A rapid and sensitive method for the quantitation of microgram quantities of protein utilizing the principle of protein-dye binding. *Analytical Biochemistry,* **72,** 248-254.
Brook, K., Bennett, J. & Desai, S. P. (2017). The chemical history of morphine: An 8000-year journey, from resin to de-novo synthesis. *Journal of Anesthesia History,* **3,** 50-55.
Campos, D. A., Coscueta, E. R., Valetti, N. W., Pastrana-Castro, L. M., Teixeira, J. A., Picó, G. A. & Pintado, M. M. (2019). Optimization of bromelain isolation from pineapple byproducts by polysaccharide complex formation. *Food Hydrocolloids,* **87,** 792-804.
Carstens, M., Mccrindle, T. K., Adams, N., Diener, A., Guzha, D. T., Murray, S. L., Parker, J. E., Denby, K. J. & Ingle, R. A. (2014). Increased resistance to biotrophic pathogens in the

Arabidopsis constitutive induced resistance 1 mutant is eds1 and pad4-dependent and modulated by environmental temperature. *Public Library of Science One,* **9,** e109853.
Cayona, R. & Creencia, E. (2021). Phytochemicals of *Euphorbia hirta* l. And their inhibitory potential against sars-cov-2 main protease. *Front Mol Biosci,* **8,** 801401.
Chaiwut, P., Pintathong, P. & Rawdkuen, S. (2010). Extraction and three-phase partitioning behavior of proteases from papaya peels. *Process Biochemistry,* **45,** 1172-1175.
Chakravarthy, P. & Acharya, S. (2012). Efficacy of extrinsic stain removal by novel dentifrice containing papain and bromelain extracts. *Journal of Young Pharmacists,* **4,** 245-9.
Chanda, I., Basu, S., Dutta, S. & Das, S. (2011). A protease isolated from the latex of *Plumeria rubra* linn (Apocynaceae) 1: Purification and characterization. *Tropical Journal of Pharmaceutical Research,* **10**.
Charney, J. & Tomarelli, R. M. (1947). A colorimetric method for the determination of the proteolytic activity of duodenal juice. *Journal of Biological Chemistry,* **171,** 501-5.
Choudhury, D., Biswas, S., Roy, S. & Dattagupta, J. K. (2010). Improving thermostability of papain through structure-based protein engineering. *Protein Engineering, Design and Selection,* **23,** 457-467.
Coates, L., Tuan, H.-F., Tomanicek, S., Kovalevsky, A., Mustyakimov, M., Erskine, P. & Cooper, J. (2008). The catalytic mechanism of an aspartic proteinase explored with neutron and x-ray diffraction. *Journal of the American Chemical Society,* **130,** 7235-7237.
Coelho-Ferreira, M. (2009). Medicinal knowledge and plant utilization in an amazonian coastal community of Marudá, Pará State (Brazil). *Journal of Ethnopharmacology,* **126,** 159-175.
Cordeiro, M. C., Pais, M. S. & Brodelius, P. E. (1994). Tissue-specific expression of multiple forms of cyprosin (aspartic proteinase) in flowers of *Cynara cardunculus*. *Physiologia Plantarum,* **92,** 645-653.
Corzo, C. A., Waliszewski, K. N. & Welti-Chanes, J. (2012). Pineapple fruit bromelain affinity to different protein substrates. *Food Chemistry,* **133,** 631-635.
Crowell, A. M. J., Wall, M. J. & Doucette, A. A. (2013). Maximizing recovery of water-soluble proteins through acetone precipitation. *Analytica Chimica Acta,* **796,** 48-54.
Cui, N., Hu, M. & Khalil, R. A. (2017). Biochemical and biological attributes of matrix metalloproteinases. *Progress in Molecular Biology and Translational Science,* **147,** 1-73.
David, K. (2017). Cell division and cell differentiation. *In:* Thomas, B., Murray, B. G. & Murphy, D. J. (eds.) *Encyclopedia of applied plant sciences (second edition).* Oxford: Academic Press.
De Freitas, C. D. T., De Souza, D. P., Araújo, E. S., Cavalheiro, M. G., Oliveira, L. S. & Ramos, M. V. (2010). Anti-oxidative and proteolytic activities and protein profile of laticifer cells of *Cryptostegia grandiflora*, *Plumeria rubra* and *Euphorbia tirucalli*. *Brazilian Society of Plant Physiology,* **22,** 11-22.
De Leo, F., Volpicella, M., Licciulli, F., Liuni, S., Gallerani, R. & Ceci, L. R. (2002). Plant-pis: A database for plant protease inhibitors and their genes. *Nucleic Acids Research,* **30,** 347-348.
De Veer, S. J., White, A. M. & Craik, D. J. (2021). Sunflower trypsin inhibitor-1 (sfti-1): Sowing seeds in the fields of chemistry and biology. *Angewandte Chemie International Edition,* **60,** 8050-8071.
Dehrmann, F. M., Coetzer, T. H., Pike, R. N. & Dennison, C. (1995). Mature cathepsin l is substantially active in the ionic milieu of the extracellular medium. *Archives of Biochemistry and Biophysics,* **324,** 93-8.
Dennison, C. & Lovrien, R. (1997). Three phase partitioning: Concentration and purification of proteins. *Protein Expression and Purification,* **11,** 149-161.
Desborough, M. J. R. & Keeling, D. M. (2017). The aspirin story - from willow to wonder drug. *British Journal of Haematology,* **177,** 674-683.
Dharmadasa, R. M., Akalanka, G. C., Muthukumarana, P. R. M. & Wijesekara, R. G. S. (2016). Ethnopharmacological survey on medicinal plants used in snakebite treatments in Western and Sabaragamuwa provinces in Sri Lanka. *Journal of Ethnopharmacology,* **179,** 110-127.
Dhiman, V. K., Chauhan, V., Kanwar, S. S., Singh, D. & Pandey, H. (2021). Purification and characterization of actinidin from *Actinidia deliciosa* and its utilization in inactivation of α-amylase. *Bulletin of the National Research Centre,* **45,** 213.
Di Cera, E. (2009). Serine proteases. *International Union of Biochemistry and Molecular Biology,* **61,** 510-5.
Dodson, G. & Wlodawer, A. (1998). Catalytic triads and their relatives. *Trends in Biochemical Sciences,* **23,** 347-352.
Dubey, R., Reddy, S. & Murthy, N. Y. S. (2012). Optimization of activity of bromelain. *Asian Journal of Chemistry,* **24,** 1429-1431.

Dubey, V. K. & Jagannadham, M. V. (2003). Procerain, a stable cysteine protease from the latex of *Calotropis procera*. *Phytochemistry,* **62,** 1057-71.
Dutta, S., Choudhury, D., Roy, S., Dattagupta, J. K. & Biswas, S. (2016). Mutation in the pro-peptide region of a cysteine protease leads to altered activity and specificity-a structural and biochemical approach. *Public Library of Science One,* **11,** e0158024-e0158024.
Ekor, M. (2014). The growing use of herbal medicines: Issues relating to adverse reactions and challenges in monitoring safety. *Frontiers in Pharmacology,* **4,** 177-177.
Ellis, K. J. & Morrison, J. F. (1982). Buffers of constant ionic strength for studying pH-dependent processes. *Methods in Enzymology,* **87,** 405-26.
Englund, P. T., King, T. P., Craig, L. C. & Walti, A. (1968). Ficin. I. Its isolation and characterization. *Biochemistry,* **7,** 163-175.
Esti, M., Benucci, I., Lombardelli, C., Liburdi, K. & Garzillo, A. M. V. (2013). Papain from papaya (*Carica papaya* l.) fruit and latex: Preliminary characterization in alcoholic–acidic buffer for wine application. *Food and Bioproducts Processing,* **91,** 595-598.
Eun, H.-M. (1996). 1 - enzymes and nucleic acids: General principles. *In:* Eun, H.-M. (ed.) *Enzymology primer for recombinant DNA technology.* San Diego: Academic Press.
Evans, S. A., Olson, S. T. & Shore, J. D. (1982). P-aminobenzamidine as a fluorescent probe for the active site of serine proteases. *Journal of Biological Chemistry,* **257,** 3014-7.
Eyssen, L. E.-A., Goldring, J. P. D. & Coetzer, T. H. T. (2021). Three-phase partitioning (TPP) of proteases from parasites, plants, tissue and bacteria for enhanced activity. *In:* Munishwar Nath Gupta, I. R. (ed.) *Three phase partitioning applications in separation and purification of biological molecules and natural products.* Susan Dennis.
Faurant, C. (2011). From bark to weed: The history of artemisinin. *Parasite,* **18,** 215-8.
Feijoo-Siota, L. & Villa, T. (2010). Native and biotechnologically engineered plant proteases with industrial applications. *Food and Bioprocess Technology,* **4,** 1066-1088.
Fernández-Lucas, J., Castañeda, D. & Hormigo, D. (2017). New trends for a classical enzyme: Papain, a biotechnological success story in the food industry. *Trends in Food Science & Technology,* **68,** 91-101.
Figueiredo, L., Santos, R. & Figueiredo, A. (2021). Defense and offense strategies: The role of aspartic proteases in plant–pathogen interactions. *Biology,* **10,** 75.
Folgado, A. & Abranches, R. (2020). Plant aspartic proteases for industrial applications: Thistle get better. *Plants (Basel, Switzerland),* **9,** 147.
Fricker, S. P. (2010). Cysteine proteases as targets for metal-based drugs. *Metallomics,* **2,** 366-77.
Furstenberg-Hagg, J., Zagrobelny, M. & Bak, S. (2013). Plant defense against insect herbivores. *International Journal of Molecular Sciences,* **14,** 10242-97.
Gagaoua, M. & Hafid, K. (2016). Three phase partitioning system, an emerging non-chromatographic tool for proteolytic enzymes recovery and purification. *Biosensors Journal,* **5**.
Gagaoua, M., Hoggas, N. & Hafid, K. (2015). Three phase partitioning of zingibain, a milk-clotting enzyme from *Zingiber officinale* roscoe rhizomes. *International Journal of Biological Macromolecules,* **73,** 245-52.
García-Lorenzo, M., Sjödin, A., Jansson, S. & Funk, C. (2006). Protease gene families in *Populus* and *Arabidopsis*. *BMC Plant Biology,* **6,** 30.
Ge, X., Dietrich, C., Matsuno, M., Li, G., Berg, H. & Xia, Y. (2005). An *Arabidopsis* aspartic protease functions as an anti-cell-death component in reproduction and embryogenesis. *European Molecualr Biology Organisation reports,* **6,** 282-288.
Geisen, U., Zenthoefer, M., Peipp, M., Kerber, J., Plenge, J., Managò, A., Fuhrmann, M., Geyer, R., Hennig, S., Adam, D., Piker, L., Rimbach, G. & Kalthoff, H. (2015). Molecular mechanisms by which a fucus vesiculosus extract mediates cell cycle inhibition and cell death in pancreatic cancer cells. *Marine Drugs,* **13,** 4470-91.
Gharib, M., Marcantonio, M., Lehmann, S. G., Courcelles, M., Meloche, S., Verreault, A. & Thibault, P. (2009). Artifactual sulfation of silver-stained proteins: Implications for the assignment of phosphorylation and sulfation sites. *Molecular & cellular proteomics : MCP,* **8,** 506-518.
Gilroy, E. M., Hein, I., Van Der Hoorn, R., Boevink, P. C., Venter, E., Mclellan, H., Kaffarnik, F., Hrubikova, K., Shaw, J., Holeva, M., López, E. C., Borras-Hidalgo, O., Pritchard, L., Loake, G. J., Lacomme, C. & Birch, P. R. J. (2007). Involvement of cathepsin B in the plant disease resistance hypersensitive response. *The Plant Journal,* **52,** 1-13.
Gracz-Bernaciak, J., Mazur, O. & Nawrot, R. (2021). Functional studies of plant latex as a rich source of bioactive compounds: Focus on proteins and alkaloids. *International Journal of Molecular Sciences,* **22,** 12427.

Graham, J. S., Xiong, J. & Gillikin, J. W. (1991). Purification and developmental analysis of a metalloendoproteinase from the leaves of *Glycine max*. *Plant Physiology,* **97,** 786-92.
Grudkowska, M. & Zagdańska, B. (2004). Multifunctional role of plant cysteine proteinases. *Acta Biochimica Polonica,* **51,** 609-24.
Gschwendt, M. & Hecker, E. (1969). Tumor promoting compounds from *Euphorbia triangularis*: Mono- and diesters of 12-desoxy-phorbol. *Tetrahedron Letters***,** 3509-12.
Gul, A., Khan, S., Arain, H., Khan, H., Ishrat, U. & Siddiqui, M. (2022). Three-phase partitioning as an efficient one-step method for the extraction and purification of bromelain from pineapple crown waste. *Journal of Food Processing and Preservation,* **46,** e16973.
Haesaerts, S., Rodriguez Buitrago, J. A., Loris, R., Baeyens-Volant, D. & Azarkan, M. (2015). Crystallization and preliminary x-ray analysis of four cysteine proteases from *Ficus carica* latex. *Acta Crystallographica Section F: Structural Biology Communications,* **71,** 459-465.
Hafid, K., John, J., Sayah, T. M., Domínguez, R., Becila, S., Lamri, M., Dib, A. L., Lorenzo, J. M. & Gagaoua, M. (2020). One-step recovery of latex papain from *Carica papaya* using three phase partitioning and its use as milk-clotting and meat-tenderizing agent. *International Journal of Biological Macromolecules,* **146,** 798-810.
Hamed, M. B., El-Badry, M. O., Kandil, E. I., Borai, I. H. & Fahmy, A. S. (2020). A contradictory action of procoagulant ficin by a fibrinolytic serine protease from Egyptian *Ficus carica* latex. *Biotechnology Reports,* **27,** e00492.
Han, J., Li, H., Yin, B., Zhang, Y., Liu, Y., Cheng, Z., Liu, D. & Lu, H. (2018). The papain-like cysteine protease cep1 is involved in programmed cell death and secondary wall thickening during xylem development in *Arabidopsis*. *Journal of Experimental Botany,* **70,** 205-215.
Hanley, M. E., Lamont, B. B., Fairbanks, M. & Rafferty, C. M. (2007). Plant structural traits and their role in anti-herbivore defence. *Perspectives in Plant Ecology Evolution and Systematics,* **8,** 157-178.
Hanspal, J. S., Bushell, G. R. & Ghosh, P. (1983). Detection of protease inhibitors using substrate-containing sodium dodecyl sulfate-polyacrylamide gel electrophoresis. *Analytical Biochemistry,* **132,** 288-293.
Hara-Nishimura, I., Shimada, T., Hatano, K., Takeuchi, Y. & Nishimura, M. (1998). Transport of storage proteins to protein storage vacuoles is mediated by large precursor-accumulating vesicles. *The Plant Cell,* **10,** 825-836.
Harrach, T., Eckert, K., Schulze-Forster, K., Nuck, R., Grunow, D. & Maurer, H. R. (1995). Isolation and partial characterization of basic proteinases from stem bromelain. *Journal of Protein Chemistry,* **14,** 41-52.
Hartl, M., Giri, A. P., Kaur, H. & Baldwin, I. T. (2011). The multiple functions of plant serine protease inhibitors: Defense against herbivores and beyond. *Plant signaling & behavior,* **6,** 1009-11.
Hatsugai, N., Yamada, K., Goto-Yamada, S. & Hara-Nishimura, I. (2015). Vacuolar processing enzyme in plant programmed cell death. *Frontiers in Plant Science,* **6,** 234-234.
Hellinger, R. & Gruber, C. W. (2019). Peptide-based protease inhibitors from plants. *Drug Discov Today,* **24,** 1877-1889.
Hermanson, G. T. (2013). *Trifunctional crosslinkers in: Bioconjugate techniques*.
Heussen, C. & Dowdle, E. B. (1980). Electrophoretic analysis of plasminogen activators in polyacrylamide gels containing sodium dodecyl sulfate and copolymerized substrates. *Analytical Biochemistry,* **102,** 196-202.
Homaei, A. & Etemadipour, R. (2015). Improving the activity and stability of actinidin by immobilization on gold nanorods. *International Journal of Biological Macromolecules,* **72,** 1176-1181.
Hosfield, C. M., Elce, J. S., Davies, P. L. & Jia, Z. (1999). Crystal structure of calpain reveals the structural basis for ca(2+)-dependent protease activity and a novel mode of enzyme activation. *The European Molecular Biology Organisation Journal,* **18,** 6880-6889.
Huang, C., Zhang, R., Gui, J., Zhong, Y. & Li, L. (2018). The receptor-like kinase atvrlk1 regulates secondary cell wall thickening. *Plant Physiology,* **177,** 671-683.
Ilany, J. & Netzer, A. (1969). Milk-clotting activity of proteolytic enzymes. *Journal of Dairy Science,* **52,** 43-46.
Istrati, D. (2008). The influence of enzymatic tenderization with papain on functional properties of adult beef. *Journal of Agroalimentary Processes and Technologies,* **14,** 140-146.
Iwai, K., Kim, M.-Y., Onodera, A. & Matsue, H. (2006). A-glucosidase inhibitory and antihyperglycemic effects of polyphenols in the fruit of *Viburnum dilatatum* thunb. *Journal of Agricultural and Food Chemistry,* **54,** 4588-4592.

Jashni, M. K., Mehrabi, R., Collemare, J., Mesarich, C. H. & De Wit, P. J. (2015). The battle in the apoplast: Further insights into the roles of proteases and their inhibitors in plant-pathogen interactions. *Frontiers in Plant Science,* **6,** 584.

Jones, G. T. (2014). Chapter seven - matrix metalloproteinases in biologic samples. *In:* Makowski, G. S. (ed.) *Advances in clinical chemistry.* Elsevier.

Kadek, A., Tretyachenko, V., Mrazek, H., Ivanova, L., Halada, P., Rey, M., Schriemer, D. C. & Man, P. (2014). Expression and characterization of plant aspartic protease nepenthesin-1 from *Nepenthes gracilis*. *Protein Expression and Purification,* **95,** 121-128.

Kalyana, P., Shashidhar, A., Meghashyam, B., Sreevidya, K. R. & Sweta, S. (2011). Stain removal efficacy of a novel dentifrice containing papain and bromelain extracts--an in vitro study. *International Journal of Dental Hygiene,* **9,** 229-33.

Kamphuis, I. G., Kalk, K. H., Swarte, M. B. A. & Drenth, J. (1984). Structure of papain refined at 1.65 å resolution. *Journal of Molecular Biology,* **179,** 233-256.

Khaparde, S. S. & Singhal, R. S. (2001). Chemically modified papain for applications in detergent formulations. *Bioresource Technology,* **78,** 1-4.

Khumalo, G. P., Van Wyk, B. E., Feng, Y. & Cock, I. E. (2022). A review of the traditional use of Southern African medicinal plants for the treatment of inflammation and inflammatory pain. *Journal of Ethnopharmacology,* **283,** 114436.

Kim, G.-J. & Kim, J.-H. (2015). Development of a simultaneous extraction and acid hydrolysis process for recovery of paclitaxel from plant cell cultures. *Process Biochemistry,* **50,** 279-284.

Kojima, S., Miyoshi, K. & Miura, K. (1996). Synthesis of a squash-type protease inhibitor by gene engineering and effects of replacements of conserved hydrophobic amino acid residues on its inhibitory activity. *Protein Engineering,* **9,** 1241-6.

Konno, K. (2011). Plant latex and other exudates as plant defense systems: Roles of various defense chemicals and proteins contained therein. *Phytochemistry,* **72,** 1510-1530.

Kurek, J. (2019). Introductory chapter: Alkaloids - their importance in nature and for human life. *In:* Kurek, J. (ed.) *Alkaloids - their importance in nature and for human life* London: IntechOpen.

Laemmli, U. K. (1970). Cleavage of structural proteins during the assembly of the head of bacteriophage t4. *Nature,* **227,** 680-685.

Langner, J., Wakil, A., Zimmermann, M., Ansorge, S., Bohley, P., Kirschke, H. & Wiederanders, B. (1973). [activity determination of proteolytic enzymes using azocasein as a substrate]. *Acta Biologica et Medica Germanica,* **31,** 1-18.

Laronha, H. & Caldeira, J. (2020). Structure and function of human matrix metalloproteinases. *Cells,* **9,** 1076.

Lawrence, P. & Koundal, K. (2002). Plant protease inhibitors in control of phytophagous insects. *Electronic Journal of Biotechnology,* **5,** 5-6.

Leo, F. D., Volpicella, M., Licciulli, F., Liuni, S., Gallerani, R. & Ceci, L. R. (2002). Plant-pis: A database for plant protease inhibitors and their genes. *Nucleic Acids Research,* **30,** 347-348.

Lev-Yadun, S. (2014). Why is latex usually white and only sometimes yellow, orange or red? Simultaneous visual and chemical plant defense. *Chemoecology,* **24,** 215-218.

Li, M., Su, E., You, P., Gong, X., Sun, M., Xu, D. & Wei, D. (2010). Purification and in situ immobilization of papain with aqueous two-phase system. *Public Library of Science One,* **5,** e15168-e15168.

Liburdi, K., Boselli, C., Giangolini, G., Amatiste, S. & Esti, M. (2019). An evaluation of the clotting properties of three plant rennets in the milks of different animal species. *Foods (Basel, Switzerland),* **8,** 600.

Lid, S. E., Gruis, D., Jung, R., Lorentzen, J. A., Ananiev, E., Chamberlin, M., Niu, X., Meeley, R., Nichols, S. & Olsen, O. A. (2002). The defective kernel 1 (dek1) gene required for aleurone cell development in the endosperm of maize grains encodes a membrane protein of the calpain gene superfamily. *Proceedings of the National Academy of Sciences of the United States of America,* **99,** 5460-5.

Liggieri, C., Obregon, W., Trejo, S. & Priolo, N. (2009). Biochemical analysis of a papain-like protease isolated from the latex of *Asclepias curassavica* l. *Acta biochimica et biophysica Sinica,* **41,** 154-62.

Lin, D., Xiao, M., Zhao, J., Li, Z., Xing, B., Li, X., Kong, M., Li, L., Zhang, Q., Liu, Y., Chen, H., Qin, W., Wu, H. & Chen, S. (2016). An overview of plant phenolic compounds and their importance in human nutrition and management of type 2 diabetes. *Molecules (Basel, Switzerland),* **21,** 1374.

Liu, Q., Luo, L. & Zheng, L. (2018). Lignins: Biosynthesis and biological functions in plants. *International Journal of Molecular Sciences,* **19,** 335.

Lopez-Otin, C. & Bond, J. S. (2008). Proteases: Multifunctional enzymes in life and disease. *Journal of Biological Chemistry,* **283,** 30433-7.
Luche, S., Santoni, V. & Rabilloud, T. (2003). Evaluation of nonionic and zwitterionic detergents as membrane protein solubilizers in two-dimensional electrophoresis. *Proteomics,* **3,** 249-53.
Lynn, K. R. & Clevette-Radford, N. A. (1984a). Euphorbain p, a serine protease from *Euphorbia pulcherrima*. *Phytochemistry,* **23,** 682-683.
Lynn, K. R. & Clevette-Radford, N. A. (1984b). Purification and characterization of hevain, a serine protease from *Hevea brasiliensis*. *Phytochemistry,* **23,** 963-964.
Lynn, K. R. & Clevette-Radford, N. A. (1984c). Three serine proteases from the latex of *Euphorbia cyparissias*. *Phytochemistry,* **24,** 925-928.
Lynn, K. R. & Clevette-Radford, N. A. (1985). Four serine proteases from the latex of *Euphorbia tirucalli*. *Canadian Journal of Biochemistry and Cell Biology,* **63,** 1093-1096.
Lynn, K. R. & Clevette-Radford, N. A. (1986). Ficin e, a serine-centred protease from *Ficus elastica*. *Phytochemistry,* **25,** 1559-1561.
Magdeldin, S. & Moser, A. (2012). Affinity chromatography: Principles and applications *In:* Magdeldin, S. (ed.) *Affinity chromatography.* IntechOpen.
Mahajan, R. & Chaudhari, G. (2014). Plant latex as vegetable source for milk clotting enzymes and their use in cheese preparation. *International Journal of Advanced Research,* **2,** 1173-1181.
Mahajan, R. T. & Adsul, Y. D. (2015). Isolation, purification and characterization of serine protease from latex of *Euphorbia prunifolia jacq. International Journal of Advanced Research,* **3,** 388-395.
Mahajan, R. T., Khan, J. V. & Khan, T. A. (2016). Evaluation of proteolytic activity of some Euphorbian garden plants. *International journal of life-sciences scientific reasearch* **2,** 355-360.
Mareri, L., Parrotta, L. & Cai, G. (2022). Environmental stress and plants. *International Journal of Molecular Sciences,* **23,** 5416.
Martin, H., Cordiner, S. B. & Mcghie, T. K. (2017). Kiwifruit actinidin digests salivary amylase but not gastric lipase. *Food & Function,* **8,** 3339-3345.
Mavundza, E. J., Street, R. & Baijnath, H. (2022). A review of the ethnomedicinal, pharmacology, cytotoxicity and phytochemistry of the genus *Euphorbia* in Southern Africa. *South African Journal of Botany,* **144,** 403-418.
Menard, R., Carriere, J., Laflamme, P., Plouffe, C., Khouri, H. E., Vernet, T., Tessier, D. C., Thomas, D. Y. & Storer, A. C. (1991). Contribution of the glutamine 19 side chain to transition-state stabilization in the oxyanion hole of papain. *Biochemistry,* **30,** 8924-8928.
Milhm, A. C. P., Bonet, L. F. S., Aiub, C. a. F. & Siqueira Junior, C. L. (2022). Biochemical characterization and phytotoxic activity of protein extract from *Euphorbia tirucalli* l. *Journal of Ethnopharmacology,* **285,** 114903.
Milošević, J., Janković, B., Prodanović, R. & Polović, N. (2019). Comparative stability of ficin and papain in acidic conditions and the presence of ethanol. *Amino Acids,* **51,** 829-838.
Miner, J. & Hoffhines, A. (2007). The discovery of aspirin's antithrombotic effects. *Texas Heart Institute Journal,* **34,** 179-86.
Miura, E., Kato, Y. & Sakamoto, W. (2008). Importance of the balance between protein synthesis and degradation in chloroplasts revealed by the studies of *Arabidopsis* yellow variegated mutants. *In:* Allen, J. F., Gantt, E., Golbeck, J. H. & Osmond, B., eds. Photosynthesis. Energy from the Sun, Dordrecht. Springer Netherlands, 1121-1124.
Mnif, I., Siala, R., Nasri, R., Mhamdi, S. & Sellami-Kamoun, A. (2014). A cysteine protease isolated from the latex of *Ficus microcarpa*: Purification and biochemical characterization. *Applied Biochemistry and Biotechnology,* **175**.
Monroe, D. M., Sherrill, G. B. & Roberts, H. R. (1988). Use of *p*-aminobenzamidine to monitor activation of trypsin-like serine proteases. *Analytical Biochemistry,* **172,** 427-35.
Monti, R., A, B., C, T. & Contiero, J. (2000). Purification of papain from fresh latex of *Carica papaya*. *Brazilian Archives of Biology and Technology,* **43**.
Morellon-Sterling, R., El-Siar, H., Tavano, O. L., Berenguer-Murcia, Á. & Fernández-Lafuente, R. (2020). Ficin: A protease extract with relevance in biotechnology and biocatalysis. *International Journal of Biological Macromolecules,* **162,** 394-404.
Mugford, S. T. & Milkowski, C. (2012). Chapter fourteen - serine carboxypeptidase-like acyltransferases from plants. *In:* Hopwood, D. A. (ed.) *Methods in enzymology.* Academic Press.
Mutlu, A. & Gal, S. (1999). Plant aspartic proteinases: Enzymes on the way to a function. *Physiologia Plantarum,* **105,** 569-576.

Mwine, J., Van Damme, P., Hastilestari, B. R. & Papenbrock, J. (2013). *Euphorbia tirucalli* l. (Euphorbiaceae) – the miracle tree: Current status of knowledge. *African natural plant products volume ii: Discoveries and challenges in chemistry, health, and nutrition.* American Chemical Society.

Nassar, A. H. & Newbury, H. J. (1987). Ficin production by callus cultures of *Ficus carica*. *Journal of Plant Physiology,* **131,** 171-179.

Ndlovu, B. (2018). *Euphorbia triangularis desf. Ex a.Berger.* [Online]. SANBI. Available: http://pza.sanbi.org/euphorbia-triangularis [Accessed 8 April 2020].

Nesterenko, M. V., Tilley, M. & Upton, S. J. (1994). A simple modification of blum's silver stain method allows for 30 minute detection of proteins in polyacrylamide gels. *Journal of Biochemical and Biophysical Methods,* **28,** 239-42.

Nicosia, F. D., Puglisi, I., Pino, A., Caggia, C. & Randazzo, C. L. (2022). Plant milk-clotting enzymes for cheesemaking. *Foods (Basel, Switzerland),* **11,** 871.

Nitsawang, S., Hatti-Kaul, R. & Kanasawud, P. (2006). Purification of papain from *Carica papaya* latex: Aqueous two-phase extraction versus two-step salt precipitation. *Enzyme and Microbial Technology,* **39,** 1103-1107.

Njoroge, G. N. & Bussmann, R. W. (2007). Ethnotherapeautic management of skin diseases among the kikuyus of central Kenya. *Journal of Ethnopharmacology,* **111,** 303-307.

Novaes, L. C. D. L., Jozala, A. F., Mazzola, P. G. & Júnior, A. P. (2014). The influence of pH, polyethylene glycol and polyacrylic acid on the stability of stem bromelain. *Brazilian Journal of Pharmaceutical Sciences,* **50,** 371-380.

Otieno, B. A., Krause, C. E. & Rusling, J. F. (2016). Chapter seven - bioconjugation of antibodies and enzyme labels onto magnetic beads. *In:* Kumar, C. V. (ed.) *Methods in enzymology.* Academic Press.

Pandhare, J., Zog, K. & Deshpande, V. V. (2002). Differential stabilities of alkaline protease inhibitors from actinomycetes: Effect of various additives on thermostability. *Bioresource Technology,* **84,** 165-169.

Patel, A. K., Singh, V. K. & Jagannadham, M. V. (2007). Carnein, a serine protease from noxious plant weed *Ipomoea carnea* (morning glory). *Journal of Agricultural and Food Chemistry,* **55,** 5809-18.

Patel, G. K., Kawale, A. A. & Sharma, A. K. (2012). Purification and physicochemical characterization of a serine protease with fibrinolytic activity from latex of a medicinal herb *Euphorbia hirta*. *Plant Physiology and Biochemistry,* **52,** 104-11.

Paulus, J. K., Kourelis, J., Ramasubramanian, S., Homma, F., Godson, A., Hörger, A. C., Hong, T. N., Krahn, D., Carballo, L. O., Wang, S., Win, J., Smoker, M., Kamoun, S., Dong, S. & Hoorn, R. a. L. V. D. (2020). Extracellular proteolytic cascade in tomato activates immune protease rcr3. *Proceedings of the National Academy of Sciences,* **117,** 17409-17417.

Pavan, R., Jain, S., Shraddha & Kumar, A. (2012). Properties and therapeutic application of bromelain: A review. *Biotechnology Research International,* **2012,** 976203.

Peer, W. A. (2011). The role of multifunctional m1 metallopeptidases in cell cycle progression. *Annals of botany,* **107,** 1171-1181.

Pelmenschikov, V. & Siegbahn, P. E. (2002). Catalytic mechanism of matrix metalloproteinases: Two-layered oniom study. *Inorganic Chemistry,* **41,** 5659-66.

Petrovska, B. B. (2012). Historical review of medicinal plants' usage. *Pharmacognosy Reviews,* **6,** 1-5.

Pike, R.N. (2020). A study of the proteinase, cathepsin L, in the context of tumour invasion. PhD thesis University of Natal, Pietermaritzburg, South Africa)

Polgár, L. (1987). The mechanism of action of aspartic proteases involves 'push-pull' catalysis. *FEBS Letters,* **219,** 1-4.

Pontual, E. V., Carvalho, B. E. A., Bezerra, R. S., Coelho, L. C. B. B., Napoleão, T. H. & Paiva, P. M. G. (2012). Caseinolytic and milk-clotting activities from *Moringa oleifera* flowers. *Food Chemistry,* **135,** 1848-1854.

Putranto, R., Siswanto, Mulyatni, A., Budiani, A. & Tistama, R. (2016). Purification, characterization, and bioassay of putative protease inhibitors from *Hevea brasiliensis* latex. *E-Journal Menara Perkebunan,* **84**.

Ragster, L. & Chrispeels, M. J. (1979). Azocoll-digesting proteinases in soybean leaves. Characteristics and changes during leaf maturation and senescence. *Plant Physiology,* **64,** 857-862.

Raju, M., Sreya, A., Sovan, R. & Sanjib Kumar, C. (2021). Programmed cell death (PCD) in plant: Molecular mechanism, regulation, and cellular dysfunction in response to development and stress. *In:* Yusuf, T. (ed.) *Regulation and dysfunction of apoptosis.* Rijeka: IntechOpen.
Ramasamy, S. & Ravishankar, M. (2018). Chapter 15 - integrated pest management strategies for tomato under protected structures. *In:* Wakil, W., Brust, G. E. & Perring, T. M. (eds.) *Sustainable management of arthropod pests of tomato.* San Diego: Academic Press.
Rawdkuen, S., Chaiwut, P., Pintathong, P. & Benjakul, S. (2010). Three-phase partitioning of protease from *Calotropis procera* latex. *Biochemical Engineering Journal,* **50,** 145-149.
Reynolds, J. A. & Tanford, C. (1970). Binding of dodecyl sulfate to proteins at high binding ratios. Possible implications for the state of proteins in biological membranes. *Proceedings of the National Academy of Sciences of the United States of America,* **66,** 1002-1007.
Rodrigo, I., Vera, P. & Conejero, V. (1989). Degradation of tomato pathogenesis-related proteins by an endogenous 37-kDa aspartyl endoproteinase. *European Journal of Biochemistry,* **184,** 663-9.
Roseiro, L. B., Barbosa, M., Ames, J. M. & Wilbey, R. A. (2003). Cheesemaking with vegetable coagulants—the use of cynara l. For the production of ovine milk cheeses. *International Journal of Dairy Technology,* **56,** 76-85.
Ryan, C. A. (1990). Protease inhibitors in plants: Genes for improving defenses against insects and pathogens. *Annual Review of Phytopathology,* **28,** 425-449.
Saleh, A. M. (2011). *Ficus sycomorus* latex: A thermostable peroxidase. *African Journal of Biotechnology,* **10**.
Salomé Abarca, L. F., Klinkhamer, P. G. L. & Choi, Y. H. (2019). Plant latex, from ecological interests to bioactive chemical resources. *Planta Medica,* **85,** 856-868.
Sánchez-Morán, E., Jones, G. H., Franklin, F. C. & Santos, J. L. (2004). A puromycin-sensitive aminopeptidase is essential for meiosis in *Arabidopsis thaliana*. *Plant Cell,* **16,** 2895-909.
Sarode, A. R., Sawale, P. D., Khedkar, C. D., Kalyankar, S. D. & Pawshe, R. D. (2016). Casein and caseinate: Methods of manufacture. *In:* Caballero, B., Finglas, P. M. & Toldrá, F. (eds.) *Encyclopedia of food and health.* Oxford: Academic Press.
Schägger, H. (2006). Tricine-SDS-PAGE. *Nature Protocols,* **1,** 16-22.
Schägger, H. & Von Jagow, G. (1987). Tricine-sodium dodecyl sulfate-polyacrylamide gel electrophoresis for the separation of proteins in the range from 1 to 100 kDa. *Analytical Biochemistry,* **166,** 368-379.
Schechter, I. & Berger, A. (1967). On the size of the active site in proteases. I. Papain. *Biochemical and Biophysical Research Communications,* **27,** 157-62.
Schwartz, W. N. & Barrett, A. J. (1980). Human cathepsin H. *Biochemical Journal,* **191,** 487-497.
Sebastián, D. I., Fernando, F. D., Raúl, D. G. & Gabriela, G. M. (2020). Overexpression of *Arabidopsis* aspartic protease apa1 gene confers drought tolerance. *Plant Science,* **292,** 110406.
Sebastián, D. I., Guevara, M. G., Rocío, T. F. & Virginia, T. C. (2018). An overview of plant proteolytic enzymes. *In:* Guevara, M. G. & Daleo, G. R. (eds.) *Biotechnological applications of plant proteolytic enzymes*
Sequeiros, C., Torres, M. J., Trejo, S. A., Esteves, J. L., Natalucci, C. L. & López, L. M. (2005). Philibertain g i, the most basic cysteine endopeptidase purified from the latex of *Philibertia gilliesii* hook. Et arn. (Apocynaceae). *Protein J,* **24,** 445-53.
Shah, M. A. & Mir, S. A. (2019). Plant proteases in food processing. *In:* Mérillon, J.-M. & Ramawat, K. G. (eds.) *Bioactive molecules in food.* Cham: Springer International Publishing.
Sharma, A., Kumari, M. & Jagannadham, M. (2009). Benghalensin, a highly stable serine protease from the latex of medicinal plant *Ficus benghalensis*. *Journal of Agricultural and Food Chemistry,* **57,** 11120-6.
Sharma, P. & Gayen, D. (2021). Plant protease as regulator and signaling molecule for enhancing environmental stress-tolerance. *Plant Cell Rep,* **40,** 2081-2095.
Sharma, T., Dash, P., Das, D. & Ghosh, G. (2014). Kinetic and thermodynamic studies of purified protein isolated from *Euphorbia tirucalli latex*. *Asian Journal of Pharmaceutical and Clinical Research,* **7,** 275-278.
Shouket, H. A., Ameen, I., Tursunov, O., Kholikova, K., Pirimov, O., Kurbonov, N., Ibragimov, I. & Mukimov, B. (2020). Study on industrial applications of papain: A succinct review. *IOP Conference Series: Earth and Environmental Science,* **614,** 012171.
Siar, E.-H., Morellon-Sterling, R., Zidoune, M. N. & Fernandez-Lafuente, R. (2020). Use of glyoxyl-agarose immobilized ficin extract in milk coagulation: Unexpected importance of the ficin loading on the biocatalysts. *International Journal of Biological Macromolecules,* **144,** 419-426.

Sijwali, P. S. & Nivya, M. A. (2021). Enzymes | cysteine proteases. *In:* Jez, J. (ed.) *Encyclopedia of biological chemistry iii (third edition).* Oxford: Elsevier.
Silva-López, R. E. & Gonçalves, R. N. (2019). Therapeutic proteases from plants: Biopharmaceuticals with multiple applications. *Journal of Applied Biotechnology & Bioengineering,* **6,** 101-109.
Simoes, I. & Faro, C. (2004). Structure and function of plant aspartic proteinases. *European Journal of Biochemistry,* **271,** 2067-75.
Simões, I., Faro, R., Bur, D. & Faro, C. (2007). Characterization of recombinant cdr1, an *Arabidopsis* aspartic proteinase involved in disease resistance*. *Journal of Biological Chemistry,* **282,** 31358-31365.
Simpson, D. M. & Beynon, R. J. (2010). Acetone precipitation of proteins and the modification of peptides. *Journal of Proteome Research,* **9,** 444-50.
Siritapetawee, J., Teamtisong, K., Limphirat, W., Charoenwattanasatien, R., Attarataya, J. & Mothong, N. (2020). Identification and characterization of a protease (eurp-61) from *Euphorbia resinifera* latex. *International Journal of Biological Macromolecules,* **145,** 998-1007.
Smith, P. K., Krohn, R. I., Hermanson, G. T., Mallia, A. K., Gartner, F. H., Provenzano, M. D., Fujimoto, E. K., Goeke, N. M., Olson, B. J. & Klenk, D. C. (1985). Measurement of protein using bicinchoninic acid. *Analytical Biochemistry,* **150,** 76-85.
Soares, A., Ribeiro Carlton, S. M. & Simões, I. (2019). Atypical and nucellin-like aspartic proteases: Emerging players in plant developmental processes and stress responses. *J Exp Bot,* **70,** 2059-2076.
Sobottka, A. M., Tonial, F., Sytwala, S. & Melzig, M. F. (2014). Proteinase activity in latex of three plants of the family Euphorbiaceae. *Brazilian Journal of Pharmaceutical Sciences,* **50,** 559-565.
Song, J., Tan, H., Boyd, S., Shen, H., Mahmood, K., Webb, G., Akutsu, T., Whisstock, J. & Pike, R. (2011). Bioinformatic approaches for predicting substrates of proteases. *Journal of Bioinformatics and Computational Biology,* **9,** 149-78.
Srikanth, S. & Chen, Z. (2016). Plant protease inhibitors in therapeutics-focus on cancer therapy. *Frontiers in Pharmacology,* **7**.
Stöcker, W. & Bode, W. (1995). Structural features of a superfamily of zinc-endopeptidases: The metzincins. *Current Opinion in Structural Biology,* **5,** 383-90.
Stührwohldt, N., Bühler, E., Sauter, M. & Schaller, A. (2021). Phytosulfokine (psk) precursor processing by subtilase sbt3.8 and psk signaling improve drought stress tolerance in *Arabidopsis*. *Journal of Experimental Botany,* **72,** 3427-3440.
Suárez, M. E. (2019). Medicines in the forest: Ethnobotany of wild medicinal plants in the pharmacopeia of the wichí people of Salta province (Argentina). *Journal of Ethnopharmacology,* **231,** 525-544.
Sufiate, B. L., Soares, F. E. D. F., Ferreira, T. D. F., Dias, J. P., Gouveia, A. D. S., Moreira, S. S. & Queiroz, J. H. D. (2021). *Euphorbia trigona* latex nematicidal activity on the root-knot nematode meloidogyne incognita. *Research, Society and Development,* **10,** e19910918037.
Takahashi, K., Niwa, H., Yokota, N., Kubota, K. & Inoue, H. (2008). Widespread tissue expression of nepenthesin-like aspartic protease genes in *Arabidopsis thaliana*. *Plant Physiology and Biochemistry,* **46,** 724-729.
Takechi, K., Sodmergen, Murata, M., Motoyoshi, F. & Sakamoto, W. (2000). The yellow variegated (var2) locus encodes a homologue of ftsh, an ATP-dependent protease in *Arabidopsis*. *Plant and Cell Physiology,* **41,** 1334-1346.
Tavano, O. L. (2013). Protein hydrolysis using proteases: An important tool for food biotechnology. *Journal of Molecular Catalysis B: Enzymatic,* **90,** 1-11.
Tomar, R., Kumar, R. & Jagannadham, M. V. (2008). A stable serine protease, wrightin, from the latex of the plant *Wrightia tinctoria* (roxb.) r. Br.: Purification and biochemical properties. *Journal of Agricultural and Food Chemistry,* **56,** 1479-87.
Tornero, P., Conejero, V. & Vera, P. (1996). Primary structure and expression of a pathogen-induced protease (pr-p69) in tomato plants: Similarity of functional domains to subtilisin-like endoproteases. *Proceedings of the National Academy of Sciences,* **93,** 6332-6337.
Trezza, A., Cicaloni, V., Pettini, F. & Spiga, O. (2020). Chapter 2 - potential roles of protease inhibitors in anticancer therapy. *In:* Gupta, S. P. (ed.) *Cancer-leading proteases.* Academic Press.
Tripathi, P., Tomar, R. & Jagannadham, M. V. (2011). Purification and biochemical characterisation of a novel protease streblin. *Food Chemistry,* **125,** 1005-1012.

Troncoso, F. D., Sánchez, D. A. & Ferreira, M. L. (2022). Production of plant proteases and new biotechnological applications: An updated review. *ChemistryOpen,* **11,** e202200017.
Uchikoba, T. & Kaneda, M. (1996). Milk-clotting activity of cucumisin, a plant serine protease from melon fruit. *Applied Biochemistry and Biotechnology,* **56,** 325-330.
Urs, A. P., Manjuprasanna, V. N., Rudresha, G. V., Hiremath, V., Sharanappa, P., Rajaiah, R. & Vishwanath, B. S. (2021). Thrombin-like serine protease, antiquorin from *Euphorbia antiquorum* latex induces platelet aggregation via par1-akt/p38 signaling axis. *Biochim Biophys Acta Mol Cell Res,* **1868,** 118925.
Van Der Hoorn, R. A. (2008). Plant proteases: From phenotypes to molecular mechanisms. *Annual Review of Plant Biology,* **59,** 191-223.
Van Der Hoorn, R. a. L. & Klemenčič, M. (2021). Plant proteases: From molecular mechanisms to functions in development and immunity. *Journal of Experimental Botany,* **72,** 3337-3339.
Veeresham, C. (2012). Natural products derived from plants as a source of drugs. *Journal of Advanced Pharmaceutical Technology & Research,* **3,** 200-201.
Verma, S., Dixit, R. & Pandey, K. C. (2016). Cysteine proteases: Modes of activation and future prospects as pharmacological targets. *Frontiers in Pharmacology,* **7**.
Verma, V., Singhal, G., Joshi, S., Choudhary, M. & Srivastava, N. (2022). Chapter 10 - plant extracts as enzymes. *In:* Mir, S. A., Manickavasagan, A. & Shah, M. A. (eds.) *Plant extracts: Applications in the food industry.* Academic Press.
Vernet, T., Khouri, H. E., Laflamme, P., Tessier, D. C., Musil, R., Gour-Salin, B. J., Storer, A. C. & Thomas, D. Y. (1991). Processing of the papain precursor. Purification of the zymogen and characterization of its mechanism of processing. *Journal of Biological Chemistry,* **266,** 21451-7.
Vernet, T., Tessier, D. C., Chatellier, J., Plouffe, C., Lee, T. S., Thomas, D. Y., Storer, A. C. & Ménard, R. (1995). Structural and functional roles of asparagine 175 in the cysteine protease papain. *Journal of Biological Chemistry,* **270,** 16645-16652.
Vorster, B. J., Cullis, C. A. & Kunert, K. J. (2019). Plant vacuolar processing enzymes. *Frontiers in Plant Science,* **10**.
Wanderley, L., Soares, A., Silva, C., Figueiredo, I., Ferreira, A., Perales, J., Mota, H., Oliveira, J. & Junior, L. (2018). A cysteine protease from the latex of *Ficus benjamina* has in vitro anthelmintic activity against *Haemonchus contortus*. *Revista brasileira de parasitologia veterinaria = Brazilian journal of veterinary parasitology: Orgao Oficial do Colegio Brasileiro de Parasitologia Veterinaria,* **27**.
Wang, D.-H., Song, W., Wei, S.-W., Zheng, Y.-F., Chen, Z.-S., Han, J.-D., Zhang, H.-T., Luo, J.-C., Qin, Y.-M., Xu, Z.-H. & Bai, S.-N. (2018). Characterization of the ubiquitin c-terminal hydrolase and ubiquitin-specific protease families in rice (*Oryza sativa)*. *Frontiers in Plant Science,* **9**.
Wang, W., Tai, F. & Chen, S. (2008). Optimizing protein extraction from plant tissues for enhanced proteomics analysis. *Journal of Separation Science,* **31,** 2032-9.
Wang, Y., Zhao, J., Deng, X., Wang, P., Geng, S., Gao, W., Guo, P., Chen, Q., Li, C. & Qu, Y. (2022). Genome-wide analysis of serine carboxypeptidase-like protein (scpl) family and functional validation of gh_scpl42 unchromosome conferring cotton verticillium der verticillium wilt stress in *Gossypium hirsutum*. *BMC Plant Biology,* **22,** 421.
Wani, M. C., Taylor, H. L., Wall, M. E., Coggon, P. & Mcphail, A. T. (1971). Plant antitumor agents. Vi. Isolation and structure of taxol, a novel antileukemic and antitumor agent from *Taxus brevifolia*. *Journal of the American Chemical Society,* **93,** 2325-2327.
Wattarantenne, K. V. (2017). The meiotic prophase aminopeptidase 1 regulates polyploidy in *Arabidopsis thaliana*.
White, N. J., Hien, T. T. & Nosten, F. H. (2015). A brief history of qinghaosu. *Trends in Parasitology,* **31,** 607-610.
Wiechelman, K. J., Braun, R. D. & Fitzpatrick, J. D. (1988). Investigation of the bicinchoninic acid protein assay: Identification of the groups responsible for color formation. *Analytical Biochemistry,* **175,** 231-237.
Wolfson, J. L. & Murdock, A. L. (1995). Potential use of protease inhibitors for host plant resistance: A test case. *Environmental Entomology,* **24,** 52-57.
Wyk, B.-E. V. & Wink, M. (2017). *Medicinal plants of the world an illustrated scientific guide to important medicinal plants and their uses*, Briza Publications.

Yadav, S., Pande, M. & Jagannadham, M. (2006a). Highly stable glycosylated serine protease from the medicinal plant *Euphorbia milii*. *Phytochemistry,* **67,** 1414-26.

Yamada, K., Basak, A. K., Goto-Yamada, S., Tarnawska-Glatt, K. & Hara-Nishimura, I. (2020). Vacuolar processing enzymes in the plant life cycle. *New Phytologist,* **226,** 21-31.

Yamagata, H., Masuzawa, T., Nagaoka, Y., Ohnishi, T. & Iwasaki, T. (1994). Cucumisin, a serine protease from melon fruits, shares structural homology with subtilisin and is generated from a large precursor. *Journal of Biological Chemistry,* **269,** 32725-31.

Zakharova, E., Horvath, M. P. & Goldenberg, D. P. (2009). Structure of a serine protease poised to resynthesize a peptide bond. *Proceedings of the National Academy of Sciences of the United States of America,* **106,** 11034-11039.

Zhang, Y., Kua, J. & Mccammon, J. A. (2002). Role of the catalytic triad and oxyanion hole in acetylcholinesterase catalysis: An ab initio qm/mm study. *Journal of the American Chemical Society,* **124,** 10572-10577.

Zimmermann, D., Gomez-Barrera, J. A., Pasule, C., Brack-Frick, U. B., Sieferer, E., Nicholson, T. M., Pfannstiel, J., Stintzi, A. & Schaller, A. (2016). Cell death control by matrix metalloproteinases *Plant Physiology,* **171,** 1456-1469.

Zollner, H. (1992). *Handbook of enzyme inhibitors*, Wiley-Blackwell.